

To detect anomalies in diaphragm walls

PROEFSCHRIFT

ter verkrijging van de graad van doctor
aan de Technische Universiteit Delft,
op gezag van de Rector Magnificus prof. ir. K.C.A.M. Luyben,
voorzitter van het College voor Promoties,
in het openbaar te verdedigen

op 9 november 2015 om 15:00 uur

door

Rodriaan SPRUIT

mijnbouwkundig ingenieur
geboren te Schiedam

Dit proefschrift is goedgekeurd door de promotor:
Prof. ir. A.F. van Tol

Copromotor:
Dr. ir. W. Broere

Samenstelling promotiecommissie:

Rector Magnificus
Prof. ir. A.F. van Tol
Dr. ir. W. Broere

Technische Universiteit Delft, voorzitter
Technische Universiteit Delft, promotor
Technische Universiteit Delft, copromotor

Onafhankelijke leden:

Prof. dr. ir. E.C. Slob
Prof. dr. ir. N.C. van de Giesen
Prof. M.A. Mooney Ph.D., P.E.
Dr. rer. nat. E. Niederleithinger
Prof. ir. J. Maertens

Technische Universiteit Delft
Technische Universiteit Delft
Colorado School of Mines
Bundesanstalt für Materialforschung Berlin
Katholieke Universiteit Leuven

Printed by:

IPSKAMP Drukkers

ISBN 978-94-6259-897-3

© 2015 by R. Spruit

All rights reserved. No part of the material protected by this copyright notice may be reproduced or utilized in any form or by any means, electronic or mechanical, including photocopying, recording or by any information storage and retrieval system, without written consent of the publisher.

Printed in the Netherlands

Abstract

Diaphragm walls are potentially ideal retaining walls for deep excavations in densely built-up areas, as they cause no vibrations during their construction and provide structural elements with high strength and stiffness. In the recent past, however, several projects using diaphragm walls as soil and water retaining elements have encountered severe problems. The problems primarily arise around the joints between panels. After excavation of the building pit, the joints slowly or suddenly start to leak. If a leak coincides with a permeable soil layer outside the building pit, the soil can erode, causing settlements adjacent to the retaining wall. An average 16% chance of leakage per project has been estimated from previous projects, making the chance of a calamity due to a leaking joint unacceptably high for current litigious society.

Detection techniques have traditionally focused on groundwater flow, as groundwater flow through the wall is an important link in the calamity chain: no groundwater flow: no transportation of soil: no settlements. The flaw in such a detection system is the nature of the anomalies in diaphragm walls. Due to the production procedure of diaphragm walls, anomalies in most cases consist of bentonite (clay) pockets in the joint. These clayey anomalies have a high hydraulic resistivity, making them almost impossible to detect based upon the groundwater flow detection principle. After excavation and thus exposing the anomaly, the clayey material is too weak to retain the groundwater pressure, causing a leak which can quickly erode the remaining material in the anomaly.

In contrast with the above mentioned detection principle, this research has primarily focused on the quality of concrete around the joints between the diaphragm wall panels. It is assumed that when persistent high quality concrete in the joint area is present, no leakage or soil transport through the wall can take place.

Based on the physical characteristics of concrete, soil and bentonite slurry, several measurement techniques have been chosen for examination in the laboratory and in the field.

Using the test results from pilot projects, three techniques have been chosen for further validation and, if possible, cross correlation with the other techniques and the actual shape of the anomalies.

The validated techniques are (in order of effectiveness in a project setting): Crosshole Sonic Logging (CSL), Distributed Temperature Sensing (DTS) and Electrical Resistivity (ER).

The effectiveness of all three methods has been based upon the cost of the measurements, the accuracy of the interpretation, the ease of interpretation and the interference with the production process.

CSL is commonly used in large diameter bored pile integrity testing and is based upon the sound velocity in a medium. The velocity is determined by the stiffness and density of the material. For concrete these parameters are relatively high compared to the characteristics of the material that is expected to be present in an anomaly (soil or bentonite). An increase in the observed travel time of the ultrasonic signal indicates an anomaly. The simultaneously observed attenuation of the signal offers additional information about the properties of the anomaly. In this study the CSL technique has been verified for the novel application investigating the joints between diaphragm walls. This research has shown that the ultrasonic signal of current CSL devices can pass the joint between diaphragm wall panels while remaining interpretable. With the reference measurements of this study showing linear correlation between delay in arrival time and anomaly width, the size and material of an anomaly can be estimated, making preemptive repair decisions possible.

DTS is generally accepted in diverse monitoring applications such as monitoring power lines, hydrological flow patterns, concrete curing temperature distribution and down-hole oil production parameters. The technique uses optical fiber sensors that provide a continuous temperature profile along the length of the fiber when read out by a DTS device. In this study the DTS technique has been validated for application during diaphragm wall production. The spatial resolution for tracing a progressing temperature front has been determined. This resolution is an order of magnitude better than suggested by the specifications of the measurement equipment. With the appropriate processing of the recorded temperature profiles in the time domain, the bentonite refreshing and concrete casting

processes can be monitored meticulously. During bentonite refreshing, the temperature of the freshly mixed slurry should ideally show up at all depths of each recorded profile (positioned at critical locations in the trench e.g. in the joints). If locally the arrival of fresh slurry is not observed, the refreshing process can be repeated after additional clean-up of the trench. This ensures consistent slurry characteristics before concrete casting takes place. During concrete casting, the interpreted DTS recordings will show the casting progress in time for each DTS profile position. The observed temperatures also reveal valuable information about the purity of the concrete, making an estimate of the local concrete quality possible.

Electrical resistivity methods are often mentioned as a possibility for detecting leaks. The method is based upon differences in electrical resistivity of soil and concrete. It is assumed that a continuous (fully cured) concrete wall will have a relatively high resistivity compared to a wall with clayey anomalies. In this study the method has been tested for detecting anomalies in diaphragm walls. Detection limits for several electrode configurations have been determined. From the test results, requirements for field tests have been derived. To obtain adequate measurements, at least a four electrode setup must be used with the potential electrodes placed no further than 0.2 m from the diaphragm wall.

The research comprised laboratory and site testing in several projects. The project experiences are an important component of this research, as they illustrate the practical implications of the measurement techniques. As a result, it was possible to derive a manual for the execution of the measurements, containing practical tips for the interpretation of the measurement results.

CSL is the primary recommended method because of the relatively low cost, low impact on the building process and reliable and fast interpretation. DTS shows great potential for a step forward in quality control during diaphragm wall production. Currently, the method will be beneficial for verifying concrete flow in pilot panels with rebar spacing beyond the design code requirements. The still relatively high cost of data acquisition and interpretation (about 100% of one panel building cost) limit large scale application.

Electrical resistivity has been least successful in determining anomalies in diaphragm walls. In specific circumstances, the method could provide useful information, especially if other methods have not been applied and

Abstract

preemptive repair of the diaphragm wall with jetgrout poses a risk to the surroundings. Due to the data acquisition time and space requirement, this method is more costly than the other methods.

Samenvatting

Diepwanden zijn in potentie ideale keerwanden voor diepe ontgravingen in dichtbebouwde gebieden omdat ze tijdens de bouw geen trillingen veroorzaken en ze structurele elementen leveren met hoge sterkte en stijfheid. Echter, in het recente verleden heeft een aantal projecten waar diepwanden werden toegepast als grond- en waterkerende elementen ernstige problemen ondervonden. De problemen traden vooral op rond de voegen tussen de diepwandpanelen. Na het uitgraven van de bouwput begonnen de voegen geleidelijk of plotseling te lekken. Als een lek ontstaat op de diepte van een doorlatende grondlaag buiten de bouwput, kan grond eroderen, waardoor naast de diepwand zettingen optreden. Uit eerdere projecten is de kans op een lekkage in een project geschat op 16%, wat onaanvaardbaar hoog is in de huidige kritische samenleving.

Detectietechnieken hebben zich van oudsher gericht op grondwaterstroming, want grondwaterstroming door de wand is een belangrijke schakel in het faalmechanisme: geen grondwaterstroming: geen transport van zand: geen zettingen. De tekortkoming in een dergelijk detectiesysteem is de aard van de afwijkingen in diepwanden. Door het productieproces van diepwanden, bestaan onregelmatigheden in de meeste gevallen uit bentoniet (klei) insluitingen in de voeg. Deze volumes kleiig materiaal hebben een hoge hydraulische weerstand, waardoor ze vrijwel niet te vinden zijn op basis van grondwaterstroming. Na het uitgraven en dus het blootstellen van de anomalie, blijkt het materiaal te zwak om de grondwaterdruk te weerstaan. Zodra een grondwaterstroming door het lek optreedt, kan het resterende materiaal in de anomalie snel eroderen.

In tegenstelling tot het bovengenoemde detectieprincipe heeft dit onderzoek zich vooral gericht op de kwaliteit van beton rondom de voegen tussen de diepwandpanelen. Er is vanuit gegaan dat bij een doorgaande goede

kwaliteit beton in de zone van de voeg, geen lekkage kan optreden zodat ook grondtransport door de wand kan worden uitgesloten.

Op basis van de fysische eigenschappen van beton, grond en bentonietmengsels zijn verschillende meettechnieken gekozen voor beproeving in het laboratorium en in het veld.

Op basis van de voorlopige testresultaten zijn drie technieken gekozen voor verdere validatie en, indien mogelijk, correlatie met andere technieken en de werkelijke vorm van de afwijkingen.

De gevalideerde technieken zijn (in volgorde van effectiviteit in een project omgeving): Crosshole Sonic Logging (CSL), Distributed Temperature Sensing (DTS) en Elektrische weerstand (ER).

De effectiviteit van een meetmethode werd gebaseerd op de kosten van de metingen, de nauwkeurigheid van de interpretatie, het gemak van interpretatie en de inpasbaarheid binnen het productieproces.

CSL wordt vaak gebruikt om de kwaliteit van grote diameter boorpalen te bepalen. De methode is gebaseerd op de geluidssnelheid in een medium. De snelheid wordt bepaald door de stijfheid en dichtheid van het materiaal. Voor beton zijn deze parameters relatief hoog in vergelijking met de eigenschappen van het materiaal dat wordt verwacht in een anomalie (grond of bentoniet). Een toename van de waargenomen looptijd van het ultrasone signaal duidt op een anomalie. De eveneens waargenomen demping van het signaal biedt aanvullende informatie over de eigenschappen van de anomalie. In deze studie is de CSL techniek geïkt voor de nieuwe toepassing waarbij de voegen tussen diepwandpanelen worden onderzocht. Met het onderzoek is aangetoond dat het ultrasoon signaal van de huidige CSL meetapparaten de voeg tussen diepwandpanelen kan passeren en van voldoende kwaliteit blijft voor een bruikbare interpretatie. Met de referentiemetingen van dit onderzoek, die een lineaire correlatie tussen vertraging van het signaal en de dikte van de afwijking in de voeg laten zien, kan de grootte en het materiaal van een anomalie worden geschat, waardoor kan worden besloten of preventieve reparaties nodig zijn.

DTS wordt veelvuldig gebruikt in diverse monitoringstoepassingen zoals bewaking van hoogspanningskabels, het in kaart brengen van hydrologische stromingspatronen, het uitharden van beton en het volgen van olieproductieparameters in het boorgat. De techniek maakt gebruik van optische (glasvezel) sensoren die een continu temperatuurprofiel over de lengte van de vezel opleveren als ze met een DTS apparaat worden uitgelezen. In deze studie is de DTS-techniek gevalideerd voor gebruik

tijdens diepwandproductie. De plaatsresolutie voor het volgen van een zich verplaatsend temperatuurfront is bepaald. Deze resolutie is een orde van grootte beter dan de specificaties van de meetapparatuur doen vermoeden. Met de juiste verwerking van de geregistreerde temperatuurprofielen in het tijddomein, kan het ontzanden van de steunvloeistof en het betonstorten nauwgezet worden gevolgd. Tijdens het ontzanden van de steunvloeistof moet de temperatuur van de vers gemengde bentoniet op elke diepte van elk geregistreerd temperatuurprofiel verschijnen. Als lokaal geen aankomst van verse bentoniet wordt waargenomen, kan het ontzanden worden herhaald. Dit garandeert optimale bentonieteigenschappen voor aanvang van het betonstorten. Tijdens het betonstorten, zal het geïnterpreteerd DTS-sigitaal de vooruitgang van het stortfront in de tijd laten zien voor elke positie waar een DTS profiel wordt gemeten. De waargenomen temperaturen blijken ook betrouwbare informatie over de zuiverheid van het beton te bieden zodat een schatting van de plaatselijke betonkwaliteit kan worden gemaakt.

ER wordt vaak genoemd als mogelijkheid voor lekdetectie. De methode is gebaseerd op verschillen in elektrische weerstand. Er wordt in de toepassing in diepwanden vanuit gegaan dat een doorgaande (volledig uitgeharde) betonnen wand een relatief hoge elektrische weerstand zal hebben vergeleken met een betonnen wand met afwijkingen gevuld met klei. In deze studie is de methode getest voor het opsporen van afwijkingen in de diepwanden. Detectielimieten voor meerdere electrode configuraties zijn bepaald. Voor bruikbare metingen moet op zijn minst gebruik worden gemaakt van een test opzet met 4 electrodes waarvan de potential electrodes niet verder dan 0,2 m van de diepwand af staan.

Het onderzoek bestond uit laboratoriumproeven en veldproeven in verschillende projecten. De projectervaringen vormen een belangrijk onderdeel van dit onderzoek, omdat ze de praktische waarde van de meettechnieken illustreren.

Dit bood de mogelijkheid om een handleiding voor het uitvoeren van de metingen op te stellen, waarbij ook praktische tips voor de interpretatie van de meetresultaten worden gegeven.

CSL is de aanbevolen methode om anomalieën in diepwanden op te sporen vanwege de relatief lage kosten, de geringe impact op de bouwlogistiek en de snelle en betrouwbare interpretatie van de meetresultaten.

DTS biedt op termijn de kans op een verbetering van de kwaliteitscontrole tijdens diepwandproductie. Momenteel is de methode vooral geschikt om betonstroming tijdens het storten te controleren van een (proef-) paneel waarvan de wapening niet voldoet aan de ontwerpvoorschriften. De relatief hoge kosten voor het meten en interpreteren (ongeveer 100% van de productiekosten van een paneel) staan vooralsnog grootschalige inzet van deze toepassing in de weg.

De elektrische weerstandsmethode is het minst succesvol gebleken om anomalieën in diepwanden op te sporen. Onder specifieke omstandigheden kan de methode nuttig zijn, vooral als de andere methoden niet zijn toegepast en preventieve reparatie met jetgrout een risico voor de omgeving oplevert. Door de benodigde tijd en ruimte voor de metingen, is deze methode duurder dan de andere.

Table of contents

Abstract	4
Samenvatting.....	8
Table of contents.....	12
Chapter 1 Introduction.....	15
1.1 State of the art quality control and leakage prevention.....	17
1.2 Research vision and outline.....	20
1.3 Research scope	21
Chapter 2 Pilot projects and verification experiments.....	23
2.1 Chronology of the research	23
2.2 Pilot test Franki Oosterhout	25
2.3 Pilot project Kruisplein Rotterdam	27
2.4 Spoorzone Delft	31
2.5 Laboratory tests at TU Delft	35
2.6 Test Electric conductivity TU Delft	37
Chapter 3 Detection of anomalies in diaphragm walls with Crosshole Sonic Logging	38
3.1 Abstract	38
3.2 Introduction.....	38
3.3 Crosshole Sonic Logging	39
3.4 Test models.....	41
3.5 Results from the test models.....	43

3.6	Discussion	50
3.7	Frequency domain analyses.....	52
3.8	Results from field tests	54
3.9	Conclusions	59
3.10	Acknowledgements	60
Chapter 4 Distributed Temperature Sensing applied during diaphragm wall construction.....		61
4.1	Abstract.....	61
4.2	Introduction	61
4.3	Hypothesis	62
4.4	Measurement principle	63
4.5	Laboratory measurements.....	65
4.6	Field measurements	72
4.7	Correlation with manual concrete level measurements	76
4.8	Discussion	84
4.9	Conclusions	85
Chapter 5 To detect anomalies in diaphragm walls with apparent resistivity measurements.....		87
5.1	Abstract.....	87
5.2	Introduction	87
5.3	Measurement principle	88
5.4	Tests.....	90
5.5	Conclusions and recommendations	113
Chapter 6 Discussion.....		116
6.1	Production projects	116
6.2	Discussion of the tests and results	145
6.3	Recommended measurements	153
Chapter 7 Conclusions and recommendations.....		155
7.1	Conclusions	155

Table of contents

7.2 Recommendations	162
References.....	165
Acknowledgements.....	171
About the author.....	172

Chapter 1 Introduction

On the 19th of June 2008 the 'Noord-Zuid-lijn' metro project in Amsterdam caught the attention of Dutch national media, because adjacent 17th century buildings subsided 140 mm due to a leaking diaphragm wall of the deep excavation for the construction of an underground metro station (van Tol and Korff 2012). The leak occurred when the excavation had reached the depth of a sand layer. This sand layer served as the foundation layer for the wooden pile foundations of the adjacent monuments. The sand eroded, causing a reduction of in-situ stresses which resulted in loss of bearing capacity and settlement of the wooden piles of the monuments. After stopping the leak, a geophysical survey with a multi-sensor electrical resistivity method was conducted, showing many small leaks, but no major defects. Just after restarting the project, (on the 10th of September) another severe leak occurred, causing groundwater and soil inflow. Settlements up to 250 mm occurred adjacent to the same excavation, affecting different buildings. This major defect in the diaphragm wall had not been noticed by the geophysical detection method (van Tol and Korff 2012).

As a result, diaphragm walls were suddenly considered unsafe in the Netherlands for application close to existing buildings, especially because around the same time other projects, like metro construction projects in Rotterdam and Cologne showed similar problems with diaphragm walls (van Tol et al 2010, Sieler et al. 2012). However, apart from these calamities, diaphragm walls seem ideally suited to the built-up environment due to their vibration-free execution and their obtainable high strength and stiffness.

Before the problems in Amsterdam occurred, diaphragm walls were considered an expensive but safe concept for building a retaining wall. Investigation into previous Dutch projects (van Tol et al. 2010) showed however, that generally for 0.16% of the panels, severe problems have occurred. These leakages did not lead to dominant exposure in the media due to less densely built-up areas where the problems occurred, the simple fact that not every leak causes a major problem and luck. Leaks are often

directly stopped by immediate back filling and leakage only leads to severe problems in sandy soils. This 0.16% problem rating for diaphragm walls, may seem a low number. When considering a typical project like an underground parking or a metro station with in the order of magnitude 100 panels (and the same number of joints), this adds up to a calamity chance of 15% for a project. This seems consistent with internationally reported problems with diaphragm walls for example in Taipei, where a multistory building collapsed due to sand pockets in the diaphragm wall of a metro station under construction (Hwang et al. 2007), Boston, where major leaks in the diaphragm walls occurred in a road tunnel after completion (Poletto and Tamaro 2011) and Cologne where the city archive building collapsed due to a leaking diaphragm wall of a metro station under construction (Sieler et al. 2012).

Although not all calamities will have a big impact on the surroundings, the risk will in the future increase as the trend is still to build deeper and closer to existing buildings (Hoek 2012). Insurance companies have already long term experience with risk management in determining the insurance policy (Akindoye and MacLeod 1996). As a result, projects with retaining walls consisting of diaphragm walls may become impossible to insure. Consequential damage if a calamity occurs can be so large (both financially and socially), that many projects will not be feasible any more.

There was however some good news as well: the forensic studies (van Tol et al. 2010, Poletto and Tamaro 2011, Sieler et al. 2012) show that the joints between the panels are causing the majority of the problems. Experience has shown that reparation of joints is rather easy if no groundwater flow occurs (yet). If detection of an anomaly, that can cause a calamity, takes place before excavation of the building pit starts, the anomaly can be repaired before a groundwater flow is present, increasing the chances of a successful repair. So the major challenge is to detect the anomaly and assess its coordinates prior to excavation.

To reduce the risk profile of diaphragm walls, two research projects were initiated at Delft University of Technology.

- Improvement of the diaphragm wall installation process, in which 3D finite element modelling of the bentonite and concrete flow and large scale testing are used to better understand and predict the critical stages and geometric boundary conditions during diaphragm wall installation (van Dalen 2015).

- Detecting anomalies in diaphragm walls: with measurement techniques locating anomalies in (the joint area of) diaphragm walls, in order to be able to repair the anomalies before excavation of the building pit takes place.

The research described in this thesis is about the detection of anomalies. Before focusing on the detection techniques, the current practice of quality control and leakage prevention of the installation process will be briefly reviewed.

1.1 State of the art quality control and leakage prevention

This paragraph contains an overview of the available methods for quality control and leakage prevention during diaphragm wall installation.

The steps to install a diaphragm wall in a reliable way with an acceptable leakage risk can be subdivided into:

- Protocols and procedures that ensure proper design and installation of diaphragm walls
- Measurements during construction that verify the protocols and procedures
- Measurements after completion to verify the quality of the wall

Before this research started, leakage prevention was primarily based upon protocols and procedures supporting good workmanship.

The flow parameters of both the bentonite and the concrete, combined with the bar spacing in the rebar cage largely govern the chances of anomalies occurring. As a result, many codes include rules for rebar spacing and flow parameters. For example in the former German codes (DIN-4126, 1986 and DIN-4127, 1986), Eurocode (EN 1538, 2010) for diaphragm wall execution and the CUR231 guideline for design and execution of diaphragm walls, properties for the bentonite slurry and the concrete are specified. As a result, most quality control measurements during construction focus on bentonite and concrete flow parameters.

Another aspect that is often mentioned is the verticality of the panels (Bruce et al. 1989, van Tol et al. 2010). If panels deviate too much, the joint may not overlap any more, creating a wedge shaped anomaly with increasing width at increasing depth. In most projects the verticality of the panel is verified during or after excavation of the trench with inclinometers attached to the grab.

In addition to the use of inclinometers, the Koden ultrasonic scanner can be deployed in the excavated trench to scan for anomalies in the shape of the trench (Bruce et al. 1989).

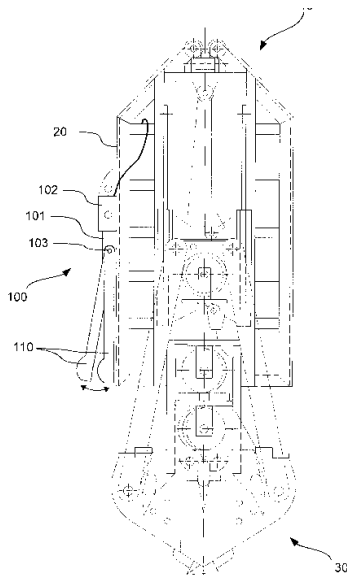


Figure 1: Device for mechanically examining panel joint (feelers indicated with number 110) (Schneider 2014)

Recently, a device (Schneider 2014) has been developed and patented to examine the exposed joint of the previously installed panel, just after the steel stop end has been removed. The device has three or more feeler arms and will be attached to the grab (Figure 1). After being lowered to the final depth and pulled towards the joint, the feelers record the shape of the joint during pull-up of the device. If irregularities are encountered, the joint can be brushed. After brushing the the device can be lowered into the trench again to verify the cleanup.

Another recent development is reported by Niederleithinger and Garcia (2014) in which the shape of the exposed joint of the primary panel is examined from the excavated secondary panel by means of an ultrasonic scan. The intended result is the same as with the previously mentioned mechanical method. Both methods can only provide information on the joint of the primary panel because the concrete of the secondary panel has not yet been cast.

In a study to safely construct diaphragm walls to a depth of 100 m (Bruce et al. 1989), Crosshole Sonic Logging (CSL) is mentioned as a reliable possibility to check the continuity of the joints between panels. CSL is commonly used in large diameter bored pile integrity testing and is based upon the sound velocity in a medium. The longitudinal compression wave velocity is determined by the stiffness and density of the material. For concrete these parameters are relatively high compared to the characteristics of the material that is expected to be present in an anomaly (soil or bentonite). An increase in the observed travel time of the ultrasonic signal indicates an anomaly. The simultaneously observed attenuation of the signal offers additional information about the properties of the anomaly. In the study by Bruce et al. (1989), the CSL technique was used with the intention to verify the verticality of the panels. An increasing deviation in the relative verticality between panels will cause a longer path length of the ultrasonic signal. It was concluded that the ultrasonic signal across the joint was usable for determining the relative verticality of two panels. It was also noted that the signal would probably contain useful information about the quality of the joint between diaphragm wall panels. After this first attempt with CSL applied across diaphragm wall joints, no further publications have been found.

To assess the quality of the concrete within the panel, the French Code NF P94-160-1, 2000, mentions crosshole sonic logging (CSL) as an option. Although this could be extended to measuring across the joint, the code does not mention this possibility.

Concrete quality monitoring based upon temperature distribution is widely used (Carino and Lew 2001). To measure the local temperature, distributed temperature sensing (DTS) is becoming increasingly popular, especially in large volumes of cast concrete, such as arched dams (Thevenaz et al. 1998). Efforts have been made to assess the properties and diameter of jetgrout columns with temperature measurements (Meinhard et al. 2014). This has not yet led to an application of DTS specifically focused on diaphragm wall quality control.

After completion of the complete perimeter of the building pit, it has been tried to determine the presence of leaks with geo-electrical methods, for example during a metro construction project in Amsterdam the TexPloer (Vanni and Geutebrück 2011) method was used (van Tol and Korff, 2012). During the project in Amsterdam it was impossible to discriminate between a

joint with a severe inclusion of remaining bentonite slurry and a proper joint with a thin film of silty material. Only when the electrodes are positioned at close range from the wall along several parallel vertical profiles, it seems possible to assess the walls permeability properties (Hwang et al. 2007).

Another method of assessing the leakage parameters of a diaphragm wall around a building pit is by performing a pumping test. The Austrian and Dutch codes (Richtlinië Dichte Schlitzwände 2002, CUR 2010) indicate what permeability of the wall can be expected. Although a pumping test provides reliable information about the average leakage, it is hard to pinpoint the relatively large leaks that deliver the main contribution to the total inflow of groundwater or to estimate their size or permeability. In a project where a large number of standpipes (every 5 m along the wall) was used to record the groundwater pressure (de Doelder and Slot 2010; Berkelaar 2011), a major leak that occurred later during excavation was not found during the pumping test. This can possibly be explained by the complicating factor that during the pumping test, anomalies will still be filled with soil, with relatively low hydraulic permeability. If after excavation the soil plug in the anomaly becomes unstable under the water and soil pressures from outside the building pit, the soil plug can erode quickly, which will strongly enhance the permeability of the anomaly.

1.2 Research vision and outline

From the above it follows that, although several tools to prevent or locate leaks are available, none of them has sufficient reliability to reduce the risk profile of the diaphragm wall substantially.

If certainty has to be based upon measurements, project managers will ask for the reliability of the measurement or test. Even though each measurement could improve the insight and thus the reliability of a retaining wall, absolute certainty can never be guaranteed. To overcome this dilemma, this research has focused from the start on the combination of several, physically independent, measurement techniques. If several techniques are available, the possibility of cross checking exists. If an anomaly has been found with one technique, another technique can be utilized to verify the findings, offering a much higher reliability profile than if the interpretation of a defect is based upon only one type of measurement.

From the recent experience with leaking D-walls in metro construction in the Netherlands (van Tol et al. 2010), it is known that especially the presence of clayey material (bentonite slurry remainings) in the joint between the panels is the major cause of problems with D-walls.

The basic idea behind this research has been that leaks in diaphragm walls are areas without concrete. If the presence of concrete at critical locations within each diaphragm wall panel can be determined, the absence of leaks can be concluded and the soil and water tightness of the wall can be proven.

In autumn 2009 construction works for a 600+ parking spaces underground garage started underneath the 'Kruisplein' in Rotterdam (more information in paragraph 2.3). This project provided the opportunity to perform pilot tests. Four methods were chosen for this pilot:

- Crosshole Sonic Logging (CSL)
- Distributed Temperature Sensing (DTS)
- Electrical Resistivity (ER)
- Natural Gamma Radiation (NGR)

From those first tests, it was concluded that CSL, DTS and ER were worth further investigation.

The NGR method seemed to be unsuitable to detect anomalies in diaphragm walls because the concrete has a higher natural gamma radiation than bentonite making bentonite detection with NGR almost impossible, as explained in paragraph 2.3.

1.3 Research scope

The research will primarily focus on the detection of the quality of the joints between diaphragm wall panels (as these seem to be the prevailing weak spot in the concept), during and after installation of the panels and before excavation of the building pit takes place. Some techniques developed in the research might be suitable for other parts of a diaphragm wall but this is not investigated.

The intention is to apply existing technology in a different setting. This is a logical thing to do: first try and apply existing technology before starting something completely new. From the already known application it will be possible to estimate the success of the new application.

If possible, the measurement should have a minimal impact on the production process. It is therefore an advantage if the measurements can be executed separately from the production of the panels. Methods should be verified in the research and translated into a practical guideline for execution and interpretation. The research will not focus on other in-situ formed elements. If the findings of the research indicate that application in other elements is expected to be effective, it will be proposed in the recommendations.

This thesis is built around three measurements techniques:

- Crosshole Sonic Logging (CSL)
- Distributed Temperature Sensing (DTS)
- Electrical Resistivity (ER)

The introductory Chapters 1 and 2 provide context and a description of the pilot and reference tests.

The description of each technique, the reference and validation tests performed in the laboratory and on site can be found in Chapters 3 to 5 respectively. These chapters form the main scientific content of the thesis and correspond to journal papers, each dealing with a separate measurement technique.

The measurement techniques and the corresponding results will be discussed in Chapter 6 combining all research output and the information from projects in which (some of) the measurement techniques have been applied. The thesis concludes with conclusions and recommendations (Chapter 7).

Chapter 2 Pilot projects and verification experiments

2.1 Chronology of the research

Project experience has been an important factor during the research described in this thesis. The projects with direct or indirect involvement will appear in chronological order and, as a result, also illustrate the evolution of the research.

The events that initiated the result are listed below:

- March 2005: Leaking diaphragm wall joint during construction of the start shaft of RandstadRail Rotterdam, Netherlands
- December 2007: Leaking diaphragm wall joint in building pit of metro station 'Centraal' under construction, Rotterdam
- June and September 2008: Calamities during construction of metro station 'Vijzelgracht' Amsterdam Netherlands

Unofficial start of the research:

- September 2009: First plans to use measurements to locate anomalies in diaphragm wall of underground parking 'Kruisplein' in Rotterdam, Netherlands, intended techniques: CSL, DTS, NGR, ER

Start of the PhD research at TU-Delft (funded by Geolmpuls) January 2010.

- February-May 2010: Pilot tests: Test blocks containing known anomalies fabricated at Franki Oosterhout Netherlands
- February-May 2010: Pilot project: Full scale tests at Kruisplein, Rotterdam
- June 2010 – August 2011: Regular production measurements on more than 200 joints at 'Sporzone Delft' Netherlands
- January-April 2011: Full scale tests with DTS (4 sensors) and CSL (6 tubes) and Singel hole Sonic Logging (SSL) techniques at 'Sporzone Delft'
- May-July 2011: Large scale laboratory tests CSL and SSL test TU-Delft

- May-July 2011: Laboratory tests DTS TU-Delft
- June 2012: After excavation of tunnel 'Spoorzone Delft', an anomaly was discovered at a location indicated with CSL. This anomaly had been repaired with jetgrout based upon the CSL results: confirmation of the method
- Oktober 2012: CSL measurements A2 Maastricht, Netherlands
- June 2013: CSL measurements dry dock 'Oceanco' Alblasserdam, Netherlands
- September 2013: CSL measurements adaptation railway bridge foundation Deventer, Netherlands
- September 2013-April 2014: DTS and CSL measurements in two test panels in the 'Spoorzone Delft' railway tunnel project (see also van Dalen 2015)
- November 2013: CSL measurements adaptation railway bridge foundation Nijmegen, Netherlands
- April-May 2014: Electrical conductivity measurements TU Delft

For a more consistent structure of this thesis, the projects or laboratory tests described in this chapter include:

- the pilot tests that form the basis of this research
- the validation and/or calibration tests that aim to define the detection limits of the measurements.

These projects and tests will be described in detail in the chapters describing the CSL, DTS and ER methods.

Projects where (mainly CSL) measurements were executed after January 2012 are considered to be 'regular production projects'. These projects contribute to the proof of applicability and have supplied useful information for future projects. Because the majority of the lessons learned from these projects are discussed in Chapter 6 the project descriptions can be found in that chapter as well.

Exceptions are:

- the 'Spoorzone Delft' project, which was a very early production project with some experimental components as well: this project is described here
- the electrical conductivity measurements: even though these tests were late in the research chronology, they are an essential part of the ER method and will thus be described here

2.2 Pilot test Franki Oosterhout

When in 2009 the test plan for the pilot field test at Kruisplein was designed, Crosshole Sonic Logging (CSL), Distributed Temperature Sensing (DTS), Electrical Resistivity (ER) and Natural Gamma Radiation (NGR) were foreseen as the measurement techniques to be used.

Of these measurements, CSL, DTS and NGR could be tested in advance using a large scale lab experiment.

To this end, in cooperation with Franki Grondtechnieken, two sets of test blocks were cast.

The aim of these blocks was to detect, a bentonite anomaly included at the casting joint between the two sections of each test block.



Figure 2: Test block casting

The blocks were cast in two halves. After curing of the first half, the joint casting form was removed. Glass fibers were installed in the casting joint. The glass fibers were covered with a bentonite volume with increasing thickness covering the fibers. The concrete of the second half of the test block was as a result cast over the temperature sensing fibers and (in part) over the bentonite covering the fibers. From to distribution of the recorded temperatures in time during the heat generation of the curing of the second

half of the test block, it was concluded that the thickness of a bentonite volume shielding the concrete from the sensor, could be estimated (Doornenbal et al. 2011). Monitoring of the casting process using DTS had not yet been thought of at the time. The blocks were equipped with PVC tubes to facilitate CSL measurements.

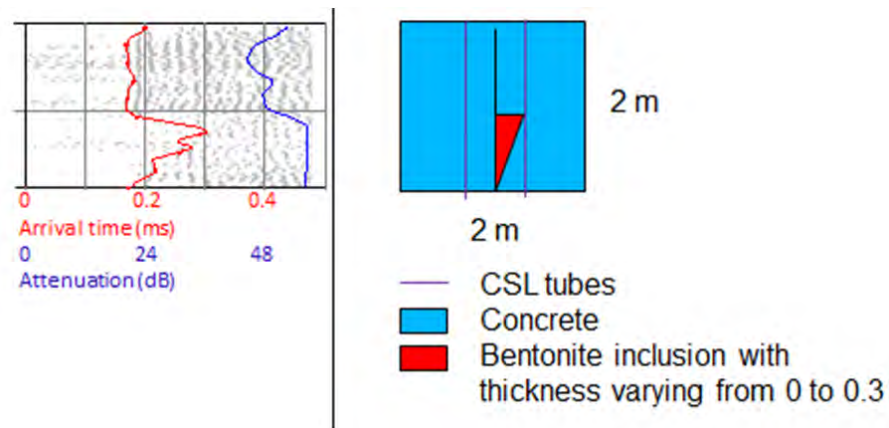


Figure 3: Correlation CSL with bentonite inclusion dimensions (first cast half on the left, second half on the right)

Figure 3 shows a simplified cross-section of one of the test blocks (on the right side) and the resulting CSL log across the inclusion. From the CSL measurements it was concluded that it should be possible to detect bentonite inclusions and even estimate the volume of the inclusion as the size of the known inclusion seemed to have a correlation with both first arrival time (FAT, red line in the graph) and attenuation (blue line in the graph). The two test blocks included only inaccessible inclusions (one with pure bentonite, the other with a sand-bentonite mixture). Based on these tests it was recommended that different types of inclusion material in the same anomaly shape should be tested.

2.3 Pilot project Kruisplein Rotterdam

After leaking joints had occurred in several underground constructions (Amsterdam, metro station 'Vijzelgracht'; Rotterdam, metro station 'Centraal Station' and start shaft of the Randstadrail tunnel), the project manager of the planned underground parking 'Kruisplein' was worried. The retaining walls of the 'Kruisplein' garage would also be constructed with diaphragm walls and the garage was planned to become the deepest building pit in the Netherlands, reaching into the sand layer (at 20 m below surface level) that provides the deep foundation for all adjacent buildings at close distance. Due to the combination of large depth (and large water pressure), excavation level in a sand layer and adjacent buildings founded in that sand layer, the project was considered to have a high risk profile.

Therefore several extra quality checks were included in the contract and it was considered worthwhile to investigate the possibilities for early detection of anomalies in the D-walls. It was accepted that the outcome of the investigations would not be directly beneficial to the project, apart from having an extra quality check based upon a few samples. The fact that such an investigation would take place during construction might already motivate the (sub-) contractor to deliver a high grade product. The Author proposed 4 different tests, each to be executed on 4 test joints (the project included a total of 60 joints)(Spruit 2011).

The tested principles were:

- Distributed temperature Sensing (DTS)
- Crosshole Sonic Logging (CSL)
- Electrical Resistivity (ER)
- Natural Gamma Radiation (NGR)(Spruit et al. 2011)



Figure 4: Top of diaphragm wall just before demolishing top meters, note the CSL tubes

The most important findings of this pilot were:

CSL:

The measurements are fast to carry out (about 30 minutes for one joint, consisting of 6 scans over 42 m). It is possible to glue PVC pipe sections together (using PVC sleeves) during connection of two sections of rebar grid. PVC tubes offer better handling on site and better signal in the measurements compared to steel tubes, no debonding between tube and concrete was noticed.

One anomaly was seen in the logs and also verified after excavation of the building pit (see 3.8.1).

From the above it was concluded that CSL seems to be the most promising method because of the combination of low cost, minimal interference with the production process and perceived high resolution and reliability of the measurements. It was decided that CSL was worth further investigation. In

Chapter 3 a detailed description of the method and the executed validation and site tests can be found.

DTS:

The measurements are not really useful for determining the concrete grade based upon curing temperature as this temperature is mainly governed by the heat conductivity properties of the surrounding soil (see Figure 36).

It is possible to monitor the concrete casting process much more accurately than expected. It is recommended to already start the measurements before slurry refreshing.

DTS sensors are much less vulnerable than expected, only 1 out of 20 failed.

DTS looked very promising for quality control during production. The detection limits of the DTS method and the impact of the measurements on the installation process have been explored during the research described in Chapter 4 of this thesis.

ER:

In this pilot the electrical method was used with two electrodes (see Chapter 5 for a more detailed description) and was not convincing in detecting anomalies. The method seemed worth further effort based upon theoretical response and positive experience in Taipei (Hwang et al. 2007). Also the measurement seemed to be the ideal confirmation tool if one (or two) other measurements would give rise to discussion.

Finally the fact that no measurement equipment needs to be installed in the wall in advance makes this method attractive for situations where initially no measurements were anticipated but production of the panels indicated a lower than usual quality standard. In Chapter 5 the research into the detection limits of the ER method in the application to detect anomalies in diaphragm walls is described.



Figure 5: Rebar cage with PVC tubes at connecting height of two sections

NGR:

It was expected that the clay minerals in the bentonite would generate a detectable natural gamma radiation. Bentonite inclusions were expected to be present at positions with relatively high detected gamma radiation. However, it was not possible to determine any consistent contrast with gamma radiation detectors lowered into the PVC access tubes. After analyzing the radiation properties of the concrete that had been applied in the walls, it came out that the concrete was more radioactive than the

30

bentonite, making detection of relatively small volumes of bentonite using natural gamma radiation almost impossible (Spruit et al. 2011). Therefore, this method has not been studied further during this research.

2.4 Spoorzone Delft

Immediately after the first interpretations of the Kruisplein and Oosterhout pilot tests, the Author presented the results at the 'Spoorzone Delft' project. At that time the Combinatie Crommelijn (CCL) contractor cooperation, responsible for both the design and the construction of the railway tunnel through the center of the historic city of Delft (Netherlands), was confronted with the city authorities being very reluctant to agree on the type of retaining wall. The proposed diaphragm wall had just before caused severe settlements of historical buildings in Amsterdam. The city of Delft wanted guarantees on the quality of the walls.

Right at that time, the preliminary results from this research offered simple to implement (CSL) and to be expected accurate information on the quality of the diaphragm walls. The contractor decided, based upon these findings, to examine with CSL all joints between the diaphragm wall panels that were closer than 5 m from adjacent buildings.

Apart from the large scale testing of the joints (more than 200 joints), a separate test site of ten additional test joints was facilitated. Here, the CSL measurements were extended with 6 instead of 4 tubes per joint and Single-hole Sonic Logging (SSL) was experimented with. With the SSL method, the same ultrasonic source is used as with CSL, but the receiver is placed above or below the source in the same measurement tube. The ultrasonic signal that spreads out from the source will be reflected on interfaces with high contrast in acoustic impedance (Paikowsky et al. 2000). Low reflection intensity was expected to indicate a good quality joint, whereas high reflection intensity would be indicating an inclusion of soft, low density material.

DTS measurements were executed during the slurry refreshing and concrete casting phases.



Figure 6: Panel after concrete casting, showing the CSL tubes and the DTS sensors

The most important findings of this field survey were:

DTS:

Slurry (bentonite) refreshing can be monitored using DTS, as well as concrete casting. The level of the interface between excavation bentonite and fresh bentonite and the level of the interface between bentonite and concrete can be monitored with an estimated accuracy of about 5 cm.

To achieve the above mentioned accuracy, a minimal latency of the sensor combined with fast read out with the DTS device should be implemented.

Using simulation of the temperature response based upon the device characteristics and the known temperatures of the media, the accuracy of determining the level of an interface can be significantly improved (see Figure 40 and Figure 47).



Figure 7: Joint between a cast panel and an excavated panel, just before concrete casting (showing a total of 6 CSL tubes)

CSL:

The measurements in this project were executed by Brem Funderingexpertise BV. The Author was involved with the interpretation of the measurement results. For one location the Author advised to execute repair works with jet grouting, which was executed by the contractor. After excavation of the building pit, the anomaly showed up exactly at the depth as expected from the CSL measurements.

CSL showed to be a very effective tool for testing the quality of the joints. There were only 2 joints out of a total of 250 joints that contained clear anomalies. Only one anomaly was considered severe enough to repair based upon the CSL results. This was a very positive result as many had feared that the measurements would not be unambiguous and would give a lot of false alerts, causing delay in the project execution.

6 measurement tubes do not offer a significantly better interpretation compared to 4 tubes. The extra tubes in the center may obstruct the

concrete flow and offer hardly any extra information compared to the diagonal scans of a 4 tube setup.



Figure 8: CSL testing (Brem Funderingsexpertise BV) at 'Spoorzone' Delft

SSL:

Single hole Sonic Logging showed no consistent results in the field tests.

ER:

At the two doubtful locations, a two electrode Electrical Resistivity measurement with a two-electrode setup has been tried. Both locations did not show convincing results.

2.5 Laboratory tests at TU Delft

After the first positive results from the tests in Rotterdam and Oosterhout, it was decided to make test objects that would provide the possibility to send the ultrasonic signal through different anomaly materials. With the resulting delay and damping characteristics per material type, it might be possible to determine the size and material in the anomaly. To reach this objective, test blocks were made with a wedge shaped opening in the middle, as depicted in Figure 12 and Figure 13. The anomaly was accessible from the top side of the test object. Concrete casting took place in a casting form (without bentonite). The joint did not include rubber water slots to focus on the influence of the fill material only.



Figure 9: Concrete casting of the one of the test objects

As a result, the anomaly could be filled with different materials. In Chapter 3 the results are described in detail.

CSL devices from three different manufacturers (PileTest 2015, Pile Dynamics Inc 2015, Olson Instruments 2015) were used. The source and

receiver differences between the devices are limited. The software behind the measurements is rather different. PileTest has the best performing autogain function and FAT-picking algorithms for the application in diaphragm walls. This company was at the time of testing also the only one that offered a raw (unprocessed data) export option in the software. The other companies offered this option on request.



Figure 10: Smooth finishing of the top of the test object

Due to the more effective autogain and FAT-picking algorithms, the measurements obtained with the PileTest CSL device provided the easiest interpretation.

The test blocks were also subjected to SSL tests from the PVC tubes situated in the center of the test blocks on both sides of the anomaly. Even the very well defined anomalies in the laboratory test block could not be located using SSL, leading to the conclusion that SSL is unsuitable in this application. The SSL test results have been studied further by Palm (2012) coming to the same conclusion. The SSL method has therefore not been studied further during the research presented in this thesis.

After completion of the CSL tests, the blocks were reserved for future ER tests (paragraph 2.6).

Also the DTS characteristics were tested in the laboratory, as described in detail in 4.5.

2.6 Test Electric conductivity TU Delft

Because of the difficulties encountered during interpretation of the field results in Rotterdam and Delft, it was decided to investigate the influence of electrode distance to the diaphragm wall and to optimize the test setup.

To this end the test blocks that were cast for the CSL validation, were setup to form a continuous wall in a water basin. The anomalies that were included in the test blocks were submerged in the water. With numerous electrode variations, the detection limits for the Electrical Resistivity (ER) method were explored. The description of this test is elaborated in Chapter 5 To detect anomalies in diaphragm walls with apparent resistivity measurements.

A time-lapse movie of the construction of the test can be watched at: <https://www.youtube.com/watch?v=BGZg0OkgcW8>

A time-lapse movie during testing can be watched at: <https://www.youtube.com/watch?v=ZYpGwPTEFIk>



Figure 11: Test setup overview (looking north-east)

Chapter 3 Detection of anomalies in diaphragm walls with Crosshole Sonic Logging¹

3.1 Abstract

Crosshole Sonic Logging (CSL) can be used to determine the quality of joints in a diaphragm wall. Tests conducted on laboratory models have provided reference information for interpretation of field data. During two large construction projects CSL has been implemented for quality control of diaphragm walls. The field experiences have shown the benefits of the tests and the predictive value of the reference measurements.

Key words: Crosshole Sonic Logging, CSL, diaphragm wall, joint, quality control

3.2 Introduction

Diaphragm walls are frequently used for deep underground constructions in densely populated areas because of their high strength and stiffness in combination with silent and vibration-less installation. Quality control for the water tightness and retaining functions has proven to be difficult, as calamities during construction works in the Netherlands and Belgium have shown (Van Tol et al. 2010; Berkelaar 2011; Van Tol and Korff 2012). Other examples of underperformance have been reported in Boston (Poletto and Tamaro 2011), Cologne (Sieler et al. 2012) and Taipei (Hwang et al. 2007). The poor quality or even absence of the concrete in the joints between the

¹ This chapter has been published as an article in Canadian Geotechnical Journal (CGJ) 2014, 51:369-380, 10.1139/cgj-2013-0204 (Spruit et al. 2014). The article was awarded the 'Editor's Choice' designation and has unlimited free access to the pdf file through CGJ's website. Minor improvements were made in the final editing of this manuscript.

diaphragm wall panels is the primary cause of these calamities (Van Tol et al. 2010).

It was therefore decided to investigate the possibilities to detect anomalies in diaphragm walls, particularly in the area around the joints between the panels, prior to excavation of the building pit enclosed by the diaphragm walls. Experiments during the construction of an underground parking facility in Rotterdam (Spruit et al. 2011) showed promising results for Crosshole Sonic Logging (CSL) and Distributed Temperature Sensing (DTS) (Doornenbal et al. 2011; Spruit et al. 2011). The CSL results demonstrated that good quality joints could be distinguished from poor quality joints. Furthermore, the position of local anomalies could be determined. Test models in an experimental set-up indicated a linear correlation between the size of the anomaly and the increase of arrival time in the CSL. Nevertheless, determining the type of material in the anomaly appeared to be difficult (Spruit et al. 2011).

To improve the interpretation of the CSL and to better determine the type of material in the anomaly, two test blocks were made in which a wedge shaped 'defect' was subsequently filled with different materials. The objective was to test the 'defective' joint several times with different types of material, in order to determine the change in CSL signal per material and allow for interpretation of the material in an anomaly encountered in the field.

3.3 Crosshole Sonic Logging

Crosshole Sonic Logging (CSL) is widely used for integrity testing of large diameter bored piles (Likins et al. 2007; ASTM 2007; ASTM 2008). The measurement is primarily based upon the physical phenomenon that the density and stiffness of the medium determine the velocity of an acoustic wave in a medium. According to Ihara (2008), for the longitudinal (p-wave) wave velocity (v_l) in a homogeneous, isotropic solid it holds:

$$[1] \quad v_l = \sqrt{\frac{E}{\rho} \cdot \frac{1-\nu}{(1+\nu)(1-2\nu)}}$$

in which E is Young's Modulus, ρ is the density and ν is Poisson's ratio. The first arrival time (FAT) is the most important parameter during CSL interpretation. Because of the higher wave velocity of longitudinal waves

compared to transversal (shear) waves, the FAT is related to the direct longitudinal waves.

The second parameter used in CSL interpretation is the attenuation of the signal (Likins et al. 2007). This is qualitatively assessed by recording the energy at the receiver for a preset time after the FAT. Apart from geometric attenuation of the signal, the signal is attenuated by reflection on interfaces between materials and by absorption. The amount of reflected (R) and transmitted (T) energy on an interface is determined by the difference of acoustic impedances (z) of the materials on both sides of the interface (Ihara 2008).

$$[2] \quad z = \rho \cdot v_l$$

$$[3] \quad R = \frac{z_1 - z_2}{z_1 + z_2}$$

$$[4] \quad T = \frac{2 \cdot z_1}{z_1 + z_2}$$

With equal acoustic impedance on both sides of the interface, the entire signal is transmitted and no reflection occurs. According to eq.[3] reflection increases and (eq.[4]) transmission decreases with increasing difference in acoustic impedance. If, instead of concrete with high stiffness and density, an inclusion of soil is present, according to eq.[1] the velocity of the acoustic waves will decrease and the transmitted signal will decrease following eq.[4].

By using preinstalled PVC or steel (Likins et al. 2004) access tubes in the element to be tested, the acoustic source and receiver can be positioned within the element, making it possible to perform the measurement very locally. As a result, depending on the number of measurement tubes and the distance in between them, high-resolution information can be obtained. According to Amir and Amir (2009) about 1/3 of the tube spacing can be regarded as the limit for detectable anomaly size for typical anomalies in an auger pile.

The CSL technique has to some extent been applied in diaphragm walls to determine the bulk concrete quality of the panel itself (Vié 2004; Horb 2005; Mendez et al. 2012). Recently the CSL technique has also been used on a test block in which a secant pile wall was simulated (Niederleithinger et al. 2010), from which the authors conclude that detection of anomalies should

be possible. According to Mendez et al. (2012) the quality of the vertical joints between adjacent wall panels cannot be assessed by CSL because joints with bentonite deposits prevent high frequency stress wave propagation. Test measurements by Spruit et al. (2011) however, have shown that CSL testing across diaphragm wall joints can be performed with useful results.

The geometry of the anomalies in diaphragm wall joints is often vertically elongated, parallel to the joint. Thus signal energy, other than with small defects in drilled shafts, will not just bypass the anomaly with minor effect on the CSL results. It is therefore expected that applying CSL across a diaphragm wall joint will allow detecting the thicknesses of non-concrete material in the joint even smaller than the above mentioned 1/3 of the tube spacing.

3.4 Test models

Because the diameter of the tubes used to introduce the source and receiver in the element cannot be scaled down, considering the sensor size of the available equipment, scaling down the test model was not a practical option. Therefore the wall thickness of the model was chosen one meter, which is a relatively common wall thickness for diaphragm walls. To eliminate the influence of the boundaries of the model, on both sides of the joint (which is in the middle of the block) 1 m of wall has been included, see Figure 12. The height of the test model was 2 meters to facilitate enough space for a reference part without anomalies and a part, which includes an anomaly. Two (double) test blocks were made. Both had an open-ended wedge shaped anomaly that could be filled with different materials. As a result of the wedge shaped form, the influence of the gradual increase of anomaly size on the CSL signal could be determined.

The first model incorporated a flat joint along the wedge (see Figure 12), the second model (see Figure 13) had a trapezoidal shaped joint along the wedge, similar to often used shapes of the stop end. On both sides of the joint 3 PVC tubes with 50 mm diameter were attached to the rebar cages. PVC tubes offer better signal to noise ratio when compared to steel access tubes (Linkins et al. 2004; Spruit et al. 2011). The PVC tubes have been filled with water prior to concrete casting to prevent debonding between tubes and concrete (Linkins et al. 2004). Debonding would prevent proper signal transmission (Adams et al. 2009). The position

of the reinforcement and the tubes is depicted in Figure 12 and Figure 13 as well.

Tests have been performed with subsequently water, saturated sand, saturated gravel and bentonite suspension with 40 kg/m^3 bentonite/water in the wedge. This sequence was followed for convenience of filling the defect, the results with water and bentonite in the anomaly will be reported first though.

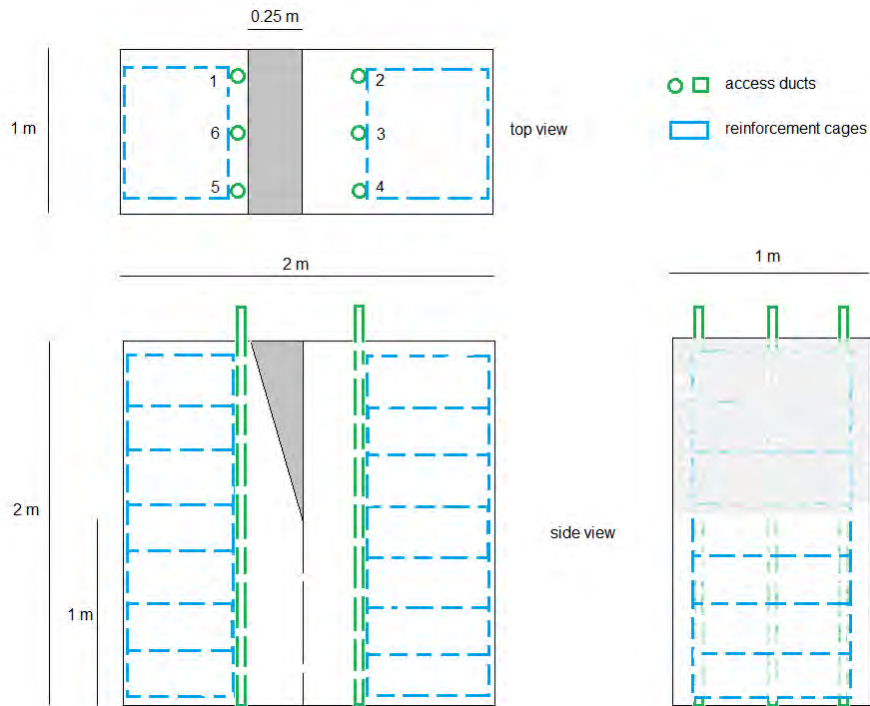


Figure 12: Test block 1 with flat joint profile

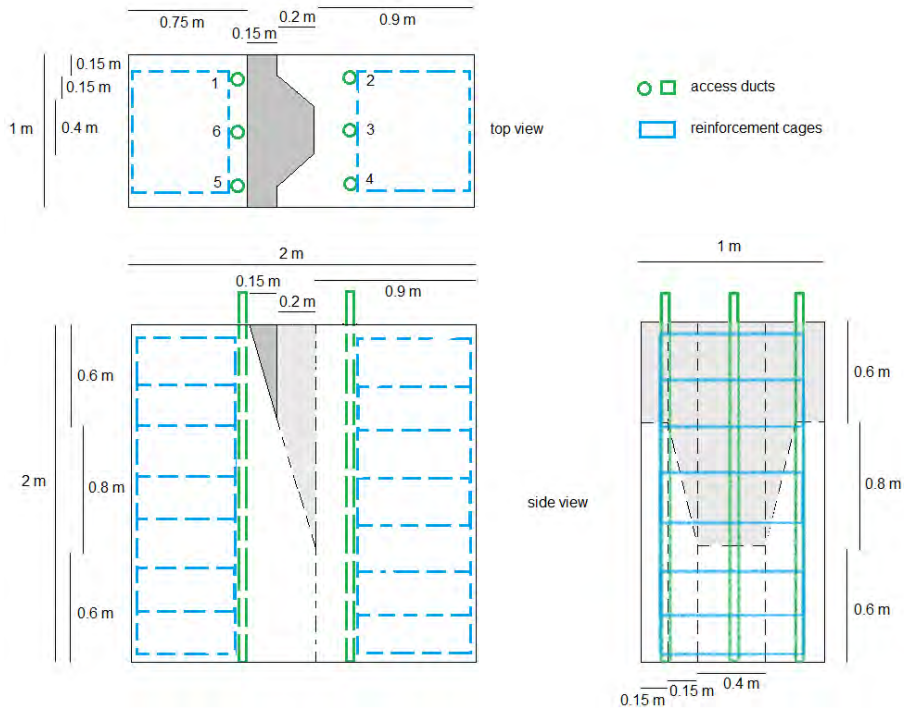


Figure 13: Test block 2 with trapezoidal shaped joint profile (dark grey: outcropping anomaly, light grey: anomaly only inside the test block)

3.5 Results from the test models

In order to investigate the influence of different brands of commercially available test equipment, devices from three different manufacturers were used on the test models. On a generic level these devices are comparable. All do use signal frequencies between 40 and 80 kHz and sample the received signal with a frequency of 500 kHz or higher (Table 1). In this paper the discussion of the results will focus primarily on the similarities of the three devices. Where appropriate, differences will be indicated.

Table 1: Key properties of the different test equipment

Manufacturer	Source frequency	Sample frequency
A	55 kHz	500 kHz
B	75 kHz	1 MHz
C	50 kHz	500 kHz

Results from an earlier investigation (Spruit et al. 2011) already indicated a linear correlation between the size of the anomaly and the increase of arrival time. In the study presented here this linear correlation has been confirmed. The propagation velocity and tube spacing are both known. Additionally, the wave velocity in concrete can be confirmed in the section of the model without anomaly. Because the size of the anomaly is known and the delay in arrival time caused by the anomaly has been measured, it is possible to determine the wave velocity of the different materials in the anomaly.

In Figure 14 to Figure 17 image-scale plots (sometimes named ‘waterfall plots’) of the measurement from the central tubes from test block 1 (from tube 3 to 6 see Figure 12) are shown. The central location was chosen as this contains the least influence of the sides of the test block. An image-scale plot shows the amplitude of the measured signal. In this case middle grey is neutral (meaning zero) signal, whereas white is maximum positive amplitude and black is maximum negative amplitude.

In addition to the image-scale plot, the first arrival time (FAT) interpreted by the measurement software of equipment set A has been plotted with black diamonds on the same scale as the waterfall plot (microseconds). The attenuation determined by equipment set A is shown with grey squares on a Decibel (dB) scale. It is clear that both FAT and attenuation increase with increasing anomaly dimensions.

The lower halves of Figure 14 to Figure 17 show the part of the test block without anomaly. Both FAT and attenuation are almost constant.

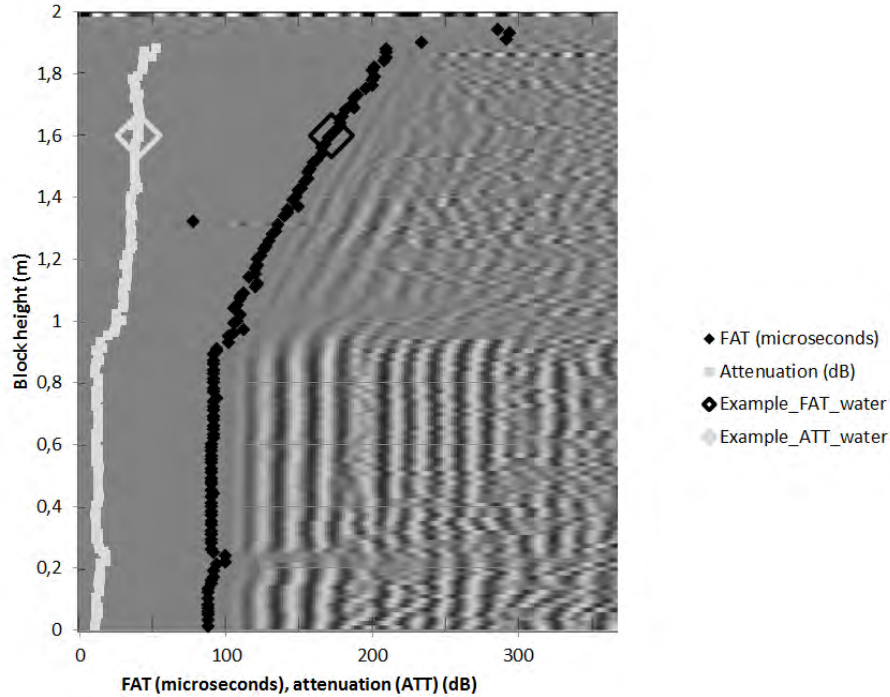


Figure 14: CSL results for an anomaly filled with water

The upper halves of Figure 14 to Figure 17 show how the signal is affected by the anomaly filled with water (Figure 14), bentonite (Figure 15), saturated sand (Figure 16) or saturated gravel (Figure 17). Figure 14 and Figure 15 show that the signal passing through the anomaly stays clearly visible up to the maximum anomaly width of 0.25 m. FAT and attenuation can be determined relatively easy.

In each Figure example points are defined, of which the numerical values have been presented in Table 2. The example from Figure 14 has been recorded at a block height of 1.6 m. The geometry of the test block (Figure 12) defines the corresponding anomaly width at that specific position: 0.17 m. The measured FAT is 172 microseconds. The average FAT in the lower half of the test block during the test with the water filled anomaly was 91 microseconds. The anomaly with 0.17 m width has caused a delay in arrival time (DAT) of $172 - 91 = 81$ microseconds.

In the same way the attenuation can be interpreted, as shown in Table 2.

Although the FAT and attenuation in the lower half of the test block vary slightly between the different measurements, the average values without anomaly are 90 microseconds for the FAT and 13.5 dB for the attenuation. The examples for each material in Figure 14 to Figure 17, each having their own sign in the Figures (diamond for water, square for bentonite, triangle for saturated sand and cross for saturated gravel), are re-used in Figure 18 and Figure 20.

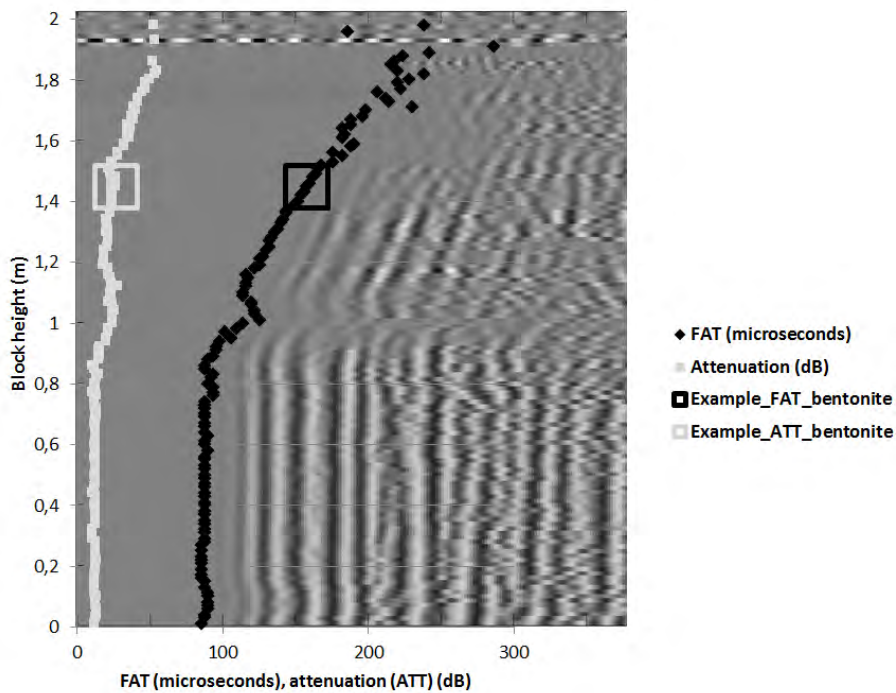


Figure 15: CSL results for an anomaly filled with bentonite

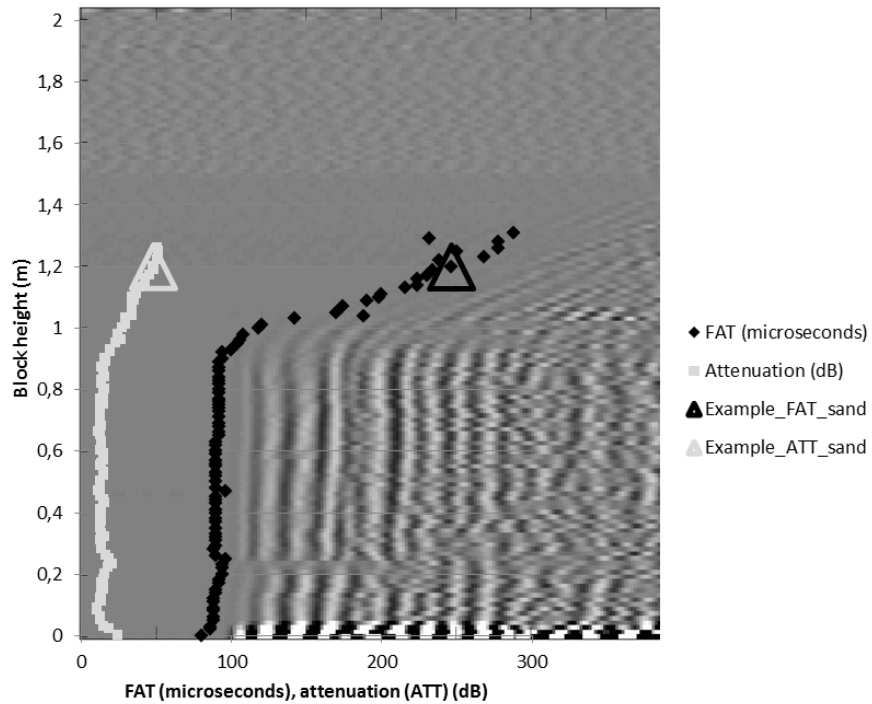


Figure 16: CSL results for an anomaly filled with saturated sand

Figure 16 and Figure 17 show that the signal passing through the anomaly filled with saturated sand (Figure 16) or saturated gravel (Figure 17) deteriorates quickly with increasing anomaly width. Fat and attenuation can only be determined up to an anomaly width of about 0.15 m.

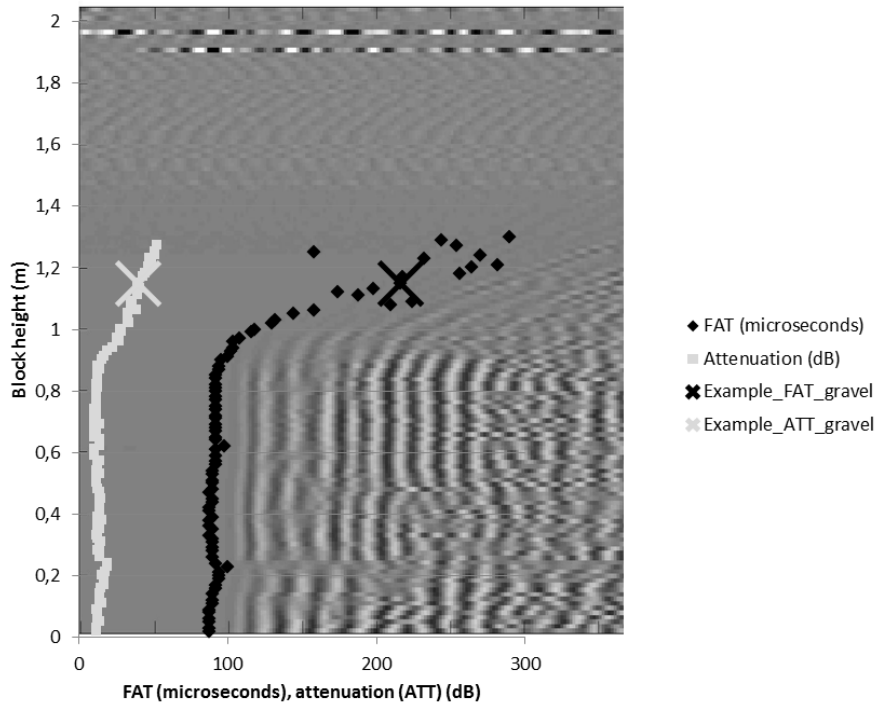


Figure 17: CSL results for an anomaly filled with saturated gravel.

Table 2: Examples showing the conversion from block height to anomaly width and FAT / attenuation to the additional values caused by the anomaly (measurements block 1)

Example	Block height (m)	Anomaly width (m)	FAT (microseconds)	DAT (microseconds)	Attenuation (ATT) (dB)	Additional attenuation (dB)
Water	1.60	0.17	172	81	40	27
Bentonite	1.45	0.13	158	70	27	14
Sat. sand	1.20	0.07	246	156	48	34
Sat. gravel	1.15	0.06	216	125	40	26

Figure 18 has been constructed using the anomaly width versus DAT data of all measurements, as illustrated with the example measurements presented in Table 2. The R^2 values indicated in Figure 18 all confirm a high level of linear correlation between anomaly width and FAT.

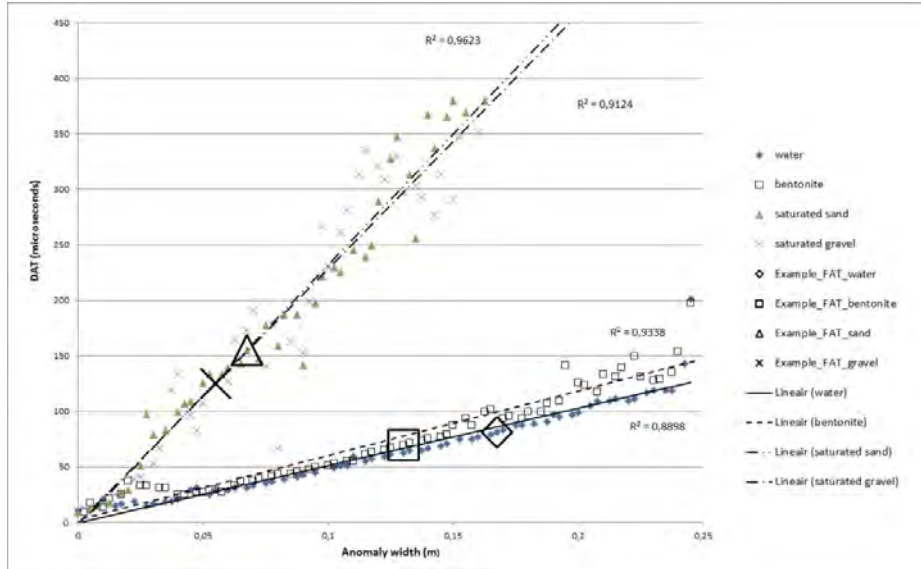


Figure 18: Delay in arrival time (DAT) as a function of anomaly width

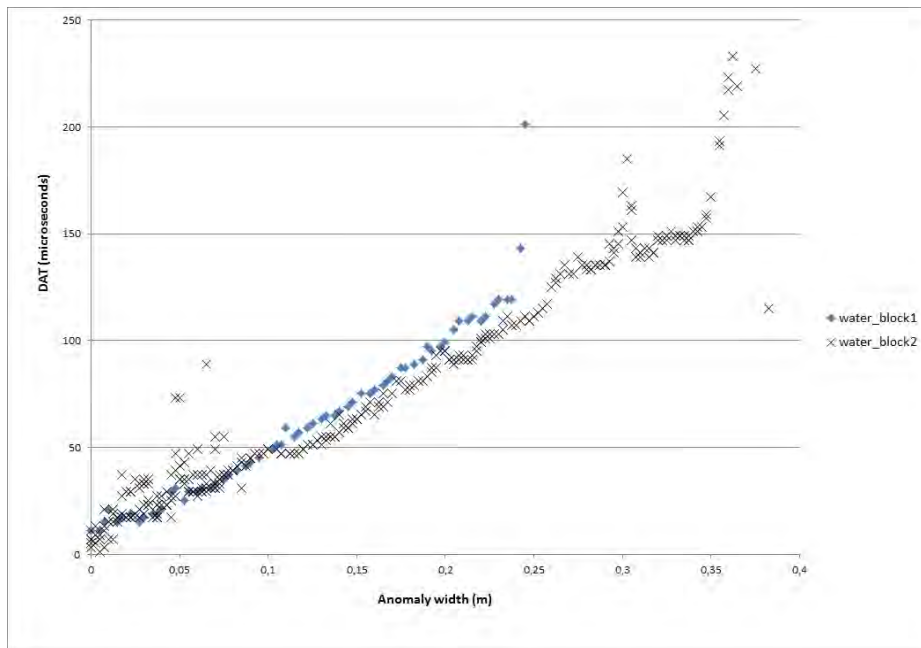


Figure 19: DAT for anomaly filled with water, comparison between blocks 1 and 2, for both blocks the measurements from tube 3 to tube 6 were used

Figure 19 shows the influence of the different geometry in the joint area on the DAT. Especially from 0.12 m to 0.28 m anomaly width, the DAT is noticeably lower for the trapezoidal shaped joint than for the flat joint, illustrating the possibility for the signal to partly pass around the anomaly through the adjacent concrete.

The additional attenuation due to the anomaly width is combined in Figure 20. The granular materials show a linear increase of attenuation (on a dB scale) with increasing anomaly width. Water and bentonite show a more complex attenuation. At narrow anomaly widths the signal loss obtained at the two interfaces (concrete to anomaly and anomaly to concrete) seems to govern the attenuation characteristics, producing almost constant attenuation, regardless of the anomaly width.

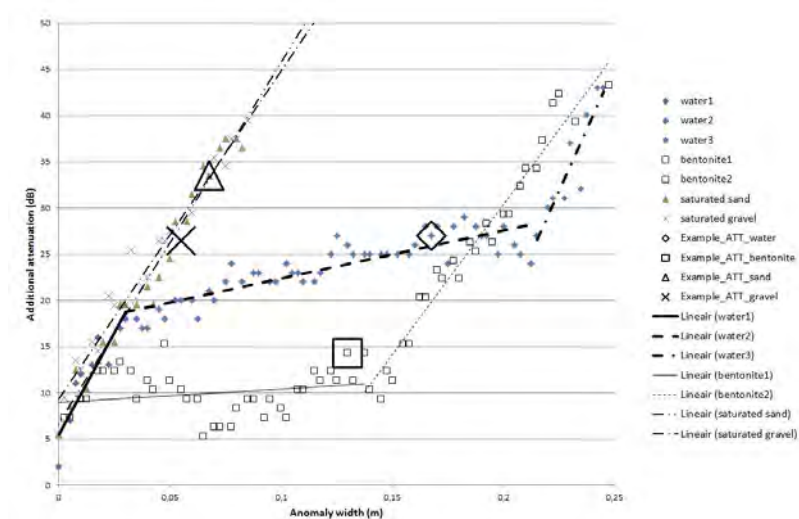


Figure 20: Additional attenuation as a function of anomaly width

3.6 Discussion

As can be seen in Figure 18, the wave velocity through water or bentonite is almost the same. The delay in arrival time caused by the water filled anomaly is 517 $\mu\text{s}/\text{m}$ and for a bentonite filled anomaly this is 578 $\mu\text{s}/\text{m}$, indicated with linear regression lines in Figure 18.

For non-granular material with high water content in an anomaly an average DAT of 550 $\mu\text{s}/\text{m}$ can be taken into account. This seems to correspond to a

wave velocity of 1800 m/s in water or bentonite. Because the anomaly replaces the concrete however, the observed extra travel time of the signal is the result of the difference in wave propagation speed between the material in the anomaly and concrete that should have been in there. If the extra travel time is corrected for this, wave propagation speed in the water filled anomaly comes down to 1432 m/s, which is close to the known average wave propagation speed in water of 1500 m/s.

The influence of the signal travelling partly through the concrete to a larger depth where the anomaly has a smaller width, and as a result slightly reduces the perceived width of the anomaly, is in this case limited to less than 3%.

As can be observed in Figure 15, from 0.95 to 1.1 m block height extra signal loss occurred in the test with bentonite. This can be explained by gravel and sand particles remaining from the previous tests in the same anomaly.

Figure 16 and Figure 17 show that sand and gravel filled anomalies are hard to distinguish from each other. They can, however, be discriminated from bentonite and water filled anomalies quite easily. The signal loss in case of granular material is so high that even with a 0.1 m wide anomaly it is very hard to determine the first arrival time of the signal. At a 0.15 m anomaly width practically no signal is picked up in the receiving tube. This means that if in a field situation the signal is almost completely lost, there is a high probability that there is an anomaly containing sand or gravel with a width of 0.15 m or more measured in the propagation direction of the waves.

The attenuations (Figure 20) are rather similar when comparing sand and gravel filled anomalies. Both filter a fixed amount of energy and a complementary amount depending on the width of the anomaly. Because of the similarity in FAT and attenuation, the results for gravel and sand filled anomalies are taken together in the résumé of the CSL results.

The additional attenuation as a function of anomaly width is formulated in Table 3.

Table 3: Résumé of the CSL results

Material	Maximum detectable thickness	DAT (ms/m)	Additional attenuation (dB) as a function of width w (m)
Water	>350 mm *	517 μ s/m	$444*w + 5$ if $w < 0.03$ ($R^2=0.82$) $52*w + 17$ if $0.03 < w < 0.2$ ($R^2=0.77$) $535*w - 88$ if $w > 0.2$ ($R^2=0.84$)
Bentonite	>350 mm *	578 μ s/m	10 ± 5 dB if $0 < w < 0.15$ ($R^2=0.05$)*** $325*w - 35$ if $w > 0.15$ ($R^2=0.96$)
Saturated sand or gravel **	<150 mm	2325 μ s/m	$8+373*w$ ($R^2=0.97$)

* 350 mm was the largest aperture of the anomaly in the test blocks

** Results for sand and gravel filled anomalies have been averaged

*** The R^2 value for bentonite $0 < w < 0.15$ shows almost perfect randomness with linear function $14.5*w + 9$. However, all attenuation is in the range of 10 dB plus or minus 5 dB.

During the interpretation of field test results it is advised to primarily use the FAT to identify suspect areas. The amount of deviation defines the width of the anomaly in the joint. As soon as a local deviation from the average FAT is encountered, the attenuation behavior, combined with the FAT can be used to derive the granular or non-granular material in the anomaly.

3.7 Frequency domain analyses

When converting the collected data from time to frequency domain, a loss of high frequencies in an area with an anomaly would be expected. Damping behavior of materials in an acoustic application (McDaniel and Dupont 2000) leads to the assumption that in the anomaly mainly the high frequency components of the signal will be lost. The results from the test blocks however do not show a clear shift to lower frequencies. On the contrary: it seems that with equipment set A a slight shift to higher frequencies occurs with water and bentonite in the anomaly in block 1 (shift to the right in the

upper part of Figure 21), combined with a higher degree of high frequency noise.

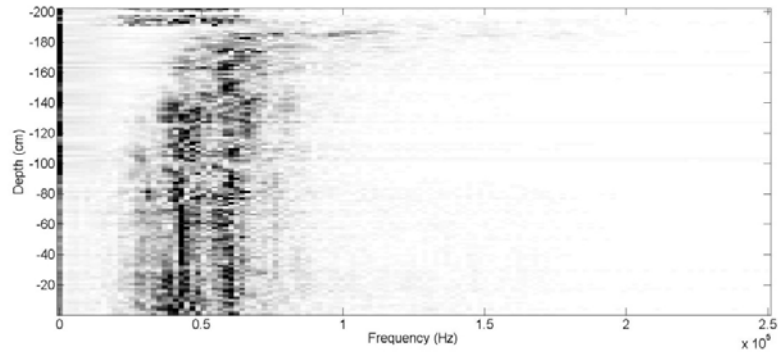


Figure 21: Frequency result through bentonite (equipment A). Greyscale indicates the relative energy after Fourier transformation

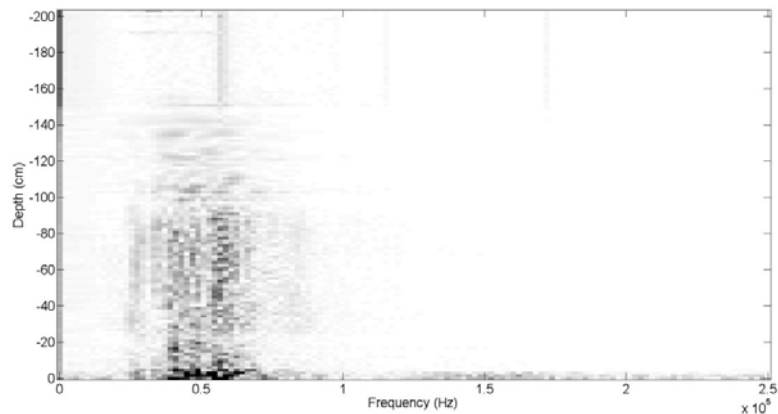


Figure 22: Frequency result through saturated sand (equipment A).

With the anomaly filled with (saturated) sand (Figure 22) or gravel, the frequency analysis becomes almost impossible because as soon as the anomaly has reached a thickness of more than 0.15 m, almost no signal is picked up. Only some very narrow banded remnants of the source frequency and higher harmonics remain visible in the signal of equipment A.

Equipment B shows similar behavior. The source signal has a slightly higher dominant frequency (75 kHz) and a larger bandwidth compared to equipment A (55 kHz). The signal from equipment B is lost even more in the sand. As soon as the signal encounters the anomaly, analyzing the frequency domain data becomes impossible.

When using equipment C, the lowest source signal frequencies are encountered but the signal loss in the anomaly filled with sand is similar to the other devices. The differences in the frequency domain have negligible influence on the interpretation of the time domain measurements, at least in the frequency domain of 40 to 75 kHz of the signals used.

3.8 Results from field tests

Field tests have been executed in two projects. During construction of an underground car park at 'Kruisplein' in Rotterdam in 2010 the CSL method was tested at 4 joints. Both steel and PVC access tubes were used.

During construction of a railway tunnel in Delft in 2011 the CSL method was implemented at all joints where the diaphragm wall was situated close to adjacent buildings. The contractor of the project installed steel access tubes.

3.8.1 Field results in Rotterdam

In one of the joints in Rotterdam an anomaly was detected. Figure 23 shows that the anomaly extends only in part of the cross section. The anomaly shows up in trace 1-2 but not in traces 3-4 and 2-4. In the diagonal trace 1-3 a slight distortion is noticeable.

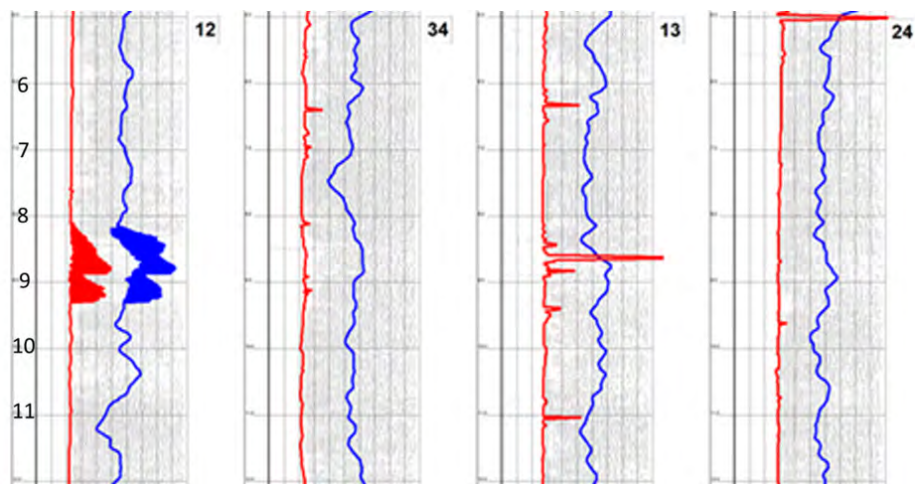


Figure 23: Four CSL results of the same joint showing an anomaly partly affecting the depth from 8.25 to 9.25 m below top level. FAT in red, Attenuation in bleu (x-scale ticks: respectively 100 microseconds, 6 dB)

Based upon preliminary lab tests this anomaly was interpreted as a bentonite intrusion of approximately $0.3 * 1 * 0.5 \text{ m}^3$ (width * height * thickness) as depicted in Figure 24. Because the anomaly did not extend through the complete cross-section of the diaphragm wall and the soil at the depth of the anomaly consisted of stiff clay with low risk of leakage, no repair works were carried out before excavation of the building pit took place.

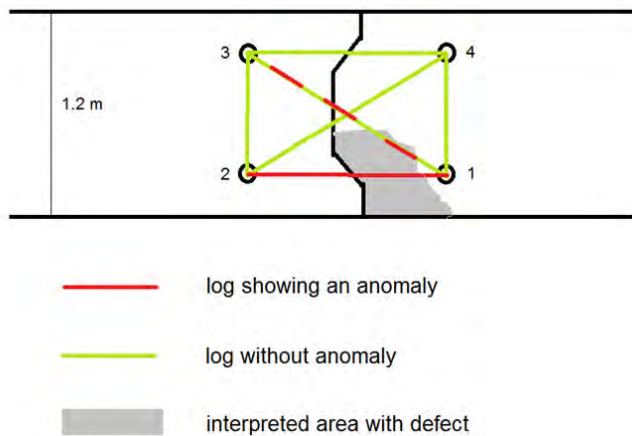


Figure 24: Interpretation of anomaly affected cross section (between 8.25 m and 9.25 m below top level)

After the excavation, the anomaly showed up on the expected location and consisted of a gravel pocket or low grade concrete with slightly larger horizontal dimensions than interpreted from the measurements. Re-examination of the original test results without filtering showed a very irregular shape of the first arrival interpretation, showing either a FAT close to the average FAT of that joint, or an extra-long FAT, see Figure 25. This more or less 'double staged' behavior of the FAT could be explained by the partly concrete / partly granular nature of the anomaly.

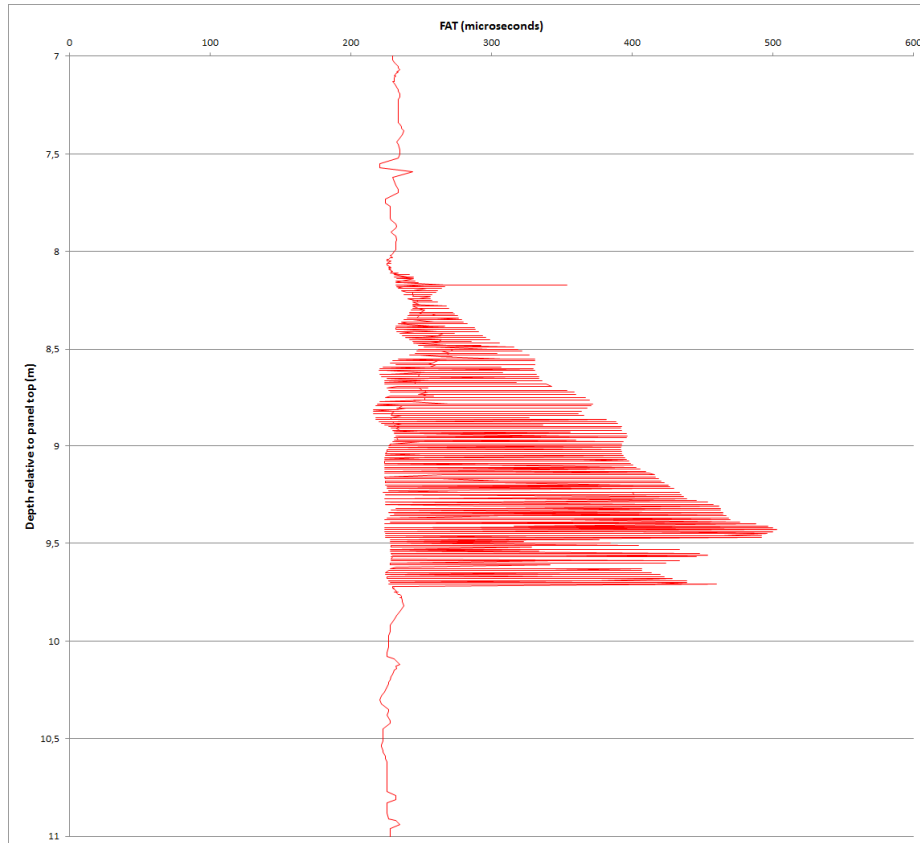


Figure 25: Zoomed part of scan 1-2 with anomaly

3.8.2 Field results in Delft

One of the tested joints in Delft showed almost absent signal over a height of 1 m (from 6 to 7 m below surface level) in 5 out of 6 logs (Figure 26). Log 34, perpendicular through the joint and log 24, diagonally through the joint, both show a clear defect between 6 m and 7 m from the top of the panel. Logs 12 and 13 are not shown but are similar to respectively 34 and 24. Log 14 (parallel to the joint) shows that the left panel (Figure 27) is even affected as far as the rebar cage onto which the access tubes are installed. The only log showing no defect is 23, parallel to the joint in the right panel.

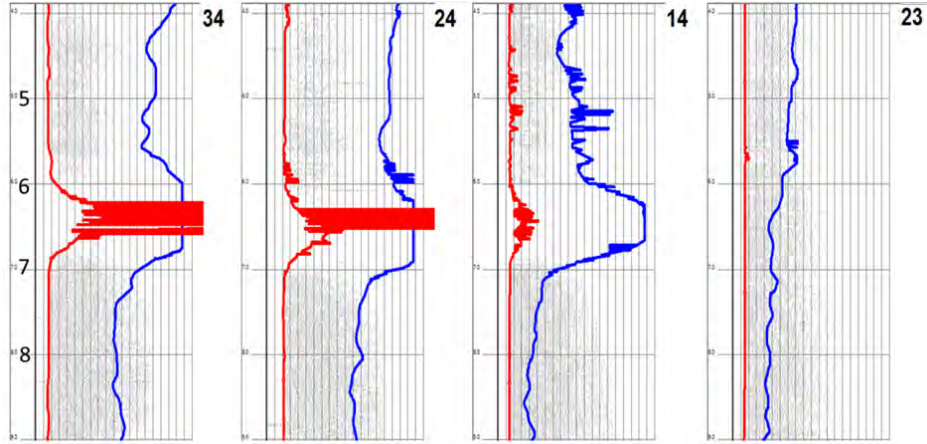


Figure 26: CSL results showing an anomaly from 6 to 7 m below reference level. FAT in red, Attenuation in bleu (x-scale ticks: 100 microseconds, 3 dB)

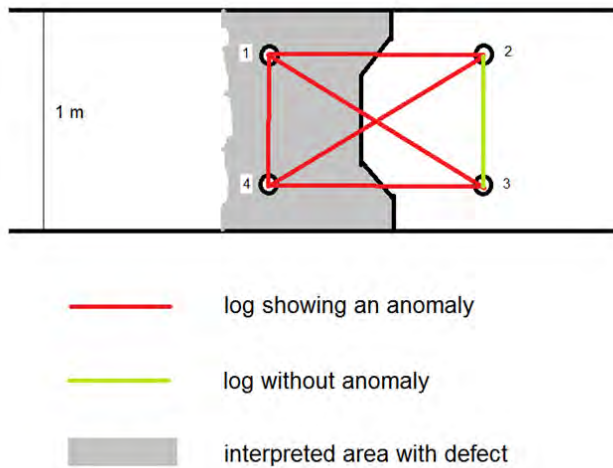


Figure 27: Interpretation of area affected by the anomaly

After comparing the characteristics of the signal to the reference measurements from the lab, it was concluded that the material in the anomaly was probably granular (sand or gravel). Due to the occurrence of the anomaly in all but one scan, it was concluded that the anomaly was situated in only one panel but did cover the full width of the diaphragm wall.

The size of the anomaly should at least be covering the measurement tubes of the affected panel as shown in Figure 27.

The soil investigations at that specific location indicated a sand layer at the same depth as the anomaly. To prevent a calamity during excavation by possible inflow of water and sand, a jetgrout column covering the height of the expected anomaly was installed on the outside of the affected joint. After the excavation the joint indeed showed an anomaly on the expected side of the joint, even showing some signs of grout from the jetgrouting that had come through the defect wall, see Figure 28.

The information about the quality of the joints between installed diaphragm walls provided by CSL, is detailed enough to make repair decisions, as has been illustrated by the two field examples.



Figure 28: Location of the sand inclusion in the Delft field case relative to the joints and panels

3.9 Conclusions

Crosshole Sonic Logging is an efficient method for determining the quality of joints in diaphragm walls. If the joint has no anomalies, this is easily recognizable from the measurements. In case of anomalies observed in the measured signal, the size of the actual anomaly can be determined quite accurately with an estimated accuracy of about 2-5 cm using the correlations shown in Table 3.

Granular material can be discriminated from bentonite or water due to the extreme signal loss that is encountered when passing through granular material. The discrimination between water and bentonite is almost impossible. Due to the method of diaphragm wall production the probability of water inclusions is very low. It seems safe enough to assume that anomalies showing similar response as water and/or bentonite contain bentonite instead of concrete.

The tests on site showed that the upper 3 meters of the panel could not be verified reliably with CSL due to low signal quality.

Steel tubes did not perform better in this respect than PVC tubes. During the tests no debonding of access tubes has occurred. The survival rate (between installation and measurement) for both PVC and steel access tubes has been around 95%.

Equipment intended for CSL integrity testing of large diameter bored piles can be used for this application without adjustments. Although there are differences in the signals used by the different manufacturers, this seems to have no significant effect on the interpretation of the results.

Analyzing the frequency domain characteristics generally does not provide useful additional information worth the effort. Considering the FAT and attenuation of the signal offers enough information for project decision-making.

3.10 Acknowledgements

The test equipment used for this paper has been manufactured by PileTest, PDI and Olson Instruments. The PileTest equipment was generously made available by PileTest and Brem Foundation Expertise. The expertise of Erez Amir of PileTest, has been highly regarded during several tests on site, in the laboratory and during interpretation of the results. Mark Bezooijen of Brem Foundation Expertise managed to provide useful measurement data in the laboratory and on site, even during harsh weather conditions. PDI equipment was provided and operated by BAM (the German governmental materials research institute) for the laboratory tests. The Olson Instruments equipment was provided by Strukton Engineering and their measurement expert Hessel Galenkamp was most helpful during the tests on site in Delft and in the laboratory.

Chapter 4 Distributed Temperature Sensing applied during diaphragm wall construction²

4.1 Abstract

Distributed Temperature Sensing (DTS) can be used to monitor the production process of diaphragm walls. DTS is able to differentiate between already present and fresh bentonite suspensions during refreshing of the bentonite slurry and excavation bentonite remaining in the trench can be observed. During concrete casting, DTS is able to differentiate between bentonite suspension and concrete. As a result, the continuity of the casting process and the arrival of good grade concrete at crucial locations in the trench can be monitored. Tests conducted on laboratory models provided reference information for interpretation of field data. Field experiences have shown the benefits of the DTS tests and the predictive value of the reference measurements. Finally, the results are compared with CSL measurements at the same location.

Key words: Distributed Temperature Sensing, DTS, diaphragm wall, joint, quality control

4.2 Introduction

Diaphragm walls (D-walls) are frequently used for deep underground constructions in densely populated areas because of their high strength and stiffness in combination with silent and vibration-free installation. Notwithstanding the extensive experience in design and construction of D-walls, quality control for both the water tightness and retaining functions has proven to be difficult, as evidenced by calamities during construction works

² This chapter is currently under review as an article for Canadian Geotechnical Journal (CGJ).

in the Netherlands and Belgium (Van Tol et al. 2010; Berkelaar 2011; Van Tol and Korff 2012). Poor quality or even absence of concrete in the joints between the diaphragm wall panels is seen as the primary cause of these failures (Van Tol et al. 2010). Other examples of below grade performance have been reported in Boston (Poletto and Tamaro 2011), Cologne (Sieler et al. 2012) and Taipei (Hwang et al. 2007).

Methods to detect anomalies in diaphragm walls are studied, particularly in the area around the joints between the panels, prior to excavation of the building pit enclosed by the diaphragm walls. CSL testing has since been verified in the laboratory and successfully implemented in several projects in the Netherlands (Spruit et al. 2014).

Distributed Temperature Sensing (DTS) is envisioned as another way of detecting anomalies.

In the DTS technique, a glass fiber which acts as a linear optical sensor is interrogated with a DTS device, delivering a continuous temperature profile along the sensor. In other engineering fields like hydrology (Selker et al. 2006, Tyler et al. 2009) and petroleum exploration (Brown and Tiwari 2010), DTS is often used to monitor fluid transportation and distribution for which a spatial resolution in the order of meters is required. However, for monitoring concrete casting a much higher spatial accuracy is required because the expected height differences within the trench are in the order of a few centimeters. Experiments during the construction of an underground parking facility in Rotterdam (Spruit et al. 2011) show promising results for monitoring concrete flow using DTS during diaphragm wall production (Doornenbal et al. 2011; Spruit et al. 2011).

This paper will focus on the verification tests of DTS in the laboratory and in field setups.

4.3 Hypothesis

During the construction process of a diaphragm wall, bentonite and concrete with different temperatures replace each other in the different construction phases. During the de-sanding operation fresh bentonite replaces the excavation bentonite, and the temperature of the fresh bentonite will differ from that of the bentonite in the trench. During concrete casting, the concrete replacing the bentonite will once again differ in temperature from the bentonite. In most cases the concrete will have a higher temperature

than the bentonite in the trench. Detailed and continuous temperature measurements near the joints during de-sanding and concrete casting would enable monitoring of the presence of concrete in a joint between two diaphragm walls. Finally, during curing the concrete will heat up and a locally lower temperature could indicate an area with sub-optimal concrete properties.

With Distributed Temperature Sensing (DTS) the required temperature measurements should be possible and practical. The principle of DTS measurements for quality control during concrete curing has been applied since the late nineties of the 20th century (Thevenaz et al, 1998), especially in large arched dams and other large volume concrete structures. More recently other applications have become common, especially in ground water monitoring (Selker et al. 2006, Tyler et al. 2009). However, the effectiveness of tracking the concrete casting of diaphragm walls or of the bentonite refreshing operation has not been published before.

4.4 Measurement principle

The DTS measurement uses glass fibers that are installed at critical locations in the diaphragm wall, such as the joint to the adjacent panel, around the water slot or behind areas with a very dense rebar grid that might obstruct the concrete flowing through. Useful installation options are:

- lowering the sensor in the bentonite with a weight attached to the sensor end;
- attaching the sensor to the rubber water slot before installation of the stop end;
- attaching the sensor to the rebar cage.

With a DTS device, the fiber is interrogated, offering a continuous temperature profile of the fiber, essentially making the glass fiber a continuous linear temperature sensor. In the rest of the paper the glass fiber will be called sensor.

In this study, DTS measurements based upon the Raman scatter principle were used. In these measurements, a monochromatic laser pulse is fed into the sensor. The vast majority of the light will be transmitted through the sensor. A small portion of light interacts inelastically with the electrons in the sensor and generates light at two frequencies symmetrical about the injected light frequency (Figure 29). The reflected light band with lower frequency is referred to as 'Stokes', and the reflected light band with higher frequency

than injected is referred to as 'Anti-Stokes'. With increasing local temperature, more electrons end up in the high energy state, thus increasing the anti-Stokes/Stokes ratio (Selker et al. 2006). As the speed of light is known, it can be determined at what position in the sensor the reflected spectrum that is recorded in time was generated. This type of DTS measurements therefore belongs to the Optical Time Domain Reflectometry (OTDR) family.

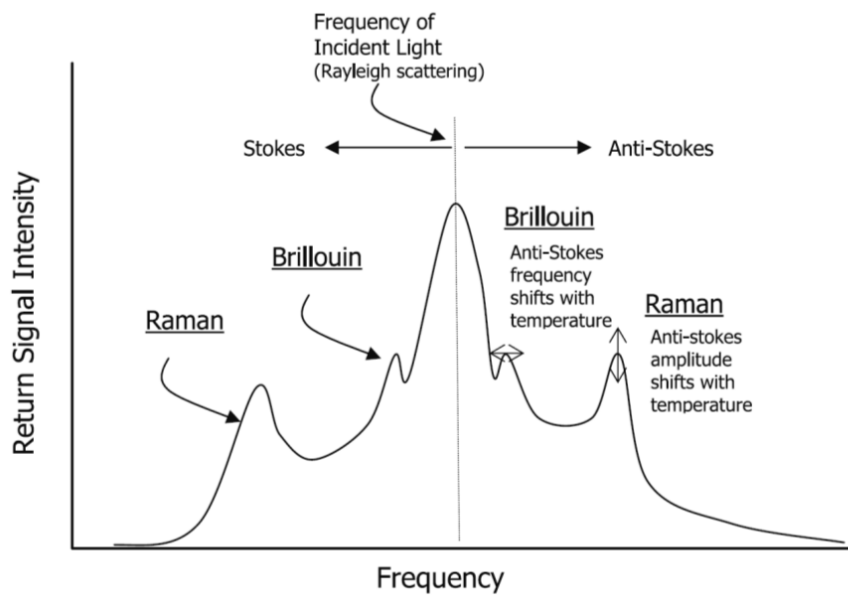


Figure 29: Raman scatter principle (Selker et al. 2006)

By analyzing the ratio of anti-Stokes over Stokes as a function of time, the local temperature of the sensor can be derived. To obtain a good signal to noise ratio for the measurements, multiple measurements need to be stacked (Selker et al. 2006). A longer measurement time will therefore lead to more accurate determination of the local temperature in the sensor, provided that the temperature is not changing during acquisition. The DTS device will produce per sensor position the local temperature along the full length of the sensor. The spatial resolution (generally every measurement is averaged over 1 m) is independent of the optical fiber and depends on the measurement equipment used.

4.5 Laboratory measurements

First, the behaviour of the DTS sensor which was intended for the field experiments has been tested in laboratory conditions. For these tests a ruggedized optical fiber (ACE-TKF CTC 8xMM) connected to a Sensornet Oryx DTS (Sensornet, 2012) has been selected. This sensor contains 8 MultiMode fibers in a gel-filled plastic tube protected with Kevlar fibers covered with a plastic outer liner, as shown in Figure 30. The external diameter of the sensor is approximately 7 mm.

The following parameters have been explored because they are not generally provided by the manufacturer: the response time of a sudden temperature change, the pressure dependency, and the accuracy of the spatial resolution.

4.5.1 Response time

A single ended sensor cable has been conditioned for at least five minutes in a container with water of about 20 degrees Celsius. Immediately after completion of a measurement cycle the sensor cable is submerged in a container with warm water (around 50 degrees Celsius) and several subsequent measurements of one minute are recorded to construct the asymptote of the temperature adjustment. Figure 31 shows the accommodation speed for this specific sensor. The ACE-TKF CTC 8xMM cable needs between 70 and 100 seconds to fully adapt to the surrounding temperature when immersed in water.



Figure 30: Cross section of the ACE-TKF CTC 8xMM cable

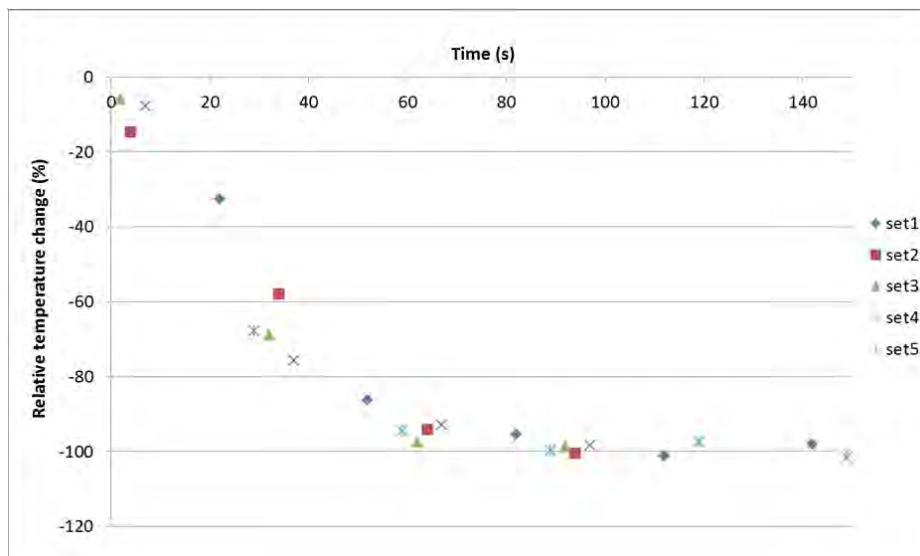


Figure 31: Temperature adaptation in time

Because the hot water was cooling down during the test, a relative temperature drop has been used instead of an absolute temperature drop so

that several measurements (in this case 5 immersion tests) can be combined.

Although this ruggedized sensor has shown a good survival rate in the field, the thick liner causes a slow equalizing of the temperature in the sensor. For fast and accurate temperature acquisition, a sensor with a thinner liner should be considered. The increased vulnerability could be compensated by installing more sensors than strictly needed (redundancy).

4.5.2 Pressure dependency

Because of the intended application in a diaphragm wall, the sensor will be exposed to external pressures ranging from 0 to 14 bar (considering a maximum depth of the diaphragm wall of about 60 m).

To check the pressure dependency, a test fiber has been installed in a pressure tank. The tank was 90% filled with water at 20 degrees Celsius to act as a temperature buffer and the air void above the water was pressurized to 6 bar. The temperature readings from the sensor did not change during this test. Temperature drift of this sensor cable due to pressure change is therefor considered negligible within the investigated pressure range.

4.5.3 Spatial accuracy and resolution

In a casting form instrumented with optical DTS sensors, the possibilities of DTS to detect a clay inclusion with varying thickness have been explored previously, as reported by Doornenbal et. al. (2011). It was concluded that the thickness of a clay layer separating the DTS sensor from the cast concrete could be derived from the measurement data.

In order to verify if fresh bentonite arrives at critical locations in the panel during slurry refreshing, or if good grade concrete arrives at critical locations in the panel during the concrete casting phase, it is necessary to determine the response curve of the sensor and DTS device in a situation with two fluids at different temperatures. This has been done using two containers with water of different temperature placed next to each other. Several meters of the same fiber have been placed in each container, as sketched in Figure 32. As the water level in the containers was almost to the top level, the transition zone of the sensor between the two containers (initially around at

position 8.389 m along the length of the fiber) was less than 0,05 m in length. During continuous recording, the sensor was kept stationary for ten minutes (ten temperature recordings) after which the transition zone was shifted 0.2 m. This was repeated until the transition zone had shifted 0.8 m in total (final position of transition zone at 7.589 m).

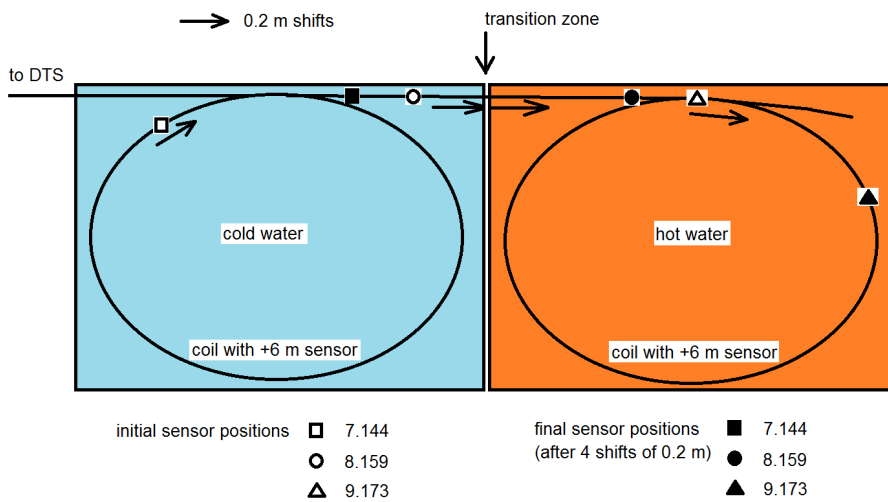


Figure 32: Test setup for determining the response curve

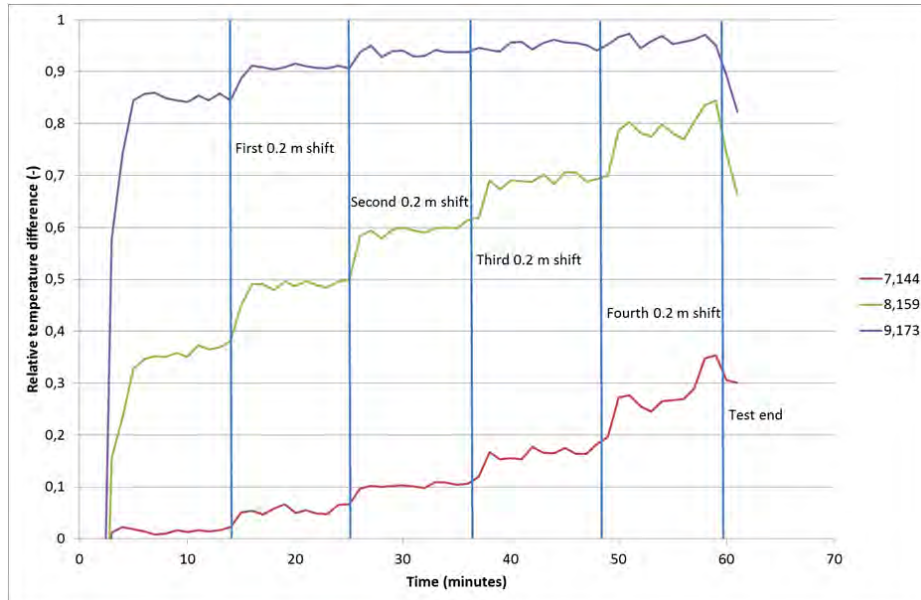


Figure 33: Relative temperature difference for 3 measurement positions (in meters relative to the DTS device) in the linear sensor near the transition zone during the response curve test

Figure 33 illustrates how the temperature readings in front and behind the transition zone are affected relative to the temperature difference between the hot and cold containers. Each of the 3 measurement positions show 5 temperature plateaus, corresponding to the 5 positions, 0.2 m apart, of the transition zone. It can also be concluded that sensor position 8.159 m is slightly off the center of the test as can be seen from the 3rd measurements (second 0.2 m shift) sequence (see Figure 4) which are at 0.6 relative temperature instead of 0.5 relative temperature.

The average of each set of ten temperature readings has been used to determine Figure 34. After the fourth shift, it seems that no equilibrium has been reached at measurement position 7.144 m. However, this does not show in Figure 34, confirming that 10 minutes is a well-chosen interpolation period.

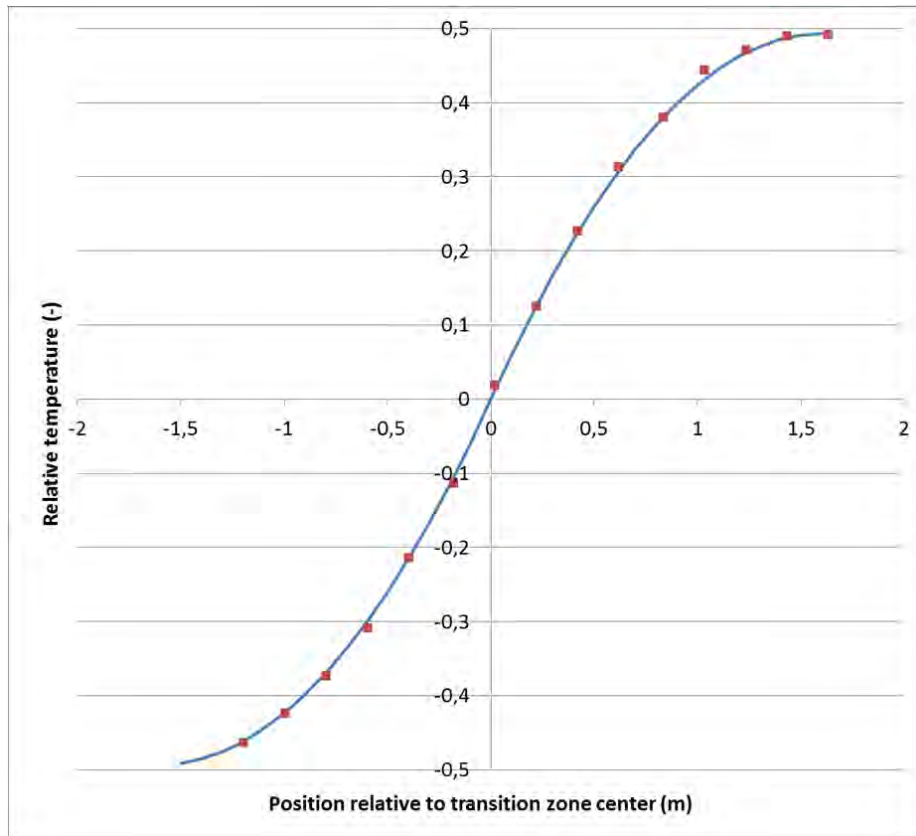


Figure 34: Response curve for Sensornet Oryx DTS and single ended ACE-TKF CTC 8xMM fiber based upon ten averaged recordings with acquisition time of 1 minute (model as line and measurements as dots)

$$\frac{T}{T_1 - T_0} = -0,1927 \cdot x^2 + 0,6164 \cdot x \quad (1)$$

In which:

T = measured temperature

T₁ = temperature of medium 1

T₀ = temperature of medium 0

x = sensor position relative to position of interface between media 1 and 0

Note that this response curve is specific for the Sensornet Oryx DTS device. If another DTS recorder is used, a different curve could be applicable. Following the procedure described above, the response curve should be determined if the manufacturer does not provide such information.

Although we generally would expect a DTS device with more measurements per meter to have a steeper response curve, theoretically it could have a less steep response curve. Without determining the actual response curve, it is not proven that a DTS device with, for example, 5 measurements per meter is 5 times more accurate than a device that only measures 1 temperature per meter.

If the acquisition time of the temperature recording is reduced, it is to be expected that the general shape of the response curve remains the same but that the individual points on the curve will show more variation.

The response curve for the Sensornet Oryx DTS shows that the local temperature between 1.5 m before and after the observation point influences the resulting measurement at the observation point.

As long as we recognize that we are dealing with only two media, each with a specific temperature, this poses no trouble for the interpretation. On the contrary, using the response curve we are able to locate the actual interface between the two media much more accurately than is suggested by the spatial resolution of 1 m that is stated in the device specifications. However, if the total sensor length in a medium is less than 3 m and we do not know the exact dimensions of the medium, we will be unable to determine the exact temperature of the sub-3 m length of sensor. If we know the temperature by means of another measurement, we will be able to determine the actual length using the characteristics from Figure 6. Consequently, if a reliable calibration of the temperature measured with the sensor is needed, a calibration coil with at least 6 m of sensor in a controlled temperature zone is recommended.

Using the response curve from Figure 34, the known sensor positions during the test and the temperature in both the warm and cold water containers, the measured absolute temperatures from Figure 33 have been simulated. These simulations are compared with the measured temperatures in Figure 35. Measured temperatures are depicted by dashed lines and simulated temperatures by solid lines. To illustrate how the temperature of the hot container (sensor position 10.188) dropped during the test and the container

with cold water (sensor position 6.129) warmed up during the test, these sensor positions are added. Note that sensor position 10.188, which was initially completely in the hot container, was slightly affected by the cold container at more than a meter distance, which is coherent with Figure 34. To determine the temperature in the hot container, the readings at sensor position 12.217 have been used.

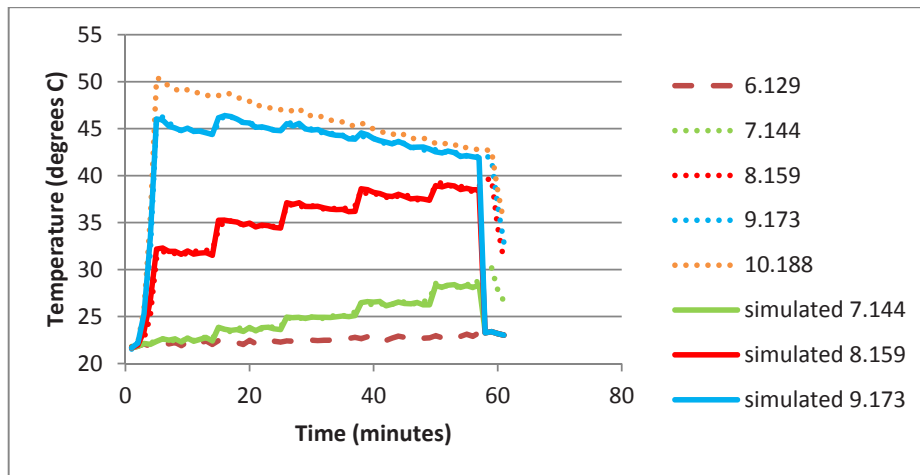


Figure 35: Measured (dashed) and simulated (continuous) temperature response curves for sensor positions near the transition zone

4.6 Field measurements

In 2010 the DTS sensors were applied in-situ for the first time in 42 m deep diaphragm walls for an underground parking underneath Kruisplein in Rotterdam. It was anticipated that the heat generated during curing of the concrete would primarily render useful information. The same ruggedized ACE-TKF CTC 8xMM sensor as tested in the lab was used. The slow response was not considered to be a problem as the temperature build-up during concrete curing is much slower than the accommodation speed of the sensor. However, the measurements started just before concrete casting.

The measurements were surprisingly illustrative for the rising concrete level in the trench during casting, although it seemed probable that for tracking concrete level changes in the trench the response time could influence the measurements. It was therefore considered worthwhile to further investigate the accuracy of concrete level determination using DTS.

The temperature measurements during curing gave less information than expected, because the permeability of the soil surrounding the diaphragm wall seemed to govern the temperature in the wall. The peak curing temperature (Figure 36) was highest in the peat layers (low permeability combined with low thermal conductivity), while within the clay layers intermediate temperatures were recorded (low permeability combined with relatively good thermal conductivity), and the lowest temperatures were recorded where the diaphragm wall was embedded in sand layers (high permeability and thermal conductivity and/or convection).

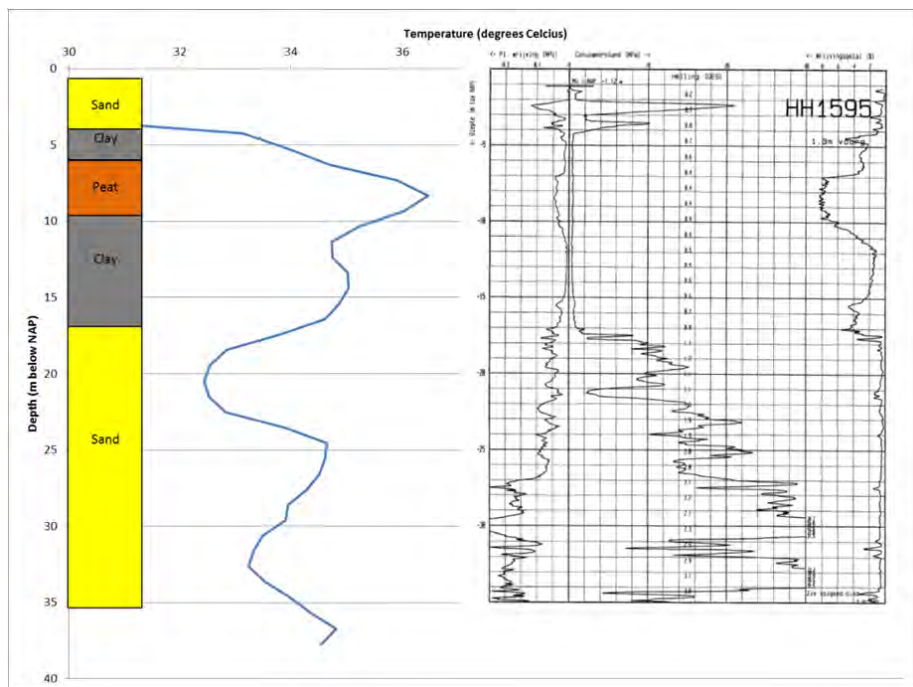


Figure 36: Peak temperature profile from concrete curing with CPT and boring

In 2011 DTS profiles were recorded in the railway tunnel project through the city of Delft in the Netherlands. The D-wall panels reached a depth of 25 m below surface level. In Figure 37 subsequent temperature profiles are shown for the center of the panel (close to the tremie pipe, see Figure 44). The interval between the profiles was four minutes because the DTS device was interrogating 4 fibers in sequence with an interpolation time of one minute for each fiber.

At the positions indicated with arrows two or more temperature profiles overlap. Depending on the number of overlapping profiles, this means a multitude of four minutes of stagnation during concrete casting. This could be caused by cutting the tremie pipe or changing the concrete truck at the tremie. Longer and therefore more hazardous discontinuations in the concrete flow would of course show up in the sequence of temperature profiles more predominantly as they would include a lot of overlapping profiles. The arrows are placed halfway between the temperatures of concrete and bentonite, as seems logical from the response curve from Figure 34.

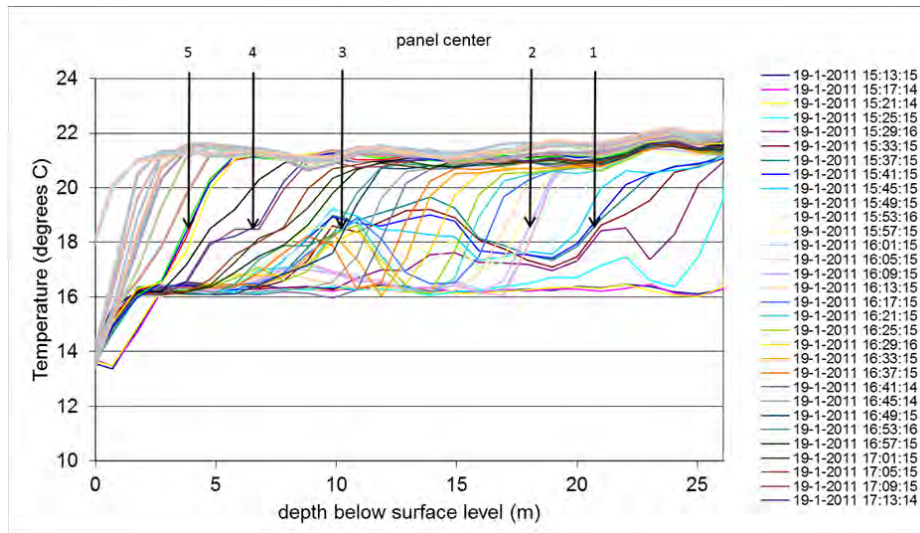


Figure 37: Subsequent temperature profiles in the center of the panel during concrete casting, arrows indicating overlapping temperature profiles of subsequent measurements

Although the arrows in Figure 37 and Figure 38 show good depth correlation, it is sometimes not clear where to interpret the level of the interface between concrete and bentonite, as is illustrated with Figure 38. The extra wiggle in the graphs around 15.5 to 16 degrees C does not correspond to the response curve of the media. The extra wiggle seems to indicate a layer of relatively constant intermediate temperature, probably consisting of a mixture of concrete and bentonite. It might be possible to simulate this using a three phase model with two superimposed response curves. A simulation of the temperature response could offer more accurate

determination of the interface between (high grade) concrete and bentonite (or low grade concrete).

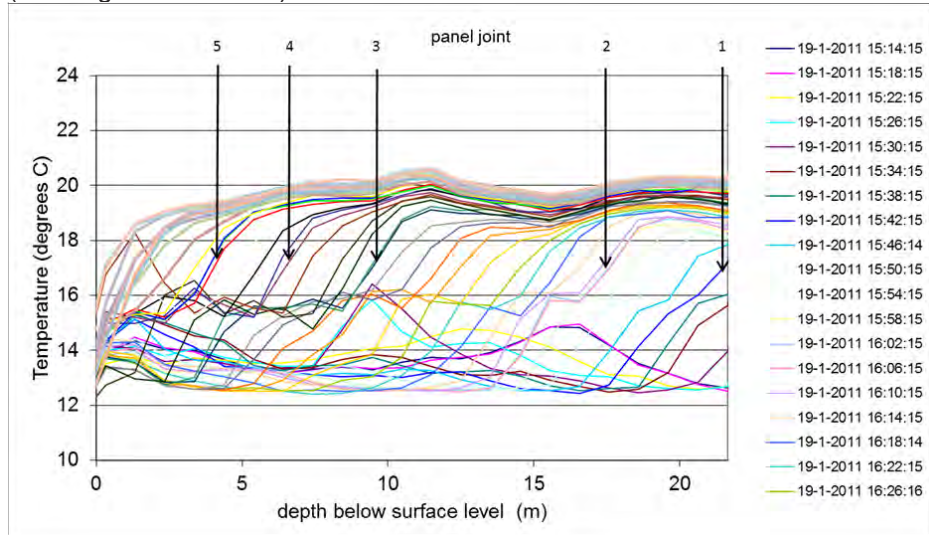


Figure 38: Subsequent temperature profiles in the joint area during concrete casting, arrows indicating overlapping temperature profiles of subsequent measurements

The DTS measurements have also been performed during the slurry refreshing operation (Figure 39). The effectiveness of replacing the slurry in the trench (16.2 degrees C) with freshly mixed slurry (12.6 degrees C) could be determined just as clearly as the concrete casting. The even spacing between the temperature profiles in Figure 39 indicates a constant slurry refreshing speed. The rising temperature between 3 and 15 m below surface level is caused by the still warm adjacent panel.

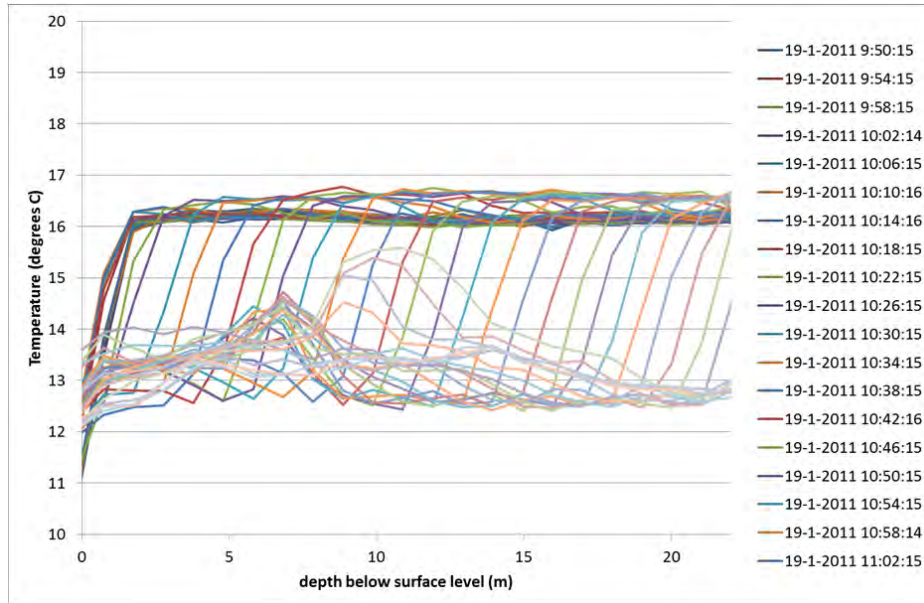


Figure 39: Subsequent temperature profiles in the joint area during slurry refreshing

From the laboratory tests and the field test, it seems possible to determine the actual concrete level using DTS much more accurately than expected regarding the manufacturers' 1 m spatial resolution.

4.7 Correlation with manual concrete level measurements

To verify the accuracy of the concrete levels determined with the DTS profiles, a comparison has been made with manual concrete level measurements of the same panel. Using the response curve as shown in Figure 34, each temperature profile from Figure 38 has been simulated. To obtain a good fit with the recorded temperature profiles, a three phase (concrete, mixed material, bentonite) system has been simulated using 2 superimposed response curves. Figure 40 shows a measured and simulated temperature profile to illustrate the simulated response of a three phase system.

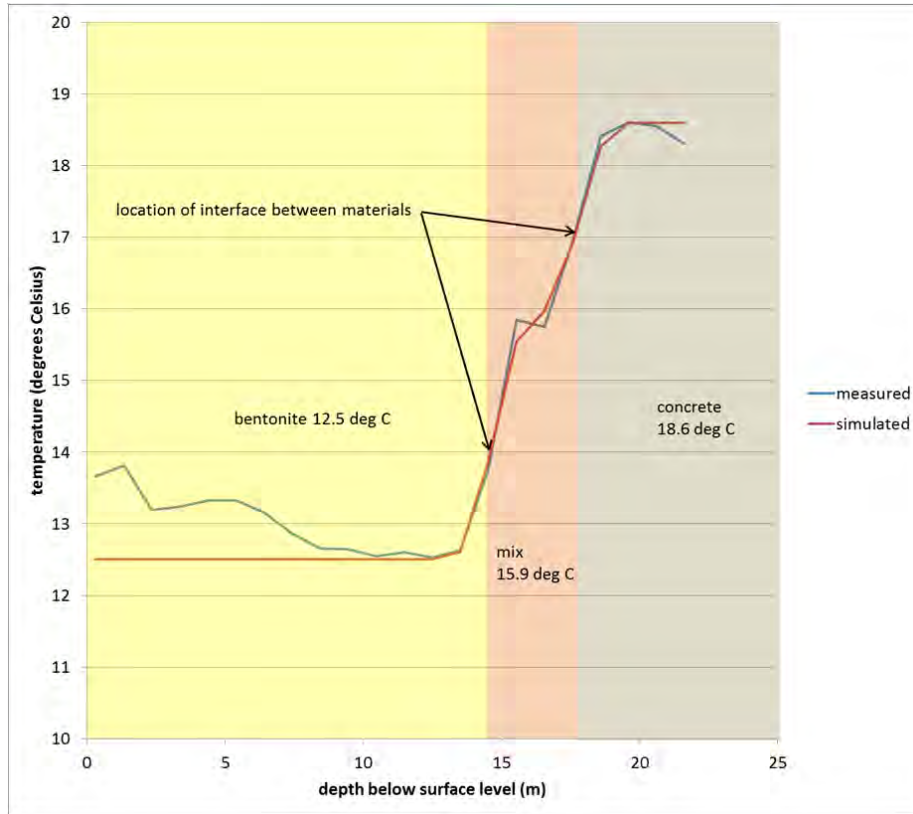


Figure 40: Measured and simulated temperature profiles in the joint at 19-1-2011 15:58:15. Correlation between measured and simulated graphs = 0.999 from 10.5 to 20.5 m below surface level

During the simulation process initially the temperatures for the bentonite, concrete and intermediate layer and the levels for the separation interfaces are assumed. The temperatures can be derived from the relatively constant temperatures in the graph above and below the interface, the interface levels are assumed from the steepest parts of the graph. During the optimization phase of the simulation, these parameters are iteratively varied to obtain a visually optimal fit with the measured temperature curve. To illustrate the simulation process, a simulated graph with the interface between bentonite and the mixed material 0.5 m too high and the interface between the mixed material and concrete 0.5 m too low is shown in Figure 41. The shape of the simulated graph in Figure 41 is correct, but the intermediate step at 16 m below surface level is too wide compared to the measured curve.

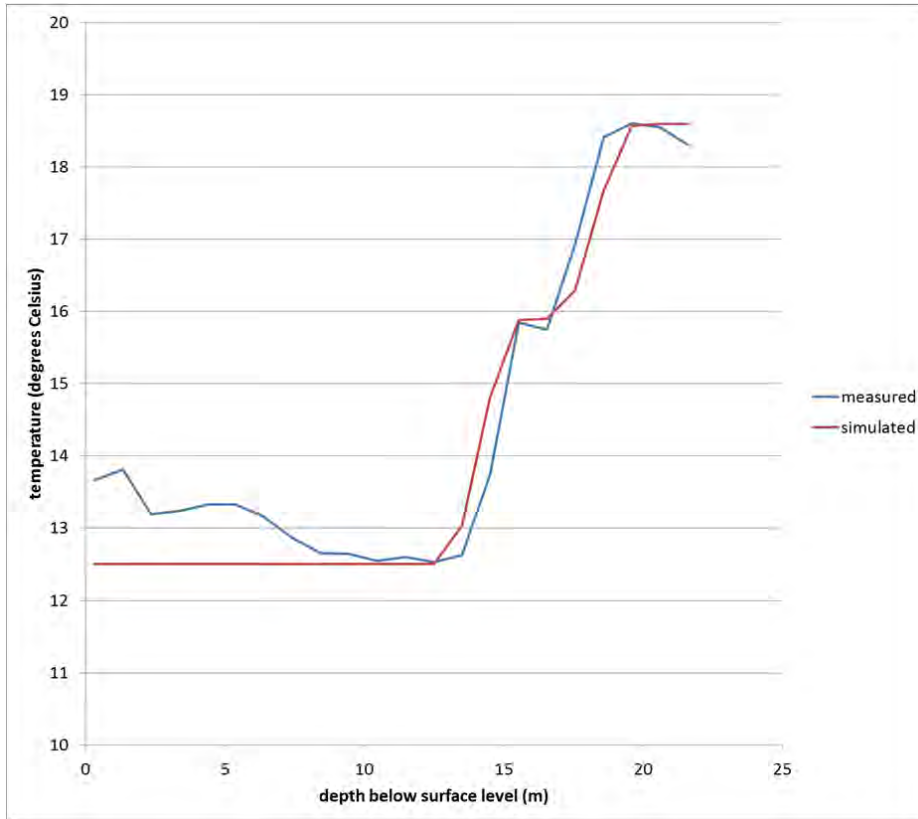


Figure 41: Measured and simulated temperature profiles in the joint at 19-1-2011 15:58:15, upper interface 0.5 m too high, lower interface 0.5 m too low. Correlation between measured and simulated graphs = 0.984 from 10.5 to 20.5 m below surface level

Between 0 and 8 m below surface level the temperature of the bentonite mixture was slightly higher because the sensor was positioned in the joint next to the still-warm panel that had been cast 4 days before. The constant temperature between 15.5 and 16.5 m below surface level indicates a layer with constant temperature. From the simulation shown in Figure 40 it can be concluded that this intermediate layer must be 3.2 m thick and have an average temperature of 15.9 degrees Celsius.

After simulating all recorded temperature profiles, it has been noticed that to obtain a correctly fitting simulated temperature profile, the position of the interface between two materials has to be accurate to 0.05 to 0.10 m. This suggests that the position of the interface between the two materials can be

determined with an accuracy of 0.05 to 0.10 m. This applies for Sensornet Oryx DTS measurements with 1 minute acquisition time per measurement. Due to this relatively long acquisition time and the adaptation time of the sensor, the interface position will be shifting during acquisition, causing a loss in spatial accuracy. A total combined latency of about one minute will cause a delay of one minute in depth recording. This corresponds to a 0.05 to 0.1 m lower perceived concrete level considering a concrete cast duration of four hours (Figure 47) for a 20 m deep diaphragm wall panel. The acquisition time of the DTS device and the latency of the sensor should therefore be shortened if possible while still maintaining acceptable temperature accuracy and ruggedness. Figure 42 shows that for relatively short sensors (during the tests the sensors were always less than 150 m long), the acquisition time does not significantly affect the temperature resolution. For reliable simulation of the temperature response, the temperature difference between the media above and below the interface should preferably be an order of magnitude higher than the temperature resolution.

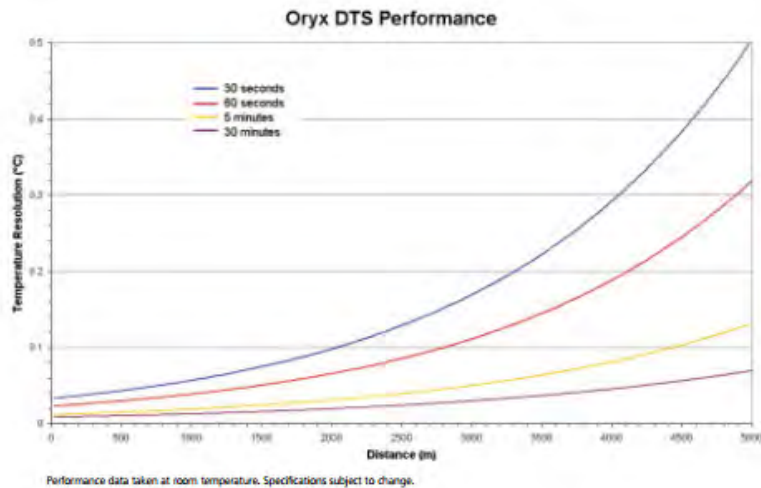


Figure 42: Temperature resolution depending on sensor length (Sensornet 2012)

Similar to Figure 40, all temperature profiles recorded in the joint and in the center of the diaphragm wall panel were analyzed. In the center of the panel, close to the tremie pipe, only a two phase system was encountered as illustrated by the temperature measurements and simulations in Figure 43. When comparing Figure 40 and Figure 43, we notice that different temperatures have been found for concrete and bentonite at these different

locations. This could partly be caused by cooling of the concrete during horizontal transportation from the tremie pipe to the joint and by variation of the bentonite temperature close to the tremie pipe. On the other hand, DTS measurements based upon Raman scatter (Tyler et al. 2009) do not offer absolute temperatures. Due to slight signal loss in an optical connector for example, the absolute values of the temperature profile can shift.

If we assume the concrete temperature in the joint to be the correct value at 18.6 degrees Celsius and shift the profile in the center of the panel accordingly, we find a bentonite temperature of 14 degrees Celsius which is much closer to the 12.5 degrees Celsius we encountered in the joint. However, the absolute value of the temperature profiles is not significant for determining the location of an interface between materials. If absolute temperature is required, all sensors should run through a temperature-controlled or isolated calibration box for at least 6 m sensor length as discussed above.

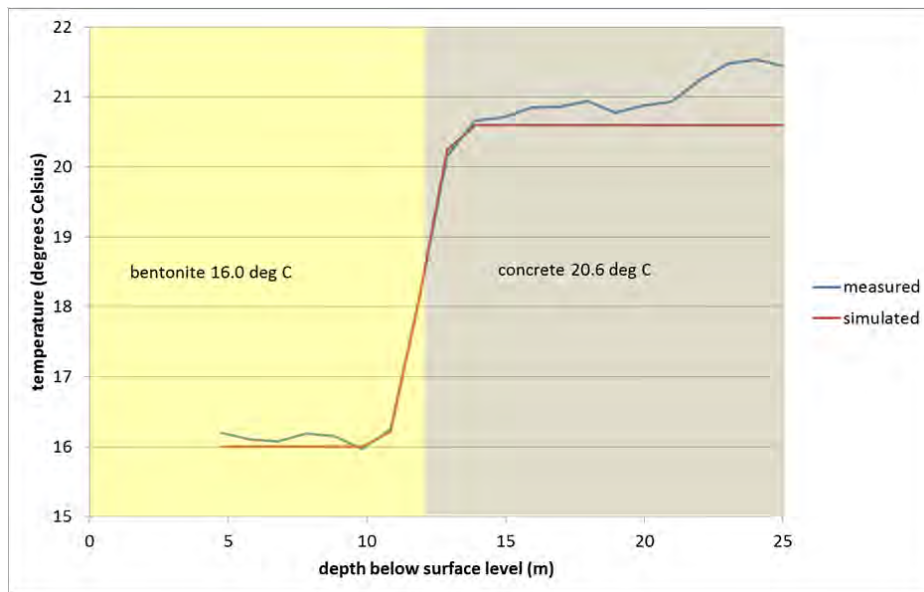


Figure 43: Measured and simulated temperature profiles in the center of the panel

The simulated temperature profiles provide a time sequence of concrete-bentonite interface levels for the center of the panel and a time sequence of concrete-mixed material and mixed material-bentonite interface levels for the

joint area. Figure 47 plots these sequences together with the manual depth registrations that were recorded by the contractor against time.

The concrete levels in the center of the panel derived from the simulations (solid line, Figure 47) show a good correlation with the manual recordings (square dots Figure 47). Between the fifth and sixth manual recordings a stagnation of the concrete casting of 12 minutes went unnoticed, but is clearly noticeable in the temperature profiles. In the joint, the top of the mixed material with intermediate temperature is rising at almost the same speed as the concrete level in the center of the panel. The stagnation of the concrete casting is also visible in the joint area. Good quality concrete, with the same temperature as the concrete in the center of the panel, is observed in the joint area on average 3 m below the level in the center of the panel. The height of the zone of mixed material gradually increases during the concrete casting. This is understandable, as mixed material will accumulate on top of the concrete in the joint area while it is pushed upwards and towards the joint by the concrete flowing from the center to the panel sides. This also explains why the top of the mixed material zone exceeds the level of the concrete towards the end of the concrete casting period. The top of the concrete in the joint never reaches the top of the panel. This corresponds perfectly with general experience with diaphragm walls: the upper meters close to a joint generally contain more contamination with bentonite and poor quality concrete than at lower levels. In this case, according to the levels derived from the temperature profiles, the upper 3 m of joint is expected to be of poor quality. This was in accordance with CSL measurements (Spruit et al. 2014) and observations on site.

When examining the upper 5 m of the CSL logs of this specific joint (*Figure 45*), we encounter a quickly deteriorating signal in the joint (straight (1-2 and 3-4) and diagonal (1-3 and 2-4) joint crossings) at 3 m below the top of the panel. The CSL logs parallel to the joint (which are located 0.4 m from the joint) show the same signal deterioration, but at 1.9 m below the top of the panel.

Correlation with manual concrete level measurements

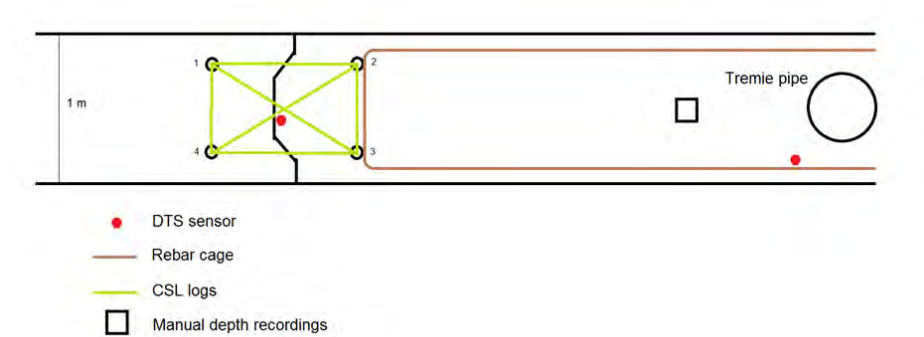


Figure 44: Position of CSL logs, manual depth recordings and DTS sensors in the panel

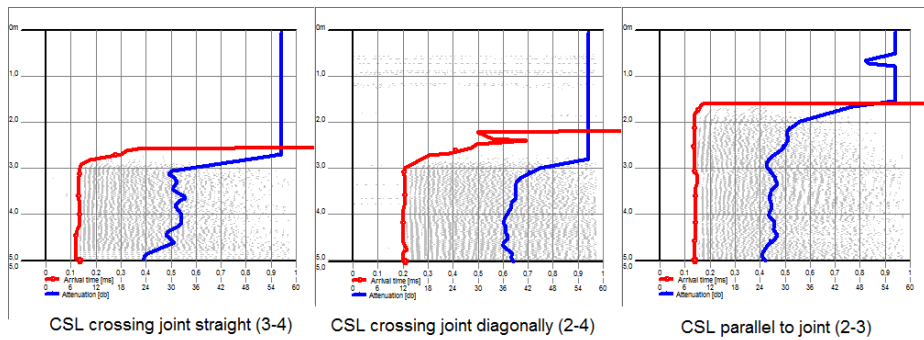


Figure 45: CSL logs, loss of signal indicating poor concrete

As the CSL logs parallel to the joint are located 0.4 m from the joint, we could estimate the slope of the concrete – mixed material interface using the level where deterioration of the signal starts and the position of the CSL logs in the panel. The DTS profiles also provide concrete level information. If the DTS and CSL interpretations are combined, this leads to the concrete boundaries as suggested in Figure 46.

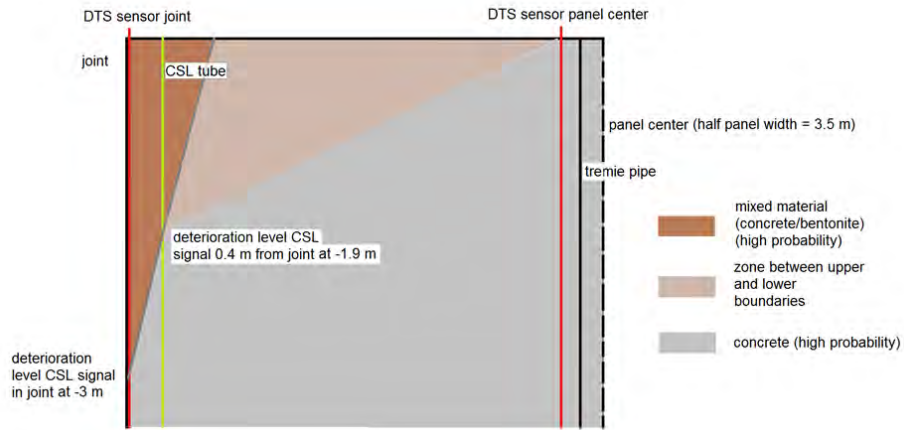


Figure 46: Interpretation of CSL and DTS concrete levels (side view of panel)

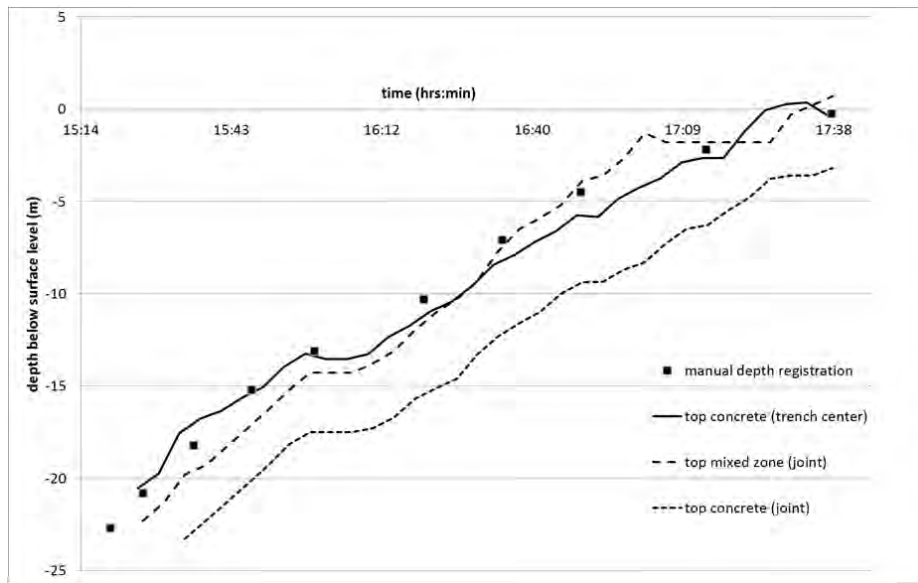


Figure 47: Concrete levels recorded in the center and joint of a panel

The correlation with the manual concrete level measurements has shown that the DTS concrete level measurements are in the same order of accuracy. The levels derived from the temperature profiles are more objective and far more frequent than manual recordings. The estimated 0.05 to 0.1 lower perceived concrete levels, based upon DTS sensor and device latency, seem insignificant compared to the accuracy of the manual depth

recordings (Figure 47). The manually recorded levels depend on subjectively sensed resistance of the dropped weight onto the concrete and are operator dependent. If a zone of mixed material is present on top of the concrete, this could be mistaken for concrete. Manual recordings are generally performed after each truckload of concrete and as a result offer only a few measurements over time. Note that the manual depth registration and the top concrete (solid line) from Figure 47 were registered near the center of the panel (see Figure 44). Both dashed lines were recorded in the joint to the next panel.

The estimated accuracy of the DTS measurements in this case study is 5-10 cm. An accuracy of about 2-5 cm is probably achievable if the acquisition time of the DTS is reduced to 15 seconds instead of the 60 seconds used here. To reach that accuracy, it is also necessary that the sensors have a liner that is as thin as possible to avoid retarding the temperature measurements. With such accuracy, otherwise difficult to monitor differences, for example the small differences in the concrete level between inside and outside the rebar cage, could be monitored.

4.8 Discussion

The DTS level measurements offer a number of advantages over other concrete level measurements during D-wall casting:

- the sensor cables are relatively low-cost
- the required space for the sensor cable is almost nil, making it possible to measure for example the concrete level between the rebar cage and the trench wall
- several sensor cables can be connected to 1 measurement device, making simultaneous concrete level measurement at several positions in one trench relatively easy
- the sensor cable could be integrated within the water slot that is often used in the joints between panels
- the sensor cable can easily be attached to the rebar cage
- the sensor has negligible influence on the concrete flow process
- vulnerability of the sensor cable is much less of a problem than expected (only 5% of the ACE-TKF CTC 8xMM sensors failed during the field tests)
- excellent recording of the slurry refreshing and concrete casting process is possible

Disadvantages of the method are:

- optical sensors are vulnerable, especially at the optical connectors where dust and/or moisture can interfere with the measurements
- in a daily operation of diaphragm wall production the sensor cables would be easily damaged if no special care is taken to prevent stepping on the sensor cables or of the sensor cables being squeezed between rebar cage and trench wall etc.
- DTS equipment is still rather expensive and not yet optimized for this specific application

Considering the above mentioned pros and cons, this measurement technique is at this moment most suitable for laboratory circumstances or field test environments intended for (further) understanding of bentonite and concrete flow during diaphragm wall production.

DTS could also be useful in specific project situations, such as when a complex and dense rebar cage with possible flow obstruction needs to be verified before serial production.

If, in time, a simple-to-operate DTS device specifically designed for this application is available, the concrete level measurement using DTS could become a standard quality control tool for D-wall production. With DTS it will be possible to check proper slurry refreshing, allowing for additional cleaning of the trench by brushing the joints and re-refreshing if stagnation or irregularities during refreshing are encountered.

During concrete casting, DTS will offer the possibility to monitor the slope of the casting front, differences between concrete level in- and outside the rebar cage and casting interruptions.

The latest generation of DTS devices promises an even higher spatial accuracy, possibly making the concrete level measurement even more accurate than obtained during the tests described in this paper. This should be determined first with response curve measurements as described above.

4.9 Conclusions

DTS measurements can be used to monitor the production of diaphragm walls. During the slurry refreshing operation the replacement of excavation bentonite by freshly mixed bentonite can be monitored. If stagnation during refreshing is encountered, additional cleaning of the trench by methods such as brushing the joints and re-refreshing could be considered. During concrete casting DTS offers the possibility to record stagnation and to verify

Conclusions

if good quality concrete arrives along the perimeter of the trench. In the joint, the detected arrival of good quality concrete ensures a high probability of a watertight joint. The optical sensor that is used for DTS might be integrated in the water slot that is often applied in joints between diaphragm wall panels. Other successful installation possibilities include lowering of the sensor using a weight attached to the sensor end or attaching the sensor to the rebar cage.

Chapter 5 To detect anomalies in diaphragm walls with apparent resistivity measurements³

5.1 Abstract

Quality control of diaphragm walls prior to excavation is often difficult. One technique that can be used to detect anomalies in diaphragm walls is Electrical Resistivity. Electrical Resistivity (ER) measurements across a diaphragm wall can (within a strict framework) be used to verify the presence of leaks in diaphragm walls as a supplement to Crosshole Sonic Logging (CSL). From measurements around a test wall conducted in this study, it is concluded that the detectability of anomalies with ER decreases exponentially with increasing distance between the measurement electrodes and the wall. ER setups with two and four electrodes have been compared. For useable results a four-electrode setup must be used in which the potential electrodes need to be placed very close to the wall (less than 0.2 m away). Based upon the test experiences, a field setup for verification of a building pit consisting of diaphragm walls is suggested, as well as a setup for determining the quality of the concrete covering the rebar in quay walls constructed with diaphragm walls.

Key words: Electrical Resistivity, diaphragm wall, joint, quality control

5.2 Introduction

Diaphragm walls are frequently used for deep underground constructions in densely populated areas because of their high strength and stiffness in combination with quiet and vibration-less installation. Quality control for water tightness and retaining functions has proven to be difficult, as

³ This chapter is currently under review as an article for Near Surface Geophysics.

disasters during construction works in the Netherlands and Belgium have shown (Van Tol et al. 2010; Berkelaar. 2011; Van Tol and Korff. 2012). Other examples of underperformance have been reported in Boston (Poletto and Tamaro. 2011), Cologne (Sieler et al. 2012), and Taipei (Hwang et al. 2007). The poor quality, or even absence, of concrete in the joints between the diaphragm wall panels is the primary cause of these calamities (Van Tol et al. 2010).

Because of these experiences, it was decided to investigate methods to detect anomalies in diaphragm walls, particularly around panel joints, prior to excavation of the building pit enclosed by the diaphragm walls. Even though CSL is the recommended method for detecting anomalies (Spruit et al. 2014), it is sometimes useful to be able to verify the outcome of such measurements with a physically independent measurement.

In Taipei, electrical resistivity has been used successfully to detect anomalies in diaphragm walls (Hwang et al. 2007). However, in three field tests described in this paper and during metro construction works in Amsterdam (Van Tol et al. 2010) the interpretation of electrical resistivity measurements showed low correlation with visually confirmed anomalies. It was therefore decided to explore the limits of anomaly detection in diaphragm walls via a series of field tests on a concrete wall with known anomalies. In the tests, the electrode configuration has been varied, revealing a different detection limit for each configuration.

Based upon the results, electrode configurations for field tests will be recommended.

5.3 Measurement principle

Electrical conductivity and/or resistivity measurements are commonly used to detect leakage of membranes or sheet piled walls (Pellerin 2002). In the case of a plastic membrane, the contrast between the electrical resistivity of a sound membrane and a leaking one is very high. During the measurement an electrical current is forced from one side of the barrier to the other using electrodes at a relatively large distance (approximately two times the investigation depth) from the barrier. By measuring the local potential with separate electrodes, the apparent resistivity can be calculated from the potential difference and the input current, or the resistivity can be determined directly by comparing the resistivity with a calibrated resistor. With increasing

potential electrode distance to the barrier, the apparent resistivity will be increasingly influenced by the larger volume of water. This will negatively affect the resolution of the measurements.

The Electrical Resistivity method can be extended to tomography in which a large number of resistivity measurements are taken with varying electrode configurations. By combining these measurements, it is possible to compute a 2D or 3D distribution of the resistivity (Pánek et al 2008, Wilkinson et al 2012). This principle is commonly used in geomorphology, archaeology, geohydrology and ecology. In such cases a 3D model of the subsurface is the intended result of the measurements.

In case of a diaphragm wall with defects, the position of the wall is known and even the areas that are prone to show defects (the joints) are predefined. As a result, there is a much lower need for a full 3D model. Also, the use of a large number of electrodes, as is required for tomography, is not suitable to most building site conditions.

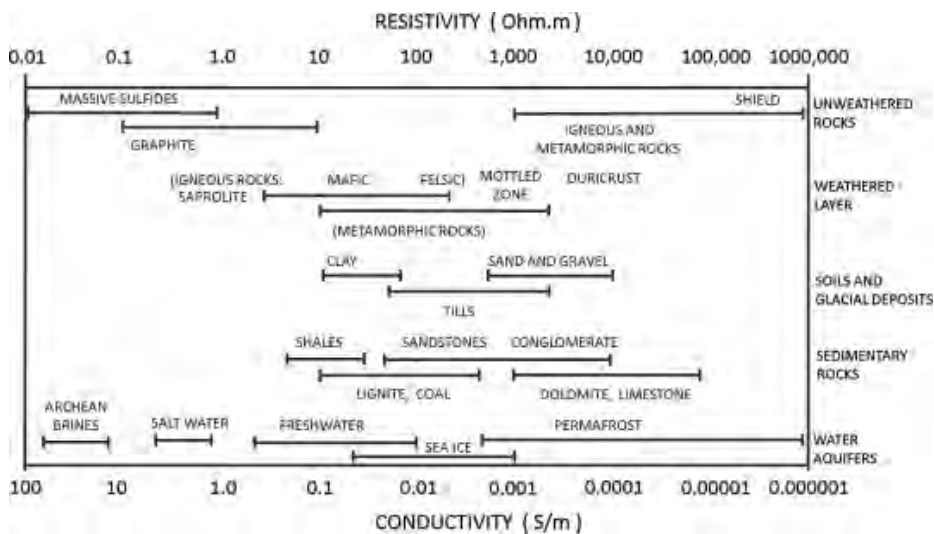


Figure 48: Indication of resistivity properties (Gunn et al. 2014)

With a resistivity of up to 100 Ohm.m (Neville 1981), saturated fully cured concrete has resistivity properties in the same range or just above clay and freshwater. Even if the defect affects the full cross-section of the wall, the resistivity of an unaffected section of the wall and a section with a hole in it is relatively small. If the defect does not extend through the full cross-section of

the wall the resistivity contrast will be even smaller. However, during construction of the Taipei metro (Hwang et al. 2007), electrical resistivity measurements were used to locate leaks in diaphragm walls and to verify if the jetgrout repair works were successful. This indicates that ER is viable in detecting anomalies in diaphragm walls.

The aim of the tests is to find a straight forward measurement setup that involves a limited number of electrodes to limit time and space requirements in the field, while still offering enough resolution to detect typical anomalies that can cause leaks in diaphragm walls.

5.4 Tests

5.4.1 Field test

During the construction of the Kruisplein underground parking in Rotterdam in 2011, CSL and DTS tests were executed on 4 joints to explore the possibilities of anomaly detection in diaphragm walls (Spruit et al. 2011). In joint 48-49 an anomaly in the CSL logs was found at 8.75 m below the top of the wall. Thus, this joint seemed suitable to test if the anomaly could also be found using an electrical resistivity measurement. This was about one month after completion of the wall.

A day prior to the actual measurement, a stationary electrode was pushed in the soil on the outside of the building pit to a depth of 35 m below NAP, directly in front of the joint and 3 m away from the wall (electrode on the left in Figure 49).

To detect anomalies in diaphragm walls with apparent resistivity measurements

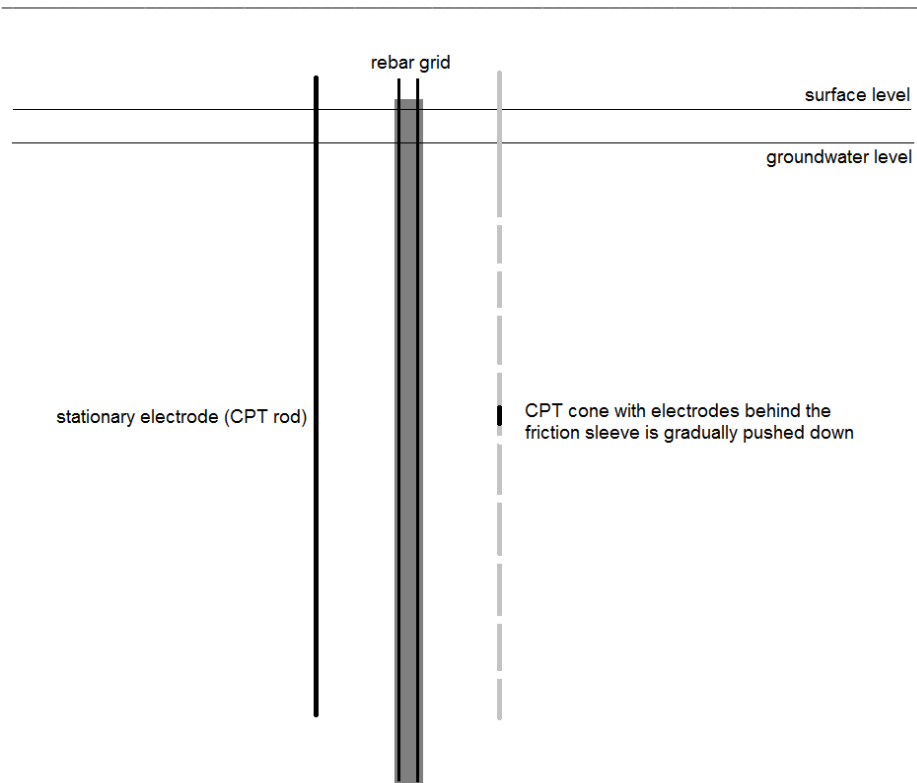


Figure 49: Schematic cross-section of the field test (not to scale)

On the test day the CPT truck (Figure 50) was placed in front of joint 48-49 on the other side of the building pit (right side Figure 49), 3 m away from the wall. The rebar cages on both sides of the joint and the previously placed stationary electrode were electrically connected to a switch box. This allowed the two electrode resistivity measurement to be taken from the CPT cone to the electrode on the other side of the wall, or from the CPT cone to the reinforcement cage north of the joint or from the CPT cone to the reinforcement cage south of the joint. Also, the local electrical ground resistance was measured in between two electrodes in the CPT cone. Each of these measurements was taken at 0.5 m interval. The cone, of which only one electrode was used for measuring the resistivity to the stationary electrode and to the rebar cages, was a 4 electrode GeoPoint earth resistivity cone.



Figure 50: CPT truck during resistivity measurements

The measurements were carried out using a two-electrode AC impedance tester Voltcraft LCR 4080 which operates at 120 Hz or 1 kHz. Using AC instead of DC avoids polarization of the electrodes. Due to the AC nature of the measurements, the obtained results should officially be called impedance instead of resistivity, but for both the unit is Ohm. For the 2-electrode tests, impedance is used, because the contact resistance causes a significant part of the measured impedance. The later used 4-electrode setup eliminates this contact resistance; therefore the measured impedance can be directly interpreted as the apparent resistivity.

The measurements show quite a lot of variation over the measured height, probably caused by variation in electrical properties of the soil, as indicated by the variation in the local impedance measured around the CPT cone.

Figure 51 shows the graphs of the local soil impedance (measured between two rings in the CPT cone), the impedance between the cone and the rebar cages of both panels, and the impedance to the electrode on the opposite

side of the diaphragm wall. All graphs run parallel to each other. In the upper five meters, high impedance has been recorded due to the partially saturated sandy top layer. Below -5 m a sequence of clay and peat layers coincide with relatively low recorded impedance, with the peat layer between -8 m and -10.5 m showing the lowest impedance values. The very local higher impedance at -14 m corresponds with a 0.3 m thick sand layer. This indicates that the contact impedance between the ring in the cone and the soil and/or the soil impedance may govern the measurements, or that the defect in this specific joint does not extend to the full width of the diaphragm wall. Because of the strong effect of the thin sand layer, it appears that the measured impedance is primarily determined by the contact impedance of the electrodes in the CPT cone. Similar results were obtained during two tests in a railway tunnel project in Delft where CSL measurements indicated anomalies in the joints.

As a result, with a two-electrode setup it will be hard to discriminate between defects in a diaphragm wall and soil impedance variation or electrode contact impedance. For better results, a different electrode setup must be considered. It also seems worthwhile to use a reference measurement on an adjacent joint with no defects. The reference profile subtracted from the profile of the suspect joint might reveal the defects more clearly, assuming that the soil profile with its impedance parameters is the same for both measurements.

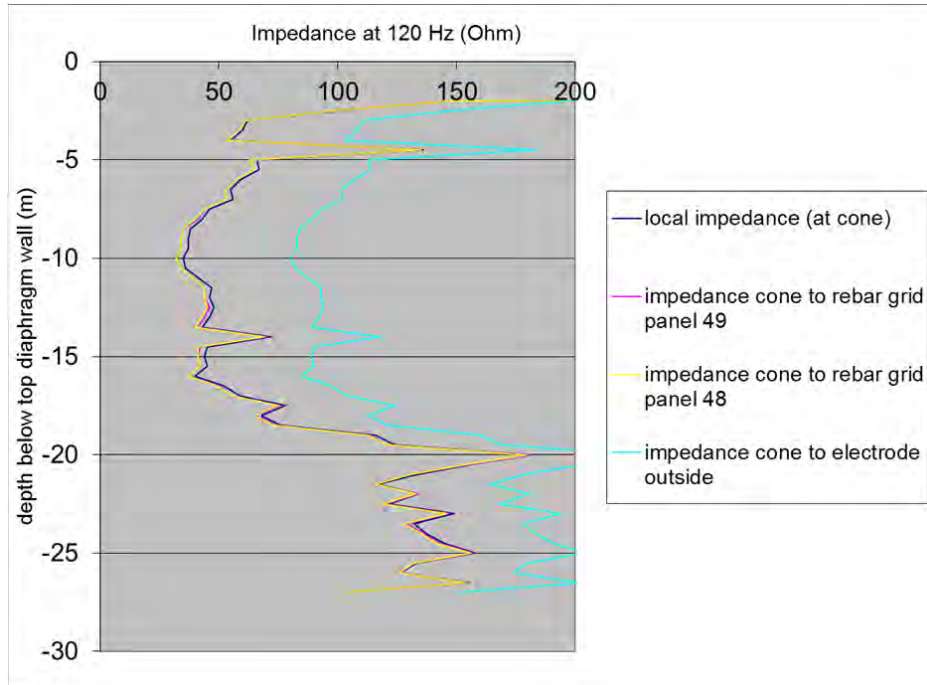


Figure 51: Impedance at 120 Hz

5.4.2 Tests on block with joint and anomaly

In 2011 a preliminary effort was conducted by a commercial company specializing in resistivity measurements, using their detection method (Vanni and Geutebrück, 2011) on one of the test blocks (Figure 52) that were produced for the CSL measurements (Spruit et al. 2014). This test block was submerged for two weeks in a large container filled with water and on the day the tests took place, the block was removed from the container. During the test, 208 sensors were connected to the outer surface of the test block in a 0.25 m grid (Figure 53). Such a test setup cannot normally be realized with in-situ D-walls.

To detect anomalies in diaphragm walls with apparent resistivity measurements



Figure 52: Test block subjected to ER measurement

The graphs provided by the company present a dimensionless parameter. Although the measurements theoretically contain resistivity information, they are always reported as relative resistivity. During the interpretation phase, the measurement results are scaled to such a degree that contrasts appear. The way this was done is not documented and depends on the engineer processing the data. Assuming that the dark areas indicate lower resistivity (Figure 53), the joint between the two blocks could be located, but the included bentonite volume (indicated with green in Figure 53) could not.

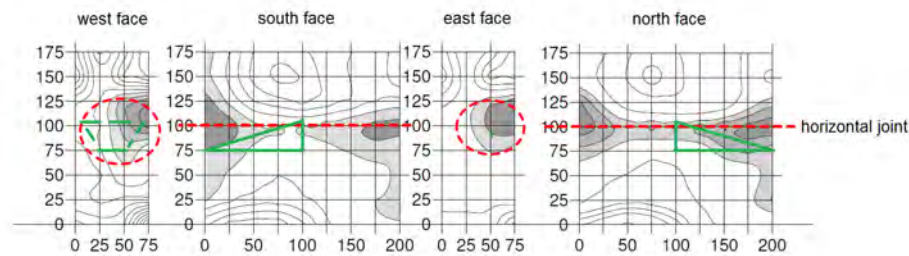


Figure 53: Measurement results (dimensionless)

The test does suggest that defects that continue throughout the total cross section of the concrete (in this case the joint between the two concrete blocks) could be located. However, the test block was saturated for 2 weeks and placed outside the water basin on the day of the tests. The concrete above and below the joint could have dried quicker than the concrete around the joint, as the joint is partially filled with bentonite and will probably retain a higher moisture content because of this and the capillary effect of the joint. If in a real situation two joints would be compared, the joint with a higher hydraulic permeability is expected to show a lower electrical resistivity relative to the better joint. If a comparative measurement setup between a known good joint and an uncertain joint is conducted, the scaling factors should remain the same for the reference and test joint.

5.4.3 Tests in plastic container with wooden barrier

Because of the unconvincing tests described above, the feasibility of resistivity measurements was first verified with a simple test.

A perforated wooden barrier was placed in the center of a plastic container of $0.9 \times 0.5 \times 0.5 \text{ m}^3$ (Figure 54). The barrier was connected to the inside of the container using silicone. The perforations were detectable with a two electrode AC impedance tester (Votcraft LCR 4080) when the electrodes were close to the barrier. This indicated that a two-electrode setup could be feasible. However, the measurements showed a strong influence of the contact resistance between the electrode and the soil, possibly limiting the resolution of a two-electrode setup.

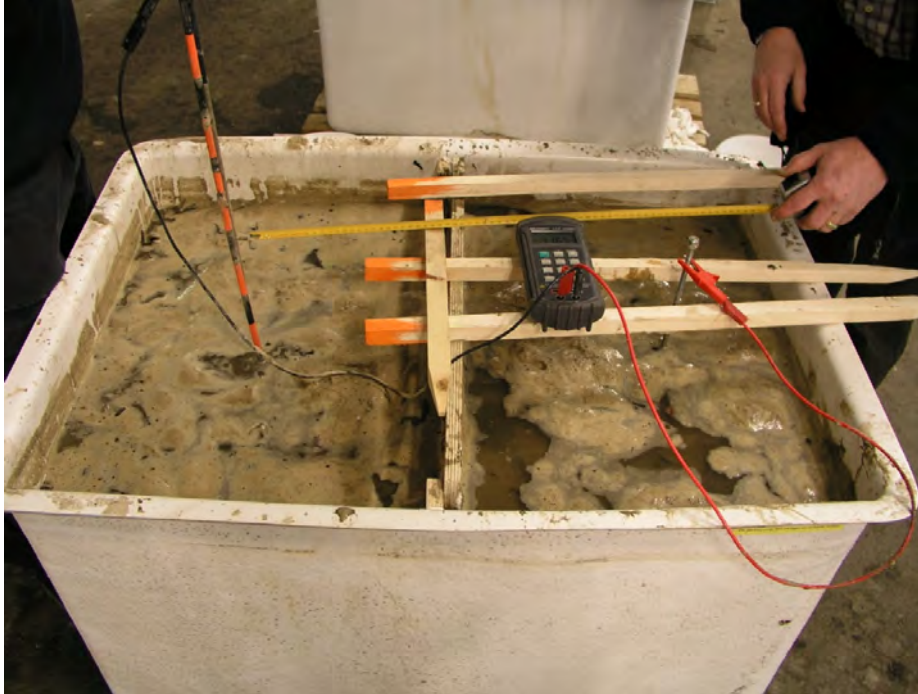


Figure 54: Test container with wooden barrier, water and sand

5.4.4 Test wall in water basin

Because of the previous test results, it was expected that only defects through the full cross-section of the wall might be detected. The simple test in the container showed that the electrodes must be placed close to the object to make detection of defects possible.

From the two batches of test blocks intended for CSL measurements (see Spruit et al. 2014) (first set from 2010, second set from 2011), a total of 4 sets of two complementary blocks were available. To investigate the possibilities of electrical testing, the following test setup was prepared:

A continuous wall (Figure 55) containing all test blocks was built (8 sections, containing 7 joints, of which 4 with defects and 3 with straight joints). This wall was placed into a basin containing water and/or soil.

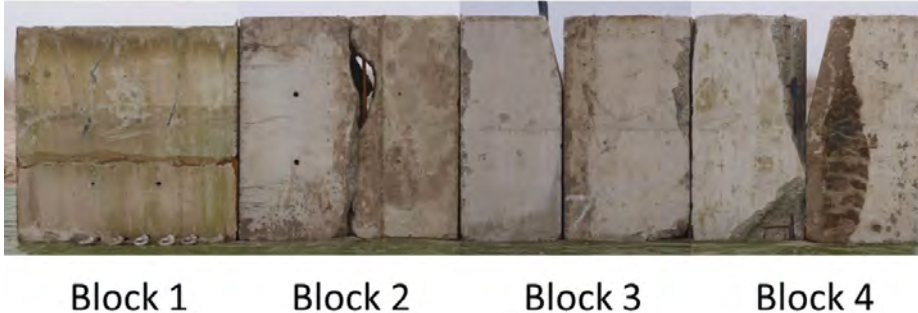


Figure 55: Test wall (side view), dimensions: height=2 m, length=8 m, width=1 m.

The configuration with soil in the basin was discarded due to practical implications (water is easy to pump into and out of the basin and varying the position of electrodes is easier). In most cases where leaks in diaphragm wall can cause problems, there will be a saturated sandy or gravelly soil, so the electrical properties are governed by the electrical properties of the groundwater.

The installation of the experiment (Figure 56) consisted of the following steps:

- Levelling and densifying the test area
- Spreading a 250 gr/m² PE sheet
- Placing the test blocks on the PE sheet
- Folding the PE sheet inwards
- Placing the mega-blocks retaining wall elements around the test wall (see Figure 60)
- Folding back the PE sheet, covering the floor and the inner vertical of the mega block wall
- Filling the joints between the test wall and the PE sheet (floor and verticals adjacent to mega blocks) with PUR foam
- Filling the 3 flat joints without defects with PUR foam
- Filling the basin with water from the nearby canal (conductivity = 134 mS/m, which is in the conductivity range of clays (Figure 48))

To detect anomalies in diaphragm walls with apparent resistivity measurements

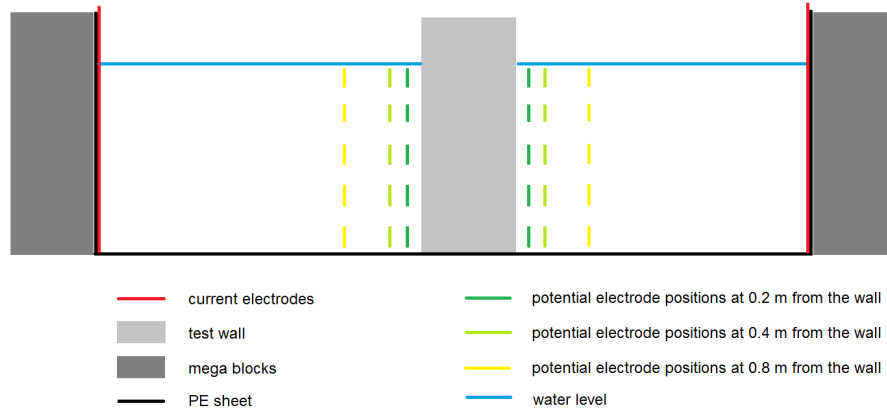


Figure 56: Cross-section of the test setup

The tests were intended to determine the maximum in-situ distance between the electrodes and D-wall that would still offer a useful resolution for detecting defects. Due to geometric spreading of the potential around areas with high permeability, it was expected that when the electrodes were relatively far from the wall, only a blurred image could be obtained, whereas when 'scanned' very close to the wall, even small defects might become visible.

It was therefore decided to test several distances between the wall and the potential electrodes, ranging from 0.2 m from the wall up to 0.8 m from the wall (see Figure 56). The current electrodes remained stationary during the tests.

The potential electrodes were installed onto a wooden frame bolted on a trolley. The trolley was able to run over a track that was installed on top of the test wall (Figure 57).



Figure 57: Top of test wall with track for positioning the potential electrodes

With the frame adjusted to the required electrode distances on both sides of the test wall and the depth below the water table, the trolley could be moved quickly (by means of a cable running through pulleys on both sides of the test wall) from one measurement position to the next (see Figure 58). The horizontal spacing of the potential electrode positions along the test wall was 0.1 m, resulting in 80 electrode positions along the wall at 5 different depths below the water table and at 3 potential electrode distances to the test wall (see Figure 56 and Figure 58).

The test was carried out using a Gossen Geohm 2 earth resistivity measurement device. The setup used 4 electrodes, 2 current (stationary) and two potential (varying position) (see Figure 56 and Figure 58). The Geohm 2 measures apparent resistivity directly by means of comparing the actual resistivity (impedance) with a calibrated internal resistor. By turning the variable resistor until no current is running through the bridge circuit, the apparent resistivity can be read directly from the variable resistor dial. The injected current is emitted at 108 Hz.

The horizontal spacing of the measurement points was 0.1 m, the vertical spacing 0.2 m, which was also the exposed electrode length. The potential electrodes consisted of 1.5 mm diameter copper wire installed vertically on a wooden frame.

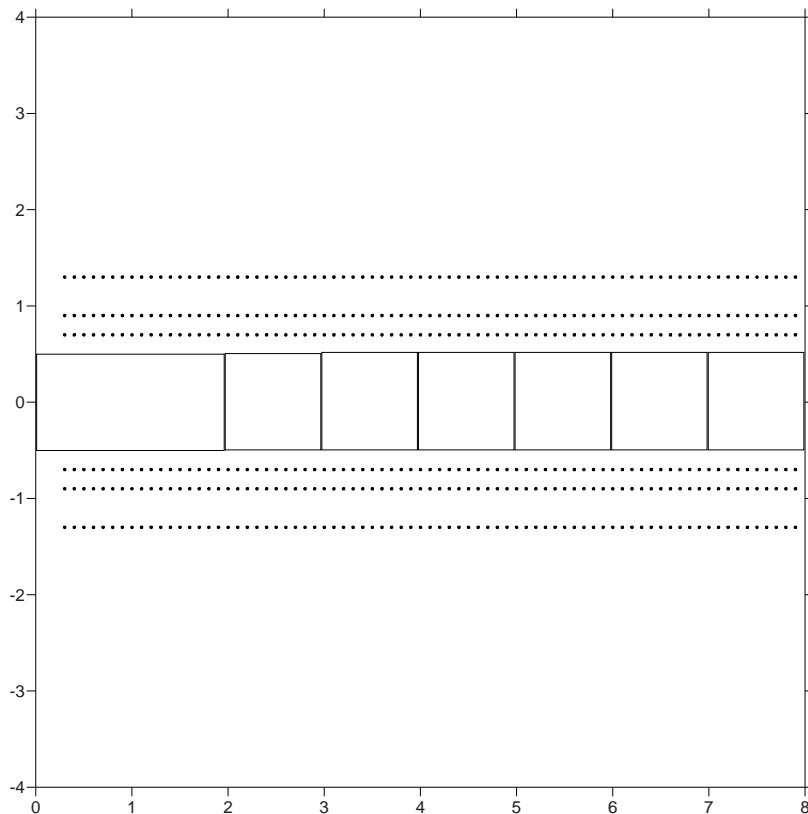


Figure 58: Top view of test wall with electrode positions (dots) for measuring the potential at 0.2, 0.4 and 0.8 m distance to the test wall, horizontal dimensions (m)

The dots presented in Figure 58 only show the horizontal distribution of the measurement locations. During the tests, 5 depths were measured, i.e. at 0.2 m, 0.4 m, 0.6 m, 0.8 m and 1.0 m below the water table.

The current electrodes were galvanized iron grids (Figure 59) fully covering the outer walls parallel to the test wall (Figure 56). This ensured current lines perpendicular to the test wall in case of a homogeneous resistivity of the test object.

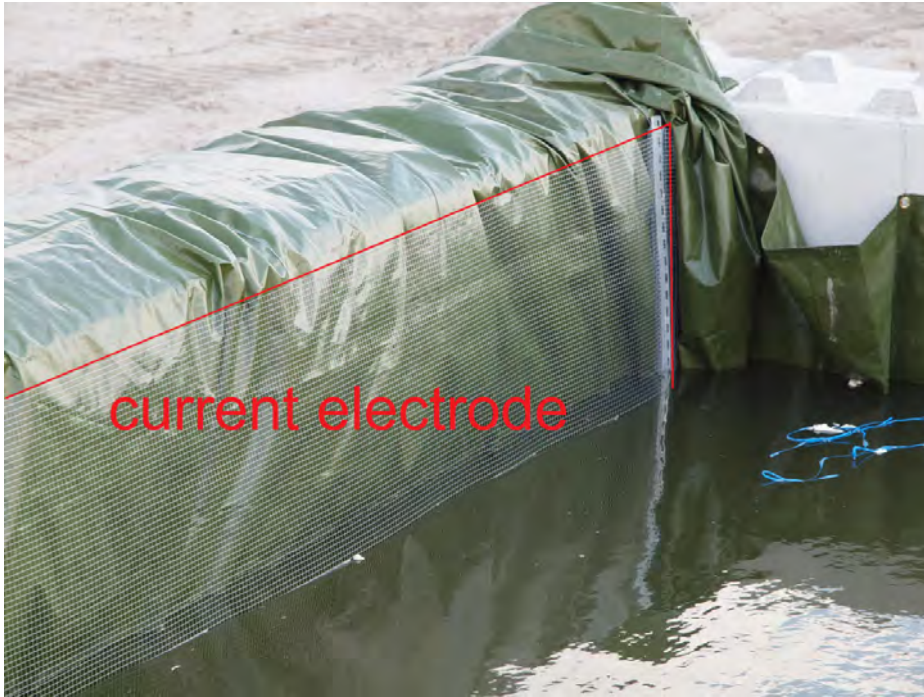


Figure 59: Current electrode grid



Figure 60: Test setup overview (looking north-east)

To detect anomalies in diaphragm walls with apparent resistivity measurements

Figure 61, Figure 62 and Figure 63 show the apparent resistivity results for the electrode distance to the test wall of 0.2, 0.4 and 0.8 m respectively.

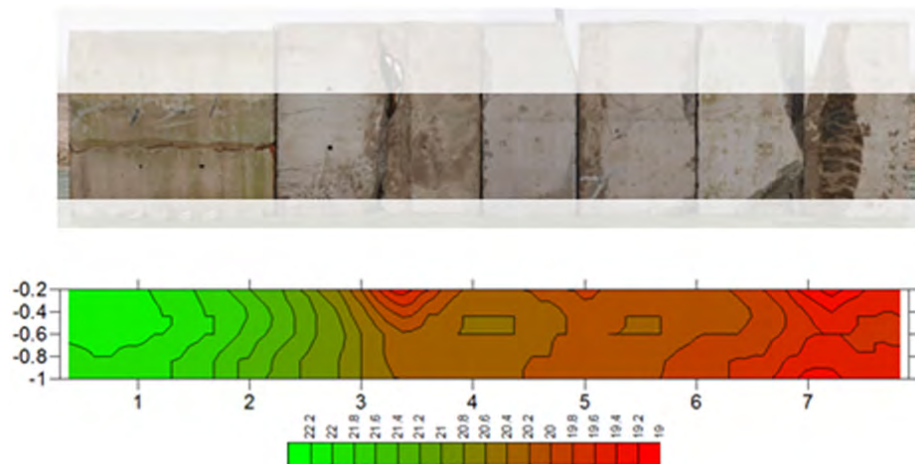


Figure 61: Apparent resistivity (Ohm) results for potential electrodes 0.2 m distance to the test wall

When the electrodes are located at 0.2 m to the test wall (Figure 61), the defects at 3.2 m, 5 m and 7 m are recognizable by the relatively low resistivity.

Block 1 does not show a defect, although a known bentonite inclusion is inside. Also the horizontal joint at half height does not show up in the apparent resistivity results. The joints that were injected with PUR foam (at 0 m, 2 m, 4 m, 6 m and 8 m) are invisible in the apparent resistivity measurements. This indicates that it is likely only defects extending the full width of the wall can be detected with these electrical resistivity measurements. This seems to be coherent with the measurements described in 5.4.2.

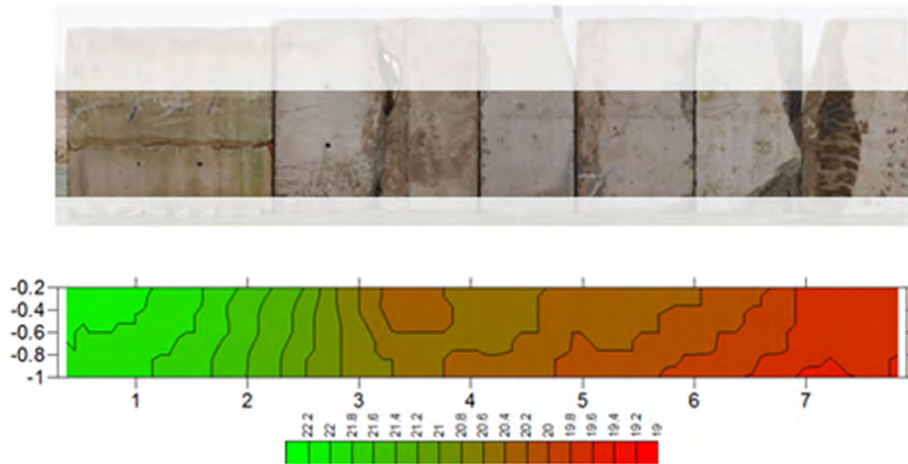


Figure 62: Apparent resistivity (Ohm) results for potential electrodes 0.4 m distance to the test wall

After increasing the distance of the electrodes to the test wall from 0.2 m to 0.4 m (Figure 62), most details are already lost. The only defect that is still recognizable is at 3.2 m. The average apparent resistivity has not changed much, suggesting that the apparent resistivity is mainly governed by the properties of the wall and that the additional water between the electrodes has a negligible effect on the absolute value of the measurements.

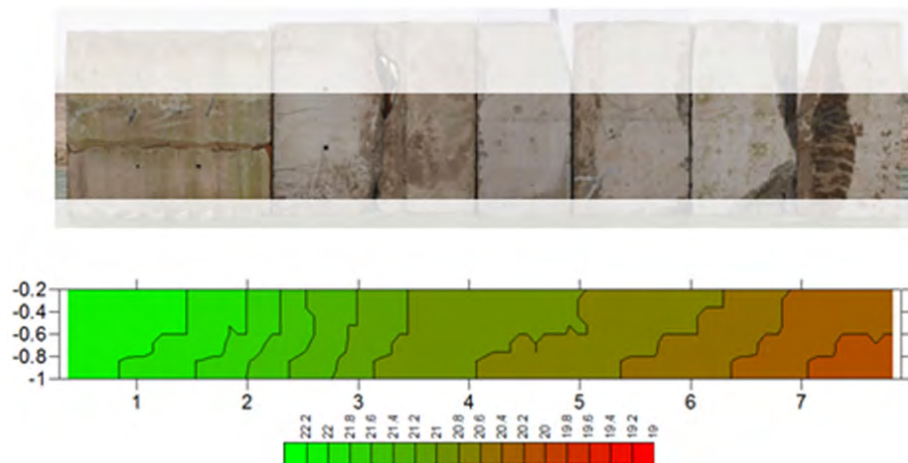


Figure 63: Apparent resistivity (Ohm) results for potential electrodes 0.8 m distance to the test wall

After increasing the distance between the electrodes and the wall from 0.4 m to 0.8 m (Figure 63), there are no longer any recognizable defects. The average apparent resistivity along the wall is still in the same league as during the tests with the electrodes closer to the test wall, confirming that the resistivity of the test wall is the predominant factor in this test.

A trend with high resistivity on the left and low resistivity on the right can be recognized in Figure 61 to Figure 63. If we subtract the resistivity results at 0.8 m between the test wall and potential electrodes from the results at 0.2 m, we effectively filter out this trend, as shown in Figure 64. Even the joints at 5 and 6 m, which were not distinguishable before, show up.

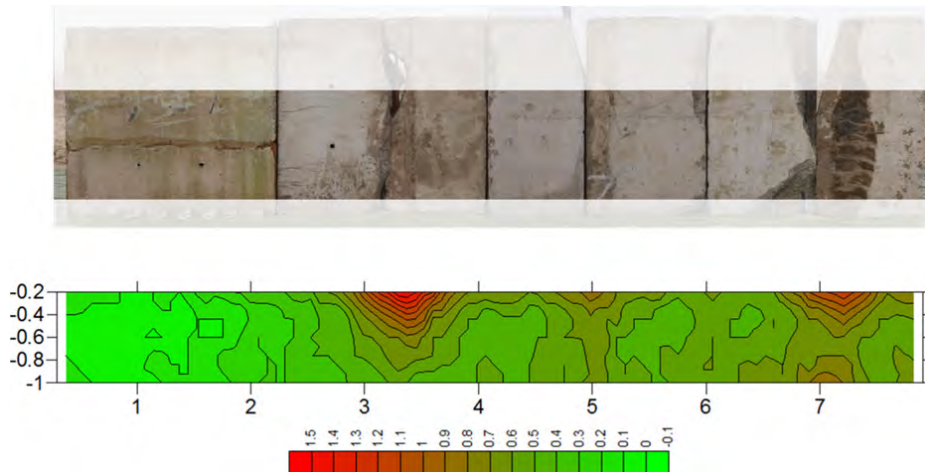


Figure 64: Apparent resistivity (Ohm) results for potential electrodes 0.2 m distance to the test wall, corrected with the results at 0.8 m distance.

An extra run at one depth with 0.1 m separation from the wall was made (see Figure 65), even though such a small distance increases the practical problems with irregularities on the outside of the D-wall. Also, push-in electrodes tend to deviate towards areas with lower horizontal stresses (due to the excavation of the D-wall trench), probably resulting in push-in electrodes hitting the concrete of the D-wall more often if introduced this close to the wall.

If the scan line at 1 m water depth is plotted for all electrode distances to the test wall (including the extra scan line at 0.1 m distance between the potential electrodes and the test wall) (see Figure 65), it becomes clear that the resolution for local anomalies dramatically decreases with increasing distance of the electrodes to the test object.

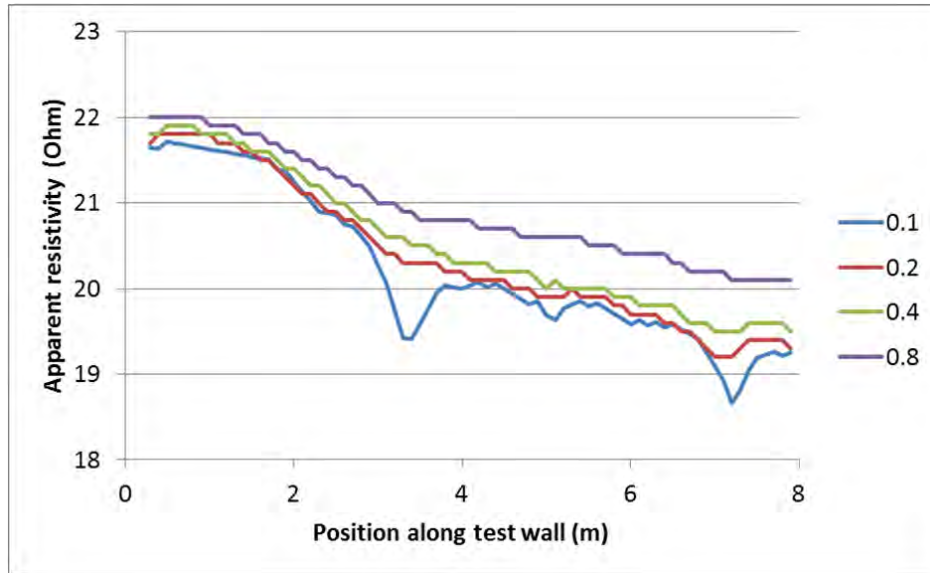


Figure 65: Apparent resistivity at 1 m below water table for 0.1, 0.2, 0.4 and 0.8 m electrode distance to the test wall.

Based on the average size of the anomalies and the limits of detection, an estimated detectable anomaly as a function of electrode distance to the object has been constructed. Table 4 shows an overview of the typical anomalies that were detectable at the different electrode distances to the test wall.

Table 4: Detected anomaly size

Electrode distance to object (m)	Detection limit illustrated	Description of known anomaly	Anomaly size (m ²)
0.1	Figure 65 at 5.0 m	Cast concrete joint of 1 mm wide and 0,1 m high	0.0001 (0.1 m * 0.001 m)
0.2	Figure 61 At x=5.0 m Y=-0.2 m	Opening of 2 cm by 5 cm	0.001 (0.02 m * 0.05 m)
0.4	Figure 62 At x=3.5 m Y=-0.4 m	Opening of 10 cm by 20 cm	0.02 (0.1 m * 0.2 m)
0.8	No anomalies detected	N/A	N/A

When the above results are plotted on a logarithmic scale for the anomaly area (Figure 66), it becomes clear that at 0.8 m electrode distance to the object, no anomalies were found because all anomalies in the test wall were smaller than 10 m².

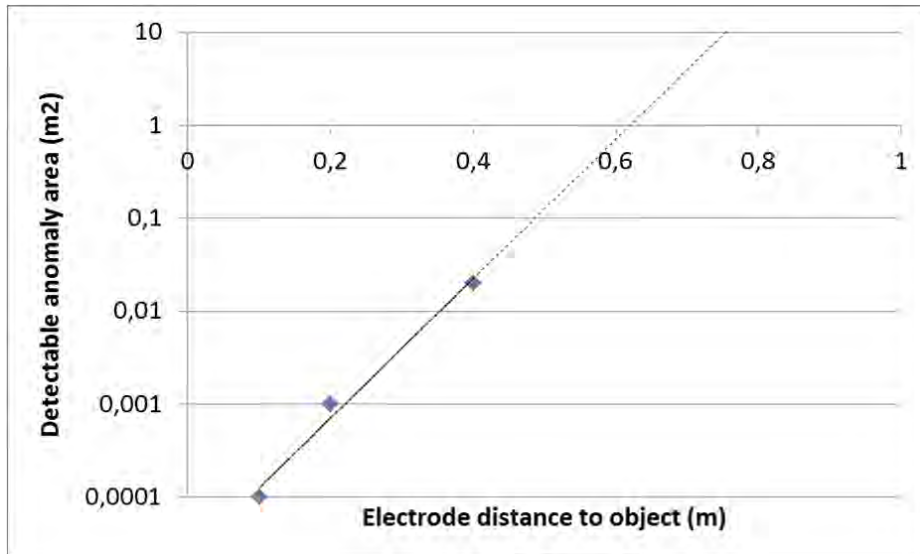


Figure 66: Detectable anomaly size and electrode distance to the test object

Because the described electrode grids cannot be used in-situ, the influence of the shape of the current electrodes on the apparent resistivity results has been investigated.

Instead of grids, single steel profiles in the middle and corners of the outer walls of the basin were used.

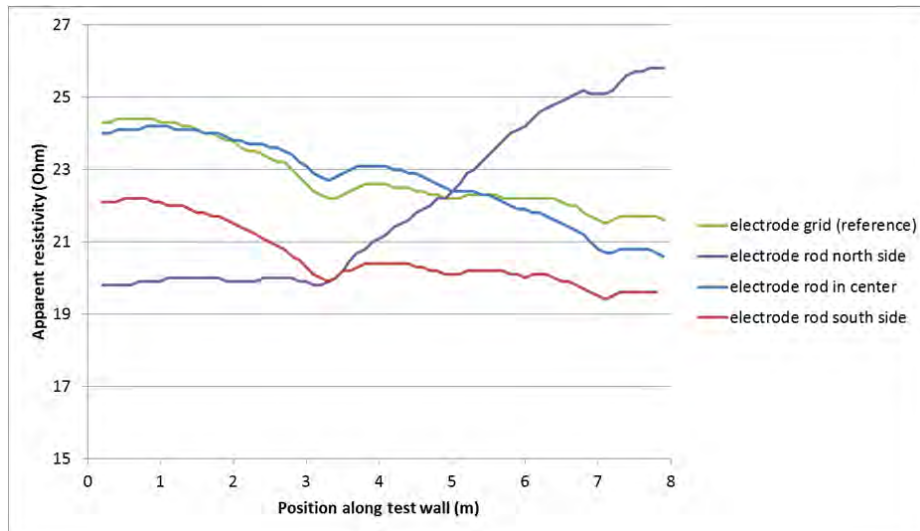


Figure 67: Current electrode shape influence (position 0 is north side of test wall)

Figure 67 shows the difference in apparent resistivity between the grid shaped current electrodes and the single steel profiles in the outer corners of the test basin (north and south) or in the center of the outer walls.

The apparent resistivity is influenced by the position and the shape of the current electrodes. The electrodes in the outer corners of the basin show a large deviation from the measurements with the electrode grids. This is probably caused by the asymmetric distribution of the current and potential lines due to the isolated walls of the basin. The image obtained with the electrodes in the center of the outer walls is rather useable. The difference between the grid electrodes and the single rods in the center of the outer walls of the test setup is almost negligible. In a field setup, single electrodes may therefore be used as long as the target area is more or less in the middle of the shortest line between the current electrodes.

5.4.4.1 Suggested measurement setup

From the measurements it can be concluded that a successful setup should include the following components:

- A 4-electrode setup in which a current is fed from current electrode 1 to current electrode 2, across the wall. The local potential at close distance to the wall is measured with potential electrodes 1 and 2, running simultaneously vertically along the joint(s) (Figure 68 and

Figure 69). It will already be hard enough to detect anomalies; contamination from electrode-soil contact resistance is unavoidable with a 2-electrode setup. The contact resistance will probably obscure the small effect of an anomaly. With a 4-electrode setup the influence of contact resistance is negligible.

- Perform a relative measurement using known good joints as references (from CSL measurements).
- Current electrodes should be placed at least 3 m into the groundwater to guarantee good contact.
- Current electrodes should preferably be placed more than 2 times the investigation depth away from the wall that is being tested.
- Potential electrodes should be located less than 0.2 m from the wall.

The image can be improved by subtracting an average resistance image, taken further away from the test object (e.g. 0.8 m), from the resistance image recorded at short distance to the test object.

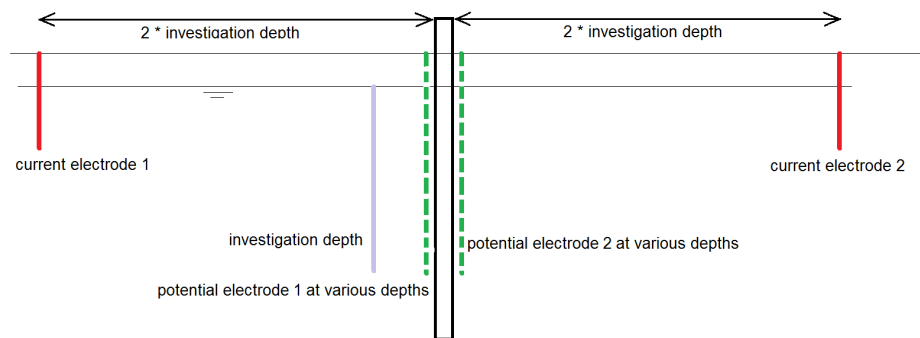


Figure 68: Suggested measurement setup for testing a diaphragm wall before excavation of a building pit (side view).

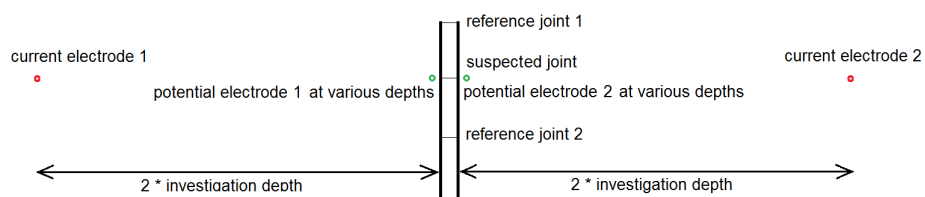


Figure 69: Suggested measurement setup for testing a diaphragm wall before excavation of a building pit (top view).

5.4.5 Test wall in water basin, tests intended for diaphragm wall as quay wall (water on one side)

Recent inspections of quay walls with diaphragm walls as retaining structures in the harbor of Rotterdam have shown areas colored by iron oxide. This could indicate that there is local insufficient quality of the concrete cover, allowing the rebar cage to corrode. Incidentally, due to transport some of the test blocks had chipped corners, exposing the rebar. This allowed for the field test to be extended to check the feasibility of an alternative measurement technique for concrete cover quality. To this end, tests were executed with one of the electrodes connected to the exposed rebar grid in the test block.

Two setups were used:

- Current electrodes as before (iron grids parallel to the test wall), with one of the potential electrodes connected to the rebar grid (4-electrode setup, Figure 70)
- One current electrode connected to the rebar grid, also acting as a potential electrode (3 electrode setup, Figure 72)

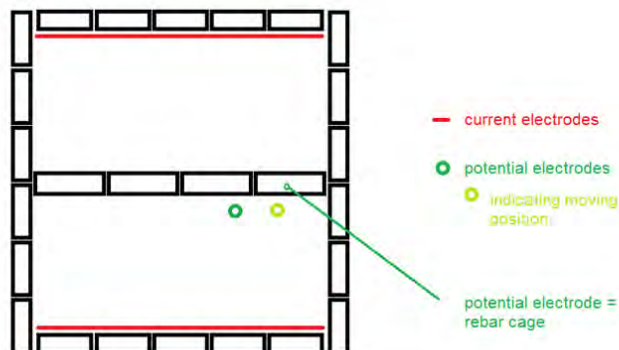


Figure 70: Test setup with 2 current electrodes, 1 mobile potential electrode and the rebar cage acting as the second potential electrode (4-electrode setup)

To detect anomalies in diaphragm walls with apparent resistivity measurements

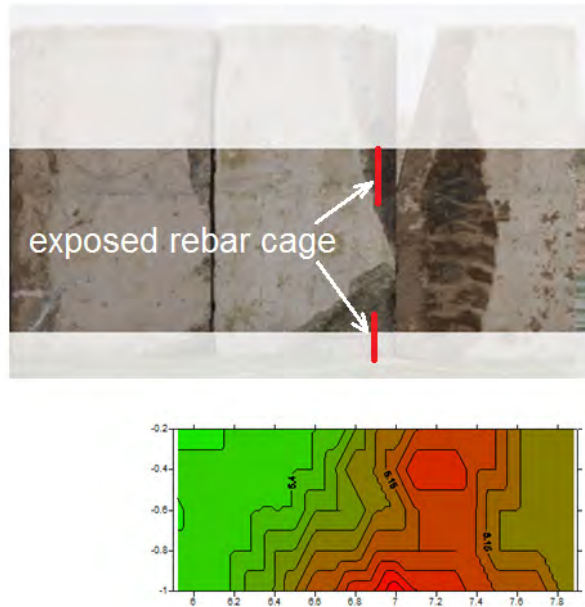


Figure 71: Apparent resistivity results for the 4-electrode test setup as indicated in Figure 70

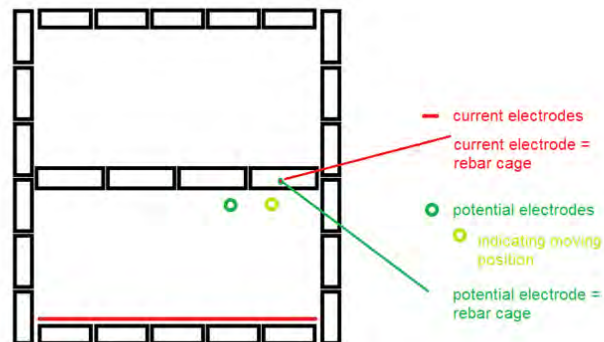


Figure 72: Test setup with 1 distant current electrode, 1 mobile potential electrode and the rebar cage acting as both the second potential and the second current electrode (3-electrode setup)

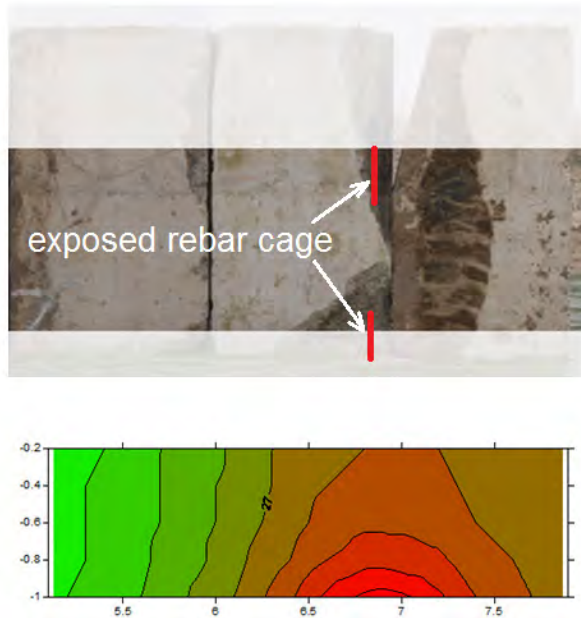


Figure 73: Apparent resistivity results for the 3-electrode test setup as indicated in Figure 72

When Figure 71 is compared with Figure 73, the 4-electrode setup (Figure 71) clearly shows a more detailed image of the exposed rebar cage. A 4-electrode setup is much more cumbersome in the field because the current electrode on the land side cannot be easily moved. As the 3-electrode setup also provides a rough identification of the exposed rebar area, a phased field survey could be effective.

First a 3-electrode setup survey can be executed to quickly discriminate between good and inferior sections. The inferior sections can be further investigated using a 4-electrode setup.

It will be necessary to calibrate the actual concrete quality and thickness of the concrete covering the rebar cage with the apparent resistivity results, as these will depend on the local conductivity of the water and concrete mixture.

To detect anomalies in diaphragm walls with apparent resistivity measurements

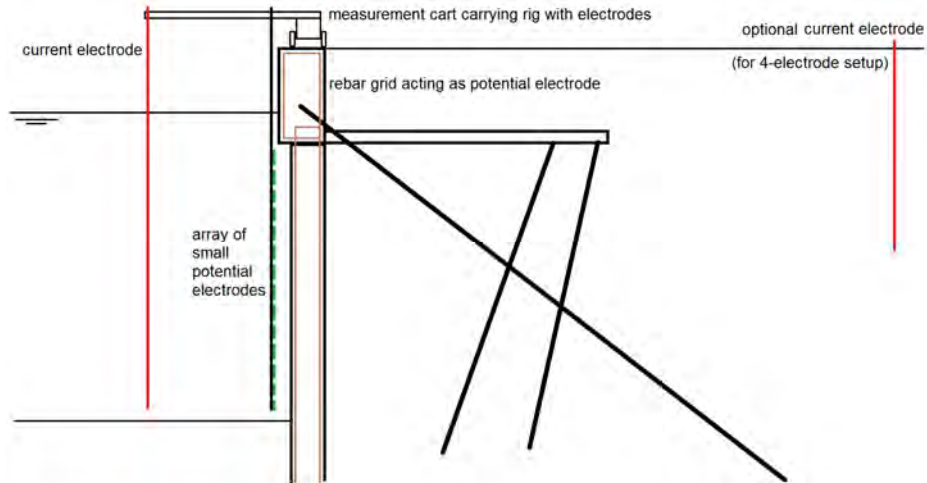


Figure 74: Suggested 3-electrode measurement setup (with optional 4th electrode) for concrete quality check quay walls

From the above results, the measurement principle illustrated in Figure 74 (without the optional current electrode on the land side) is suggested for large scale testing of the quality of diaphragm wall concrete. If anomalies are detected, a local 4-electrode measurement setup, illustrated in Figure 74 with the optional current electrode, can be used to better determine the size and shape of the anomaly. Note that such a measurement setup has not been tested within the scope of this research. Based upon the results of the test, it is expected that damaged or low-grade concrete covering the rebar cages can be detected using the above-described procedure.

5.5 Conclusions and recommendations

In this study, a test wall with known anomalies has been used to determine the detectability of the anomalies with electrical resistivity measurements. The tests described in this paper were conducted in water without the soil that would normally be present, since in permeable layers where leakage may be a problem, the resistivity is governed by the resistivity properties of the groundwater. As such, the results of these tests are expected to be applicable to permeable soil conditions.

Electrical resistivity measurements can be used to locate defects that extend to the full thickness of a diaphragm wall if the following requirements are met:

- A 4-electrode measurement setup is used
- The potential electrodes are placed very close to the wall that is being examined (potential electrodes more than 0.2 m away from the wall already seems to render the measurement useless)
- A reference measurement on a known good diaphragm wall joint at close distance (with the same geological profile) should be used to reliably identify anomalies.

Because of the limited reliability of the resistivity measurements in this application, they should always be considered as a verification option: the primary detection of anomalies in diaphragm walls should preferably be based upon CSL. As the resistivity measurements seem to only be capable of locating defects that affect the full cross section, the ER method could be used to assess the risk of leakage, provided that CSL measurements have already identified anomalies. Installing the electrodes at less than 0.2 m from the wall can best be based upon the use of perforated standpipes, installed in boreholes. Push-in electrodes will have a higher chance of hitting the wall during installation if introduced at such short distance.

Attention should be paid to:

- The effect of clay / soil / bentonite in the defect on the apparent resistivity measurements
- The effect of varying soil properties on the apparent resistivity results
- The cost and reliability of the resistivity survey should be compared to the cost and reliability of repairing the wall with jetgrouting. For some projects, preemptive repairs of anomalies will be more cost effective than re-assessment of the anomaly with resistivity measurements.

If a diaphragm wall is already exposed on one side, for example if the building pit has been excavated in submerged conditions or if a harbor along a quay wall has been dredged, the quality of the concrete covering the rebar cages can be verified with ER if:

- A galvanic connection with the rebar cages can be made
- Calibration cores are available
- There is water on the exposed side of the wall

For a quick scan a 3-electrode measurement setup can be used, to be refined with a 4-electrode setup if anomalies are detected. The 4-electrode setup requires an extra current electrode in the soil on the land side of the wall, making the measurement more time consuming and cumbersome, but

To detect anomalies in diaphragm walls with apparent resistivity measurements

delivering a much more detailed image of the quality variation of the concrete covering the rebar cages.

Ergo: Electrical measurements in a 4-electrode setup are capable of locating anomalies in diaphragm walls, but do not expect to find any anomalies with potential electrodes placed further away than 0.2 m from the test object.

Chapter 6 Discussion

6.1 Production projects

In Chapter 2 the pilot and validation tests are described. Apart from experimental testing and validation, several projects already implemented the CSL method during the period the research took place. The experience from these projects primarily adds to show the applicability of the CSL method and not fundamentally to the scientific proof. Therefore these production projects are mentioned here as part of the discussion.

Finally, a project will be described in 6.1.5, in which two test diaphragm walls were made. The test walls could be inspected over the upper 10 m because the panels were made inside the (still to be excavated) excavation for the railway tunnel in Delft. The results can be regarded as proof of concept for both DTS and CSL methods.

6.1.1 A2 Maastricht

The 'Avenue 2' project consists of the A2 freeway through the city of Maastricht and is designed and constructed by a combination of contractors with Strukton as one of the partners. Strukton Engineering had the intention to verify the quality of the D-wall panels at a section close to an existing building.

However, the sub-contractor for D-wall construction was opposed to the measurements. They stated that the PVC tubes would cause obstruction of the concrete flow, making the measurements a guarantee for joints with anomalies.

Possible obstructions are one of the reasons not to recommend a 6 tube configuration (Figure 7) for testing. Apart from the 6 tube configuration offering not much more information compared to the 4 tube configuration. Obstructions have not been observed in 4 tube configurations.

After a long debate, finally the measurements were carried out, showing only good quality joints (Galekamp 2015).

The lessons learned from this project are:

- CSL was executed in a soft rock environment without noticeable problems (other projects had been in soft soil only)
- Newly developed measurements can sometimes provoke opposition from (sub-) contractors, because the benefits are (assumed to be) uncertain, or the measurements themselves could cause problems.

6.1.2 Oceanco Alblasserdam

Contractor Cordeel was responsible for the design and construction of the new dry-dock for the Oceanco shipyard in Alblasserdam. The dry-dock uses the permanent polder principle. Diaphragm walls down to a deep clay layer form a groundwater retaining construction. To prevent the floor of the dry-dock from uplifting; a drainage system below the floor is used.

To minimize the future volumes of water that must be pumped from the drainage system, the contractor wanted the probability of leaks to be minimal.

Fugro BV was responsible for the site investigation and geotechnical monitoring. They hired Brem Funderingexpertise to execute CSL measurements. The Author was asked to interpret the measurement results and to advise where to execute repair works to reduce leakage.

Of a total of 56 joints, 1 was indicated as necessary to repair and for 2 joints it would be probable that reparation would reduce the future pumping volume.

All indicated joints were repaired by jetgrouting. Unfortunately, there was no time (and money) for pumping tests before and after the repair works, so the real benefit of the jetgrouting remains unknown.

The pumping test after reparation took place, showed remarkable high hydraulic resistance of the diaphragm wall. The actual pump flow is less than 20% of the allowed pump flow (Fugro 2013).

The lessons learned from this project are:

- Repairing three joints is hardly more expensive than repairing one joint due to the high initial cost of jet-grouting

- Aspects like accessibility can be important in deciding whether or not to repair a joint: for one of the sub-par joints, the terrain required for jetgrouting would soon be covered by a concrete floor, making future repair almost impossible

6.1.3 Railway bridge foundation adaptation Nijmegen

In 2012 the foundation of a railway bridge over de river Waal near Nijmegen needed adaptation. To better accommodate the river, the flood plains were being excavated to form a permanent side branch of the river. This meant that roughly 10 m of sand/gravel were about to be removed.

The existing foundations of the pillars of the railway bridge in the affected area were placed on raft foundations of 10m*20 m each at a depth of 5 m below surface level. Without measures, the raft foundations would be undercut by the excavation of the side channel.

To secure the raft foundations, around each raft, a rigid box consisting of 1.5 m thick diaphragm wall panels to a depth of 20 m minus surface level were designed. The panels were interconnected at the top using a rigid concrete slab around the old pillars. The slab would stay apart from the old pillars as not to introduce stress concentration in the old masonry and to allow for the horizontal forces to be transferred to the subsurface in a similar way as before the adaptation.

The concept of this in-situ formed rigid box is based upon preserving the stiffness of the soil inside the box. This implies that no soil loss from within the box is allowed and that the rigidity of the box needs to be very high to minimize bending of the panels and thus limiting the stiffness reduction of the soil and the settlements of the pillars during construction.

To assure that the box is indeed soil-tight, CSL testing on all joints was included in the contract requirements.

Because of the limited working space below the railway bridge, the contractor chose Stein (Stein 2015) flat stop ends. These stop ends are extracted vertically by hydraulic jacking before complete curing of the concrete has taken place.

During the first set of measurements (pillar 1), the height of the PVC tubes was not properly recorded to a reference level by the measurements contractor, this was hard to rectify. Also the auto-gain feature of the PDI equipment (Pile Dynamics Inc 2015) used on site proved to be unreliable. The field engineer had switched this feature off and chose the gain manually for each test. Unfortunately, this lead to hard to interpret measurement

results because of the varying gain factors between tests on one joint and varying gain factors between joints. For the next testing sessions (pillars 2 and 3) the Author demanded a fixed gain to be applied to all similar scans (e.g. gain=200 for all scans parallel to the joint, gain=400 for all scans perpendicular to the joint and gain =600 for all scans diagonally through the joint). After this change in the measurement protocol, the rest of the results were much easier to interpret. The engineer had already measured many bored piles. After the problems with the first data set, he admitted that scanning diaphragm walls is more different to scanning bored piles than he had thought. Unfortunately, the PVC tubes of the first set were no longer usable, so the CSL tests could not be re-run.

Three anomalies were detected. All three were of the same type: the scans perpendicular to the joint showing decent signal, only the diagonal scans showing low quality.

After chiseling the joints open, bentonite was found in the core over the same depths as the bad signal on the diagonal scans.

The bentonite inclusion was caused by imperfect chiseling away the spill concrete that surrounded the flat stop-end joint profiles.

Due to the remaining spill concrete, the fresh concrete of the next panel could not reach the joint, leaving the bentonite included in the center of the joint, filling the shape the joint profile had left behind (Figure 76).

Without the CSL measurements, the anomalies would probably not have been found. Although soil tightness could have been sufficient initially, during the engineering lifetime of the construction, the unreinforced joint area with the bentonite filled core, would have been a weak spot.

The lessons learned from this project are:

- Always use an absolute reference level for the CSL measurements
- Check the auto-gain feature of the equipment on several test joints. If the automatic function is unreliable, determine the optimal fixed gain settings using the previously mentioned test joints
- Make a fast interpretation of the measurements, just to check if re-running the test might be needed. Often the top of the diaphragm wall will be demolished rendering future measurements impossible
- If unprecedented results show up in the logs: investigate the presumed anomaly if possible

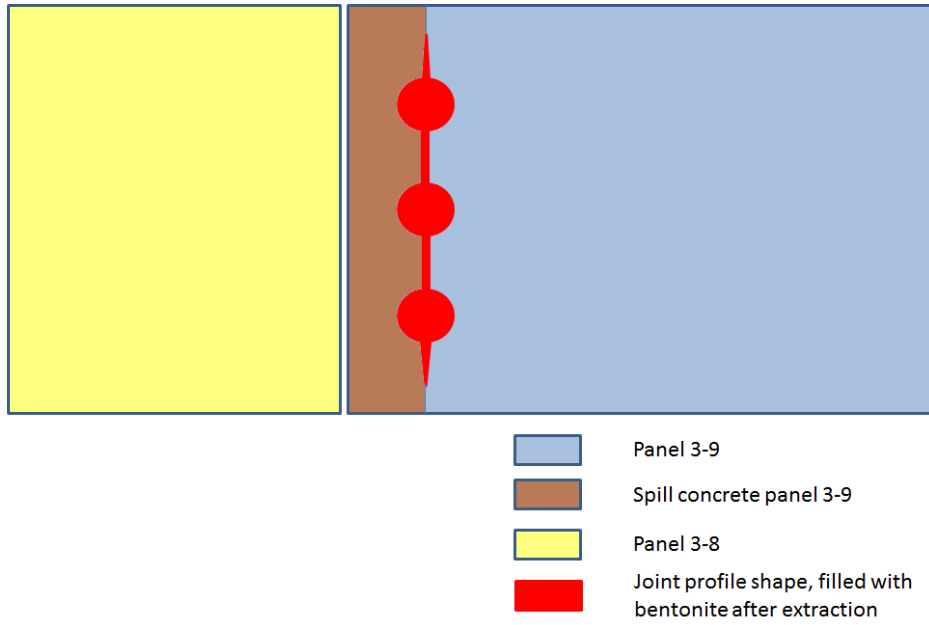


Figure 76: Interpretation of the anomaly (top view/cross section), panel 3-8 was excavated after 3-9.



Figure 77: Picture showing the intended joint and the accidental extra joint due to non-removed spill concrete



Figure 78: Temporary situation before diaphragm walls are covered with high quality concrete cover



Figure 79: Result before excavation of the channel

6.1.4 Railway bridge foundation adaptation Deventer

This was a similar project to the one described in 6.1.3.

The CSL results generally showed no defects.

The only striking anomalies in the scans were caused by the prefabricated permanent (single use) joint profiles consisting of concrete with a hollow core.

If such profiles are used, it must be accepted that those joints cannot be reliably verified with CSL.

This also applies for other objects with material with different properties than concrete: such objects could cause disturbance of the CSL measurements or hinder the interpretation of the measurement results.

The lessons learned from this project are:

- Objects with properties differing from concrete can affect the measurements. These objects could for example be prefabricated hollow concrete or steel (one-way use) joint profiles.

6.1.5 Diaphragm wall test Delft

In cooperation with J.H. van Dalen, an extensive field test has been prepared. The test was primarily intended to confirm the flow models that van Dalen has been using to simulate the flow of concrete in a diaphragm wall panel during concrete casting (van Tol et al. 2014). In this test the flow of concrete has been verified using RFID (radio-frequency identification) tags, concrete coloring and detailed concrete level recording at several locations in the trench. Results for this part of the test, as well as additional details on the test setup and execution, are given in van Dalen (2015).

Two panels were constructed within the projected (still to be excavated) railway tunnel in the 'Sporzone' project in Delft (Netherlands). In these panels, several parameters that possibly limit the concrete flow have been varied. The varied parameters were mainly: flow parameters of the bentonite slurry (e.g. fresh and very old with cement contaminated bentonite), the consistency of the concrete, the rebar spacing within the cage, distance of the rebars to the joint etc.

During slurry refreshing (only panel one) and concrete casting (both panels) DTS measurements were carried out in which all lessons learned (sensors

and acquisition time) were included. 4 automated (custom made) mechanical concrete level sounders were deployed to be able to verify the concrete levels recorded with DTS. Panel two was kept untouched for a week between excavation and concrete casting. No bentonite slurry refreshing took place. Before excavation and after full hardening of the panels, the joint in between them was tested with CSL.

After excavation of the building pit of the railway tunnel, the two panels could be inspected from both sides. During the inspection, pictures were taken and 3D laser-scans were made. With an RFID scanner, the RFID tags that had been time stamped when thrown into the concrete flow at the tremie were retrieved. After full inspection of the diaphragm walls, the panels were demolished. This allowed for inspection of the core of the panels and the joint between them.

6.1.5.1 CSL interpretation

Using the anomaly vs CSL signal correlations determined with the laboratory test blocks (Figure 18 and Table 3), the expected anomaly shape in the joint between the two panels has been derived.

The interpretation went through the following steps:

- determination of anomaly size based upon Delay in Arrival Time (DAT) (for each scan), assuming both sand and bentonite as anomaly filling material
- determination of most probable anomaly size and properties
- combination of the 4 scans running through the joint
- presenting the interpreted anomaly over the joint cross section

To make the first step possible, it is necessary to choose a base First Arrival Time (FAT) to which the DAT is defined. This has been done for each scan separately as the distance between the measurement tubes is unique for all scans (the configuration of the tubes was not in a perfect rectangle).

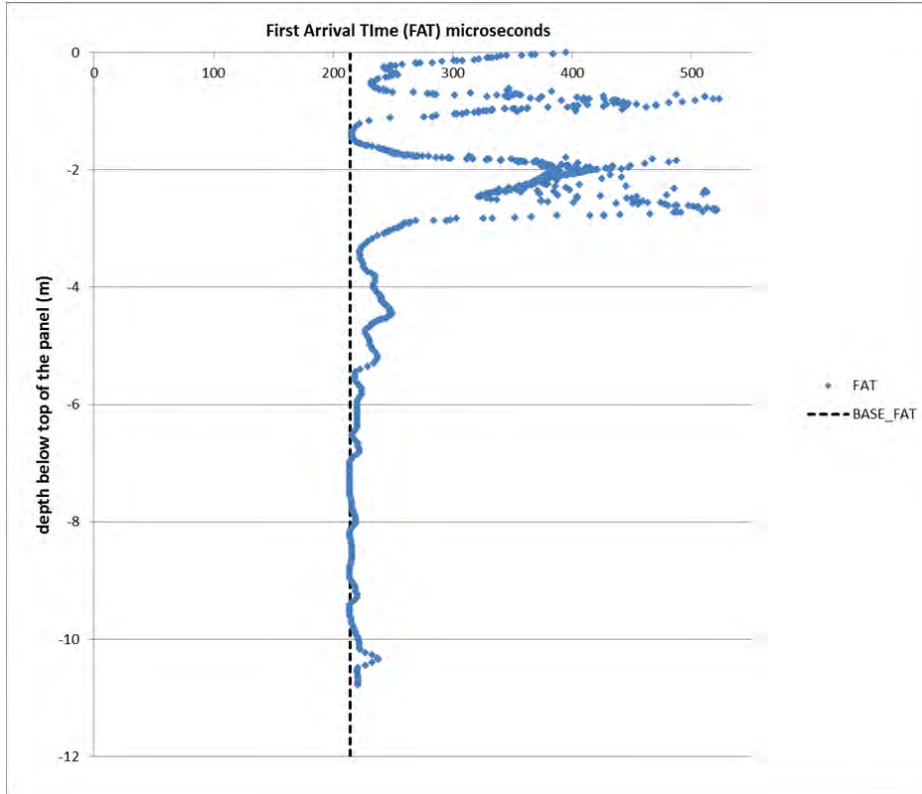


Figure 80: Determining the base-FAT to which the DAT is determined (crossing 1-3)

Using the formulae from Table 3, the anomaly size as a function of DAT has been calculated, assuming both bentonite and saturated sand as fill material, to estimate the upper and lower boundaries of the anomaly.

Figure 81 shows the expected anomaly thickness on crossing 1-3 (top view of the panels and CSL crossings in Figure 82) in the joint for two assumed fill materials. In the laboratory tests, the saturated sand showed a much higher DAT per mm anomaly as compared to the bentonite suspension. Given the recorded DAT, the resulting anomaly width assuming a saturated sand fill material will be less than when a bentonite fill is assumed.

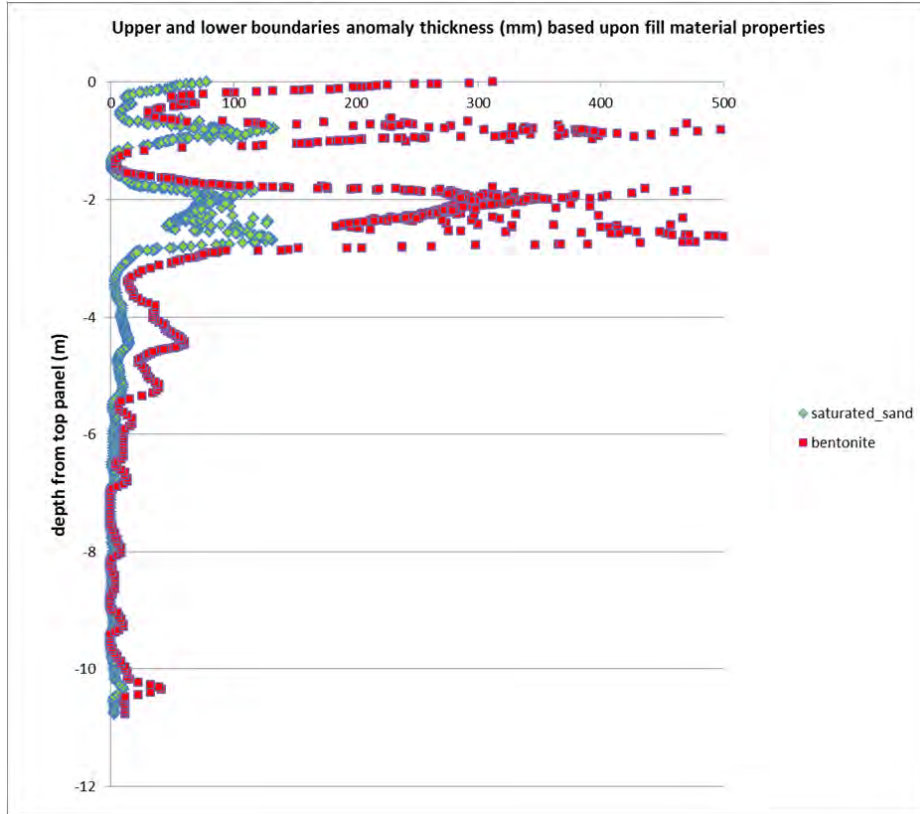


Figure 81: Anomaly thickness based upon DAT (1-3)

For each of the possible crossings (indicated in green in Figure 82) between the CSL tubes, an interpreted anomaly thickness along the depth has been determined.

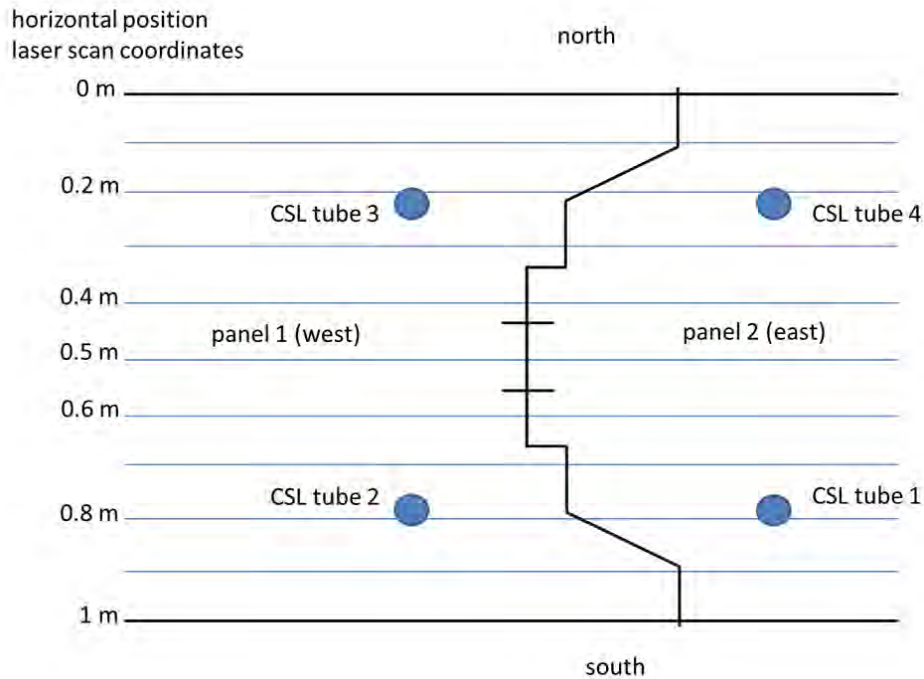


Figure 82: Schematic top view of the test panels

To convert the separate scans of the CSL measurement into an integral image of the anomaly in the joint, each scanline has been given an interpreted position within the joint.

To form an image of the joint, looking from west to east (side view of exposed joint of panel 2), the scan line between tubes 3 and 4 has been given horizontal positions 0 m and 0.2 m.

Scan line 1-3 has been referenced to horizontal position 0.4 m, whereas horizontal position 0.6 m has been coupled to scan line 2-4. Finally, the southern end of the wall has been imaged using scan line 1-2 for horizontal positions 0.8 m and 1 m.

Surface plots of the anomaly thickness in the joint have been generated assuming bentonite or sand as fill material in the anomaly (Figure 83).

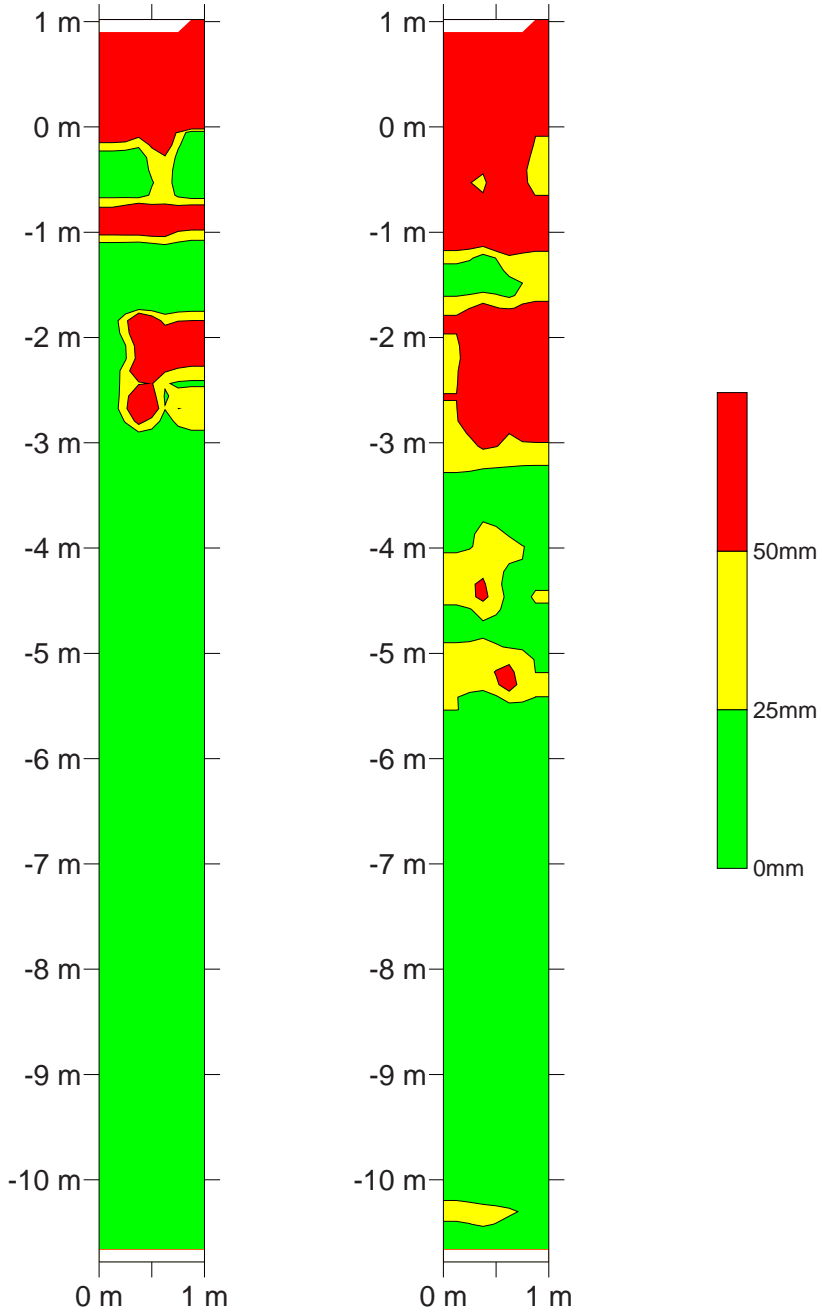


Figure 83: Interpreted anomaly thickness (mm) in the joint, assuming saturated sand fill (left) or Bentonite fill (right)

6.1.5.2 Comparison with 3D laser scan

During the phased excavation of the building pit to level -10 m, panel 1 has been demolished in steps following the excavation level of that phase. In each excavation stage, a 3D laser scan of the exposed part of the joint of panel 2 has been made using a Faro laser scanner LS (Faro 2005). The 3D laser scans of all phases have been stitched together to form a 3D model of the exposed joint.

Assuming good quality concrete along the joint in panel 1, the anomalies in the exposed joint found in the 3D laser scan should correlate with the interpreted anomalies of the CSL measurements (Figure 83).

The joint shape of panel 1 has been assumed to be without anomalies. The CloudCompare 2.6.0 software has been used to extract vertical scan lines from the 3D model with randomly distributed x-y-z dots generated by the laser scanner. The CloudCompare software offers the possibility to generate a reference raster on which the distance to the 3D object is sampled. A vertical reference grid, parallel to the joint has been used. The value that is stored in the grid, is the calculated average distance from the available randomly distributed points in the grid cell perpendicular to the reference surface (Figure 84).

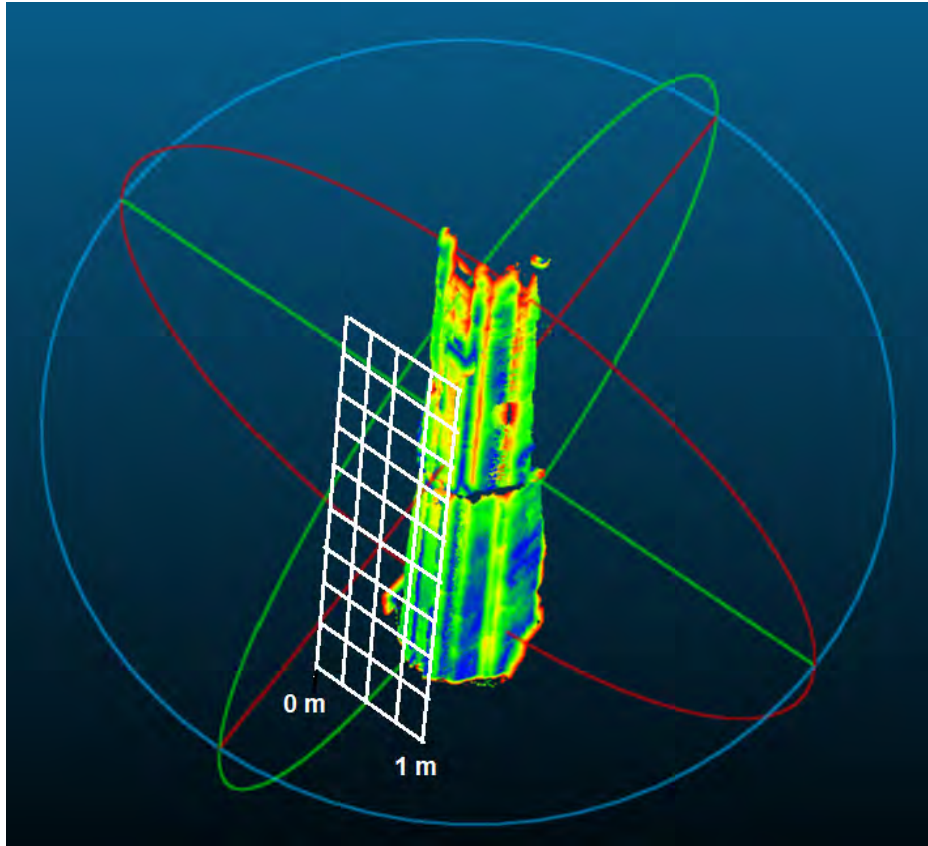


Figure 84: 3D model from laser scan data, with a sketch of the reference grid (in white)

The first comparison between the laser scan and the CSL measurements has been based upon a gridline spacing of 0.05 m. From the generated grid, the vertical scan lines of the joint have been used. These scan lines have been compared with the interpreted anomaly thickness based upon the CSL results and assuming bentonite in the anomaly. Just like the CSL interpretation, the lowest recorded value is used as a reference (anomaly width = 0 m).

The CSL results of the 3-4 scan line had the best correlation with the 3D laser scan line at position 0.4 m whereas a fit with position 0.2 was expected. In Figure 85 the CSL results from the 3-4 scan have been plotted against the laser scan results at positions 0.2, 0.3, 0.4 and 0.5. Position 0.4 clearly shows the best correlation with the CSL results. Probably the

ultrasonic signal chose the shortest route through the core of the wall with a relatively small anomaly width.

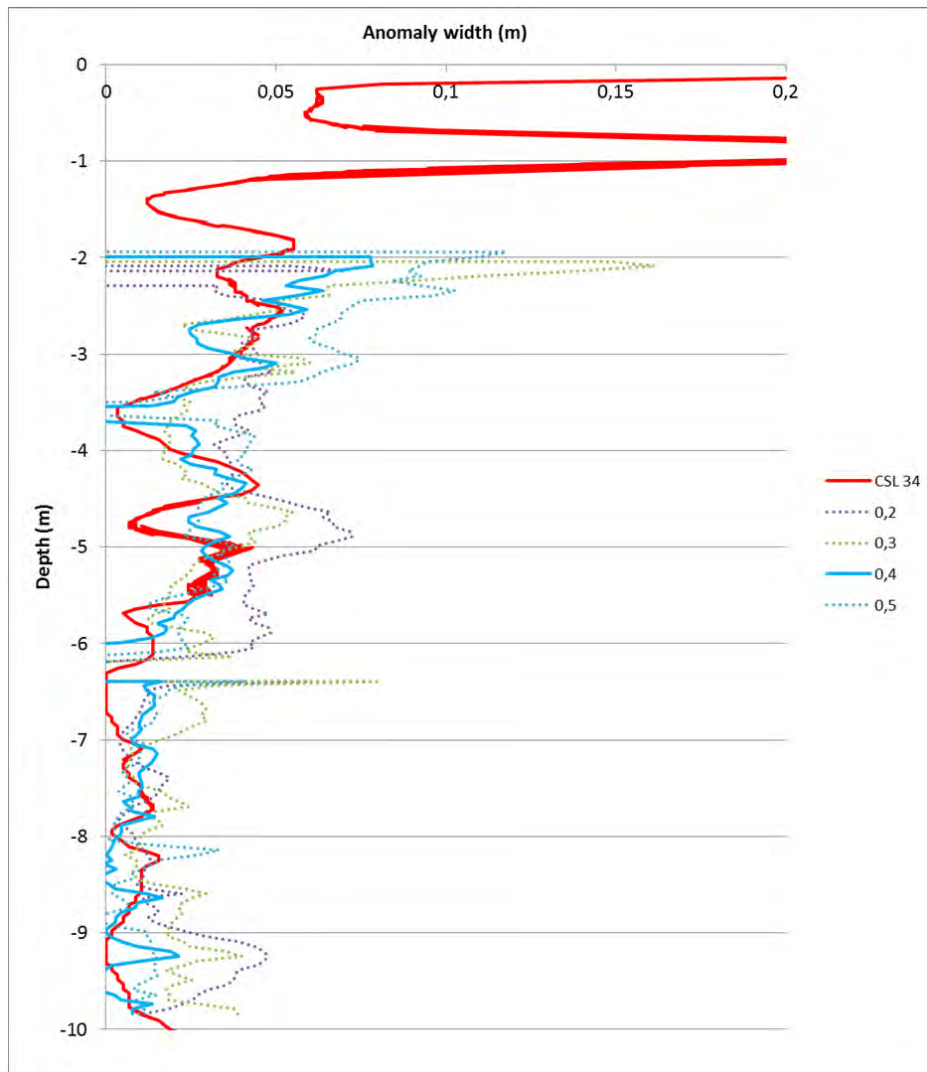


Figure 85: CSL interpretation assuming bentonite in the anomaly for scan line 3-4, compared with four scan lines from the 3D laser scan

The interpreted anomaly width of the diagonal CSL measurements (1-3 and 2-4), show the best fit with the 3D laser-scan line in the center of the wall, which is the scan line at position 0.5 m (see Figure 86).

There are discrepancies in absolute value, mainly caused by the averaging effect of the CSL measurement. Very small details will be lost because the ultrasonic signal can bypass these small anomalies.

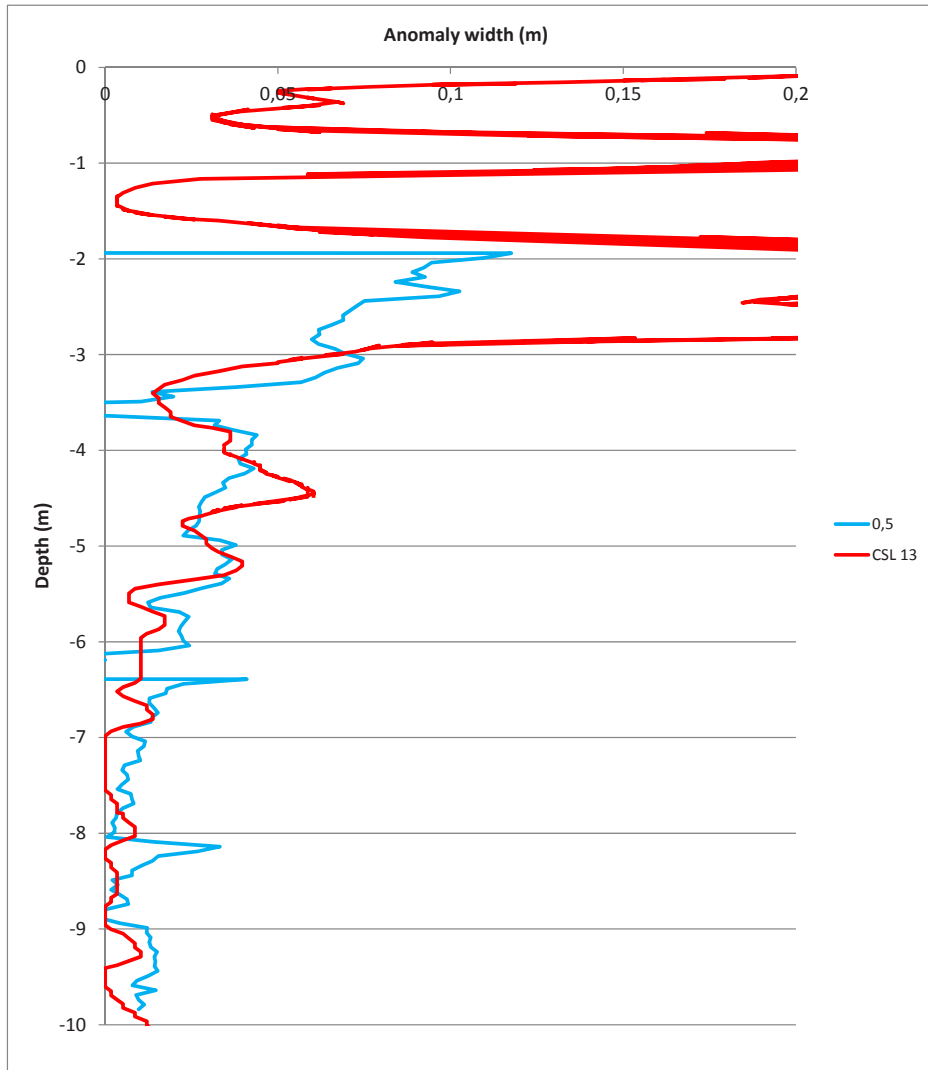


Figure 86: Example comparison of interpreted CSL results assuming a bentonite anomaly with 3D laser scan anomaly dimensions

The CSL results of the 1-2 scan line had the best correlation with the 3D laser scan line at position 0.6 m.

For all four CSL and laser scan combinations, the anomaly dimensions from the laser scan have been correlated with the in vertical direction nearest available DAT (Delay in Arrival Time) results from the CSL measurements (see Figure 87).

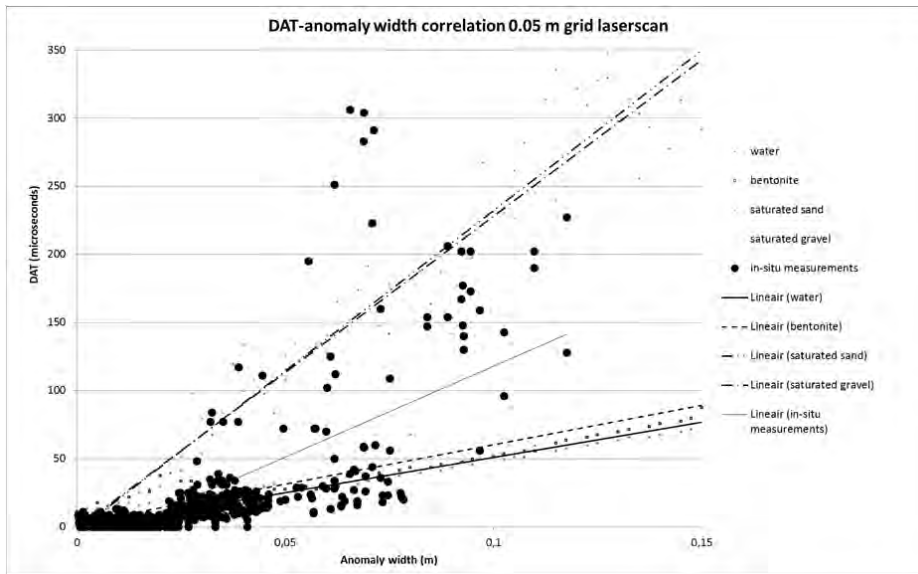


Figure 87: Measured DAT correlated with actual anomaly width from laser scan (0.05 m grid) and compared with laboratory measurements from Figure 18

The gridline spacing has been varied between 0.02 m and 0.2 m to estimate the spatial resolution of the CSL results. When comparing Figure 87 with Figure 88, Figure 88 shows more data points due to the higher grid density. In the range below 50 microseconds DAT and below 0.1 m anomaly width, the bandwidth of the measurement results appears wider for the 0.02 m grid spacing. The real bandwidth is hard to estimate graphically due to the large number of points. If the 3D model is sampled at 0.1 m and 0.2 m (Figure 89 and Figure 90), the bandwidth appears to be smaller than for 0.02 and 0.05 m grid spacing.

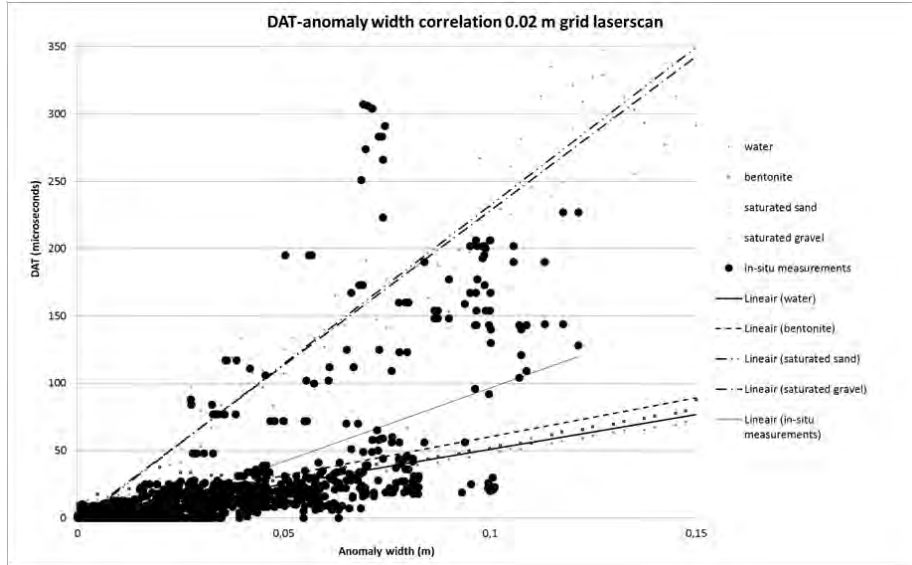


Figure 88: Measured DAT correlated with actual anomaly width from laser scan (0.02 m grid) and compared with laboratory measurements.

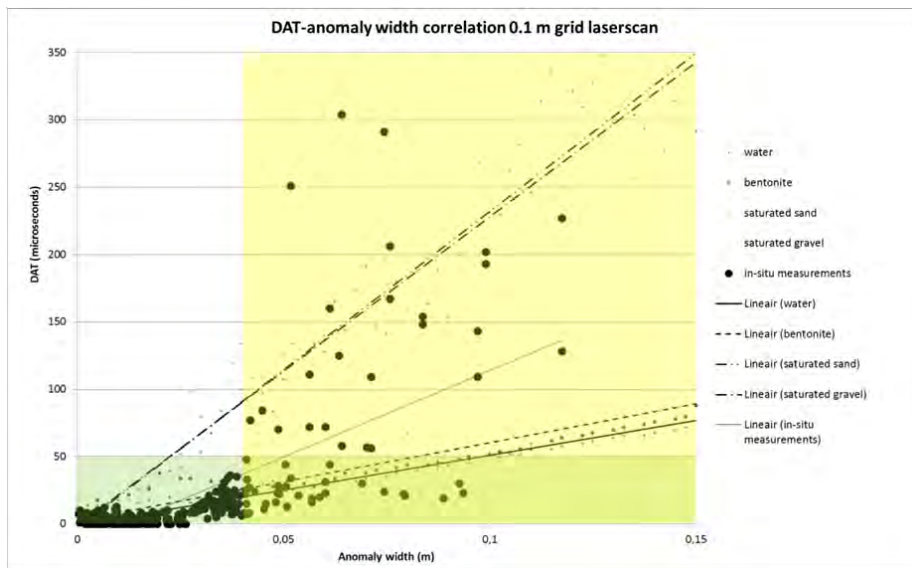


Figure 89: Measured DAT correlated with actual anomaly width from laser scan (0.1 m grid) and compared with laboratory measurements.

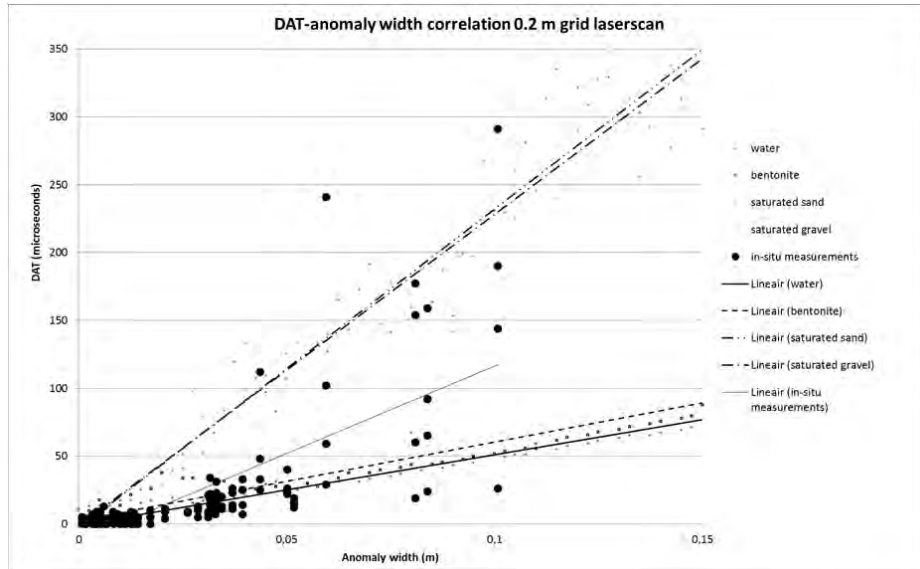


Figure 90: Measured DAT correlated with actual anomaly width from laser scan (0.2 m grid) and compared with laboratory measurements.

Below 50 microseconds DAT (green area in Figure 89), the actual anomaly width correlates well with the results obtained for water and bentonite in the laboratory tests. If the DAT is more than 50 microseconds, the results are generally between the laboratory correlation graphs for bentonite and sandy material. For anomaly widths below 0.04 m, the assumption of bentonite as material in the anomaly correlates best with the 3D laser scan results. Above 0.04 m anomaly width (yellow area in Figure 89), the results are generally between the laboratory correlation graphs for bentonite and sandy material.

To evaluate the actual bandwidth, the results have also been analyzed statistically. For each recorded DAT, the difference between the laser scanned anomaly width and the calculated anomaly width based on the assumption of bentonite in the anomaly has been analyzed. For each set of 5 subsequent DATs, the average and standard deviation have been determined.

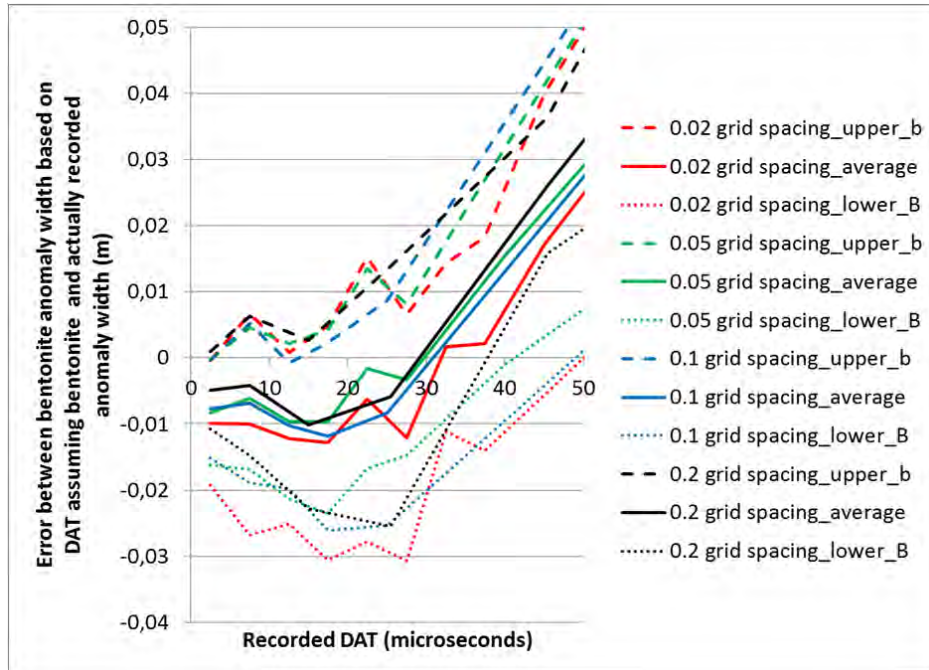


Figure 91: Error distribution as a function of DAT (up to 50 microseconds) and laser scan grid spacing. Upper and lower boundaries are set to average + and – the standard deviation.

Figure 91 shows how the average error and the standard deviation around it hardly relate to the laser scan grid spacing. Generally, there seems to be an offset of about 0.01 m, probably caused by setting the 'zero-anomaly-thickness' in both the CSL recordings and the laser scan data. The standard deviation is about 0.01 m as well for DATs below 20 microseconds. For longer DATs, the standard deviation increases together with the increasing error between the actual anomaly width as determined from the laser scan data and the anomaly width based upon DAT and assumption of bentonite. The 0.02 m grid spacing shows a slightly higher standard deviation compared to the other grid spacings.

For longer DATs, the error of the bentonite model and its standard deviation increase linearly (see Figure 92). Between DAT values of 100 and 200 microseconds, the 0.02 m grid spacing shows a smaller standard deviation due to the higher number of measurement points.

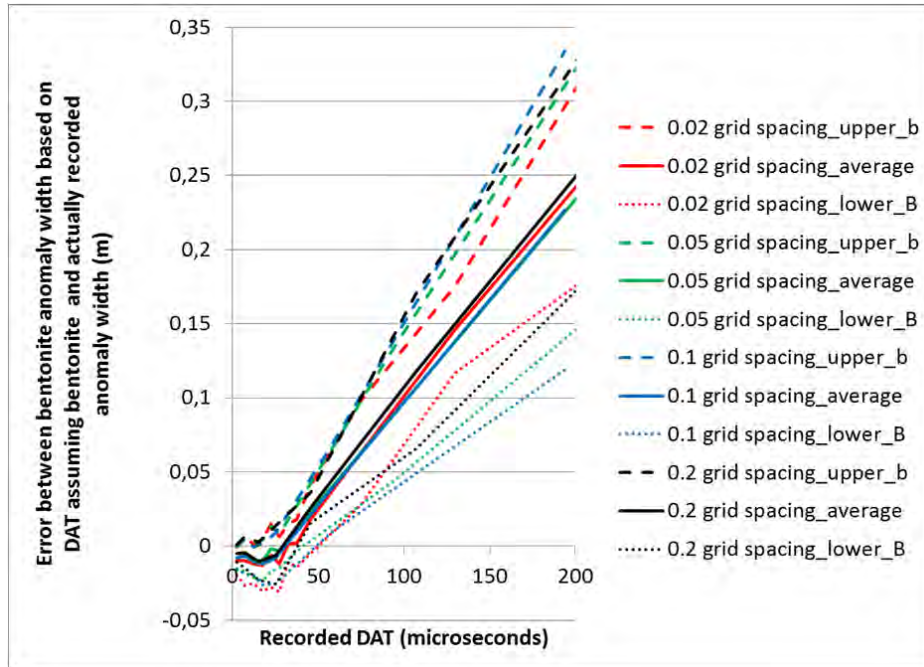


Figure 92: Error distribution as a function of DAT (up to 200 microseconds) and laser scan grid spacing. Upper and lower boundaries are set to average + and – the standard deviation.

The increasing deviation between the laser scanned anomaly width and the anomaly width based upon DAT and assuming bentonite, could be caused by the low-grade concrete at the levels with large anomaly thickness. The 3D laser scan only recognizes the reflection on an object, not the concrete quality. If poor-grade concrete is present, the CSL measurement will be affected by this local low-grade concrete quality, resulting in a higher DAT. If (during the interpretation) all concrete in the panel is assumed to be of perfect quality and all deterioration of the signal is caused by anomalies in the joint, it is logical that the interpreted anomaly thickness in the joint will increase due to adjacent low-grade concrete. It is also probable that thicker anomalies tend to consist of sandier bentonite than relatively thin anomalies, because stiffer sandier bentonite is more difficult to expel from the trench by the concrete than fresh bentonite slurry. It is important to remember that the results shown here are the result of an attempt to invoke anomalies by (among other) not refreshing the bentonite slurry, keeping the trench open for more than a week and by using relatively stiff concrete in the upper part

of panel 2. In regular production panels, the bentonite slurry will contain much less sand and the concrete should have much better flow properties. It is therefore safe (and recommended) to assume bentonite as material in the anomaly in the joint. This might give an over-estimation of the anomaly size, especially if an anomaly width of more than 50 mm is calculated from the DAT results. The degree of over estimation will depend on the actual material inside the anomaly and the concrete quality in the wall on both sides of the anomaly. Visual inspection of panel two showed poor or no concrete cover. With the CSL tube configuration on both sides of the joint between panels one and two, the thickness and/or quality of the concrete cover could not be verified.

6.1.5.3 DTS interpretation

Using the response curve characteristics of the DTS device (Figure 34), the concrete level in time has been simulated for the concrete casting of both panels.

For the measurements the Sensonet Oryx DTS was used, as in the previous tests. In order to obtain a better spatial resolution, the sensor fiber had no Kevlar protection layer (in previous tests a rather thick protective liner was used) and acquisition time was reduced from 1 minute to 15 seconds.

The accuracy of the measurements as derived from the ability to track the concrete level, showed similar characteristics as earlier tests with a rather thick liner around the sensor and an acquisition time of 1 minute. Probably, the shorter acquisition time caused a slight loss of accuracy, making the positive effect of the thinner liner of the sensor not distinguishable. On the other hand, the number of temperature profiles obtained was four times higher than before, without sacrificing spatial accuracy.

It was intended to perform the height calibration with the top level of the bentonite suspension. This proved to be rather unreliable, due to varying bentonite height and air temperature during the day. As a result, it was difficult to calibrate the relative heights of the sensors.

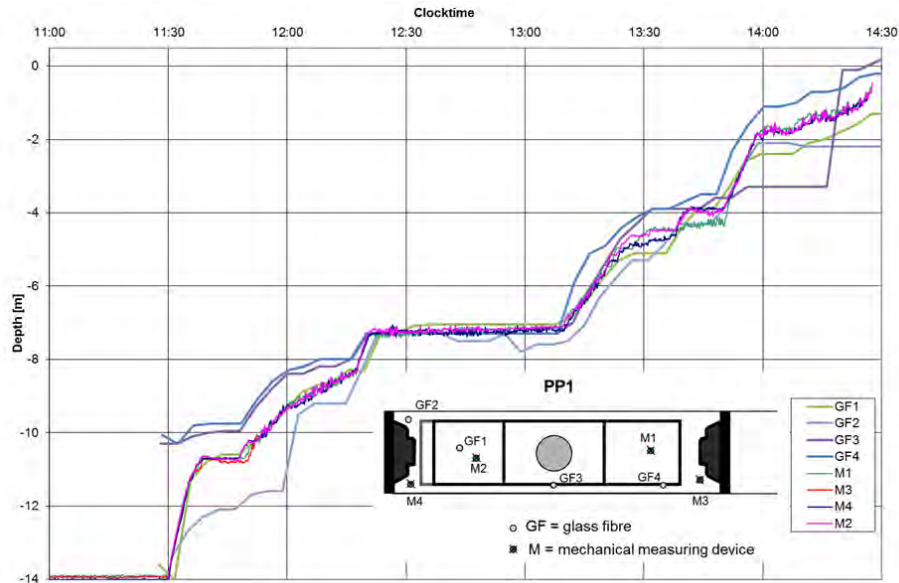


Figure 93: concrete casting progress recorded with DTS and mechanical loggers in panel 1

For panel 1, the mechanical loggers (positioned at M1 till M4 in the top view of Figure 93) showed a very constant concrete level during the casting stop for all measurement positions. The height calibration for the DTS derived concrete levels has at the beginning of the casting stop been referenced to this constant level (-7.3 m). Due to the gradual adaptation of the concrete and bentonite temperatures during such a casting stop, the DTS derived concrete level is expected to become less accurate, as is shown in Figure 93 by the deviating temperatures of GF2 during the casting stop. For future projects, a more reliable reference height should be used. This can be best based upon length markings on the sensor.

From 11:30 till 12:20 in Figure 93, the interpreted concrete levels from GF3 and GF4 seem to be between 0.5 m and 1 m too high. These sensors were attached to the rebar grid and ended at -12 m. The end of sensor effect makes interpretation of the lower meters unreliable. The influence of the steel of the rebar grid could also elongate the transition curve of the measurement, reducing the levelling accuracy. However, the sensors connected to the rebars during the cast of panel 2 did not show such a strong deviation. Sensors GF1 and GF2 of panel 1 (both placed into the bentonite using a dead weight at the sensor end), show a better correlation

with the concrete levels logged by the mechanical loggers, as shown in Figure 93. Provided that the level recorded with the mechanical loggers was the actual concrete level, an accuracy of about 0.2 m seems achievable.

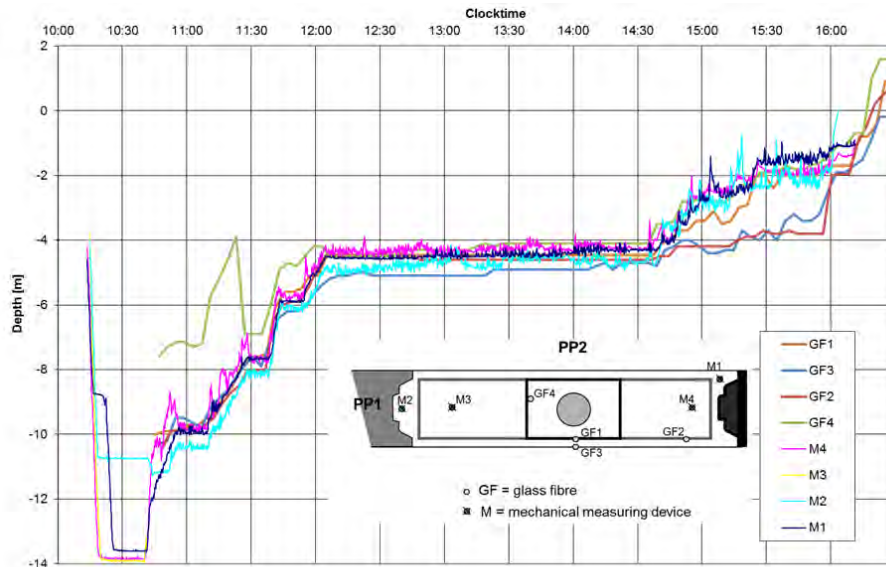


Figure 94: concrete casting progress recorded with DTS in panel 2

In the second panel (Figure 94), during the first meters of concrete casting, the interpreted levels near the tremie showed irregular results, possibly caused by dynamic effects of the concrete flow. During the casting stop around -4.5 m, the height differences did not completely equalize. The gradual rise of the interpreted concrete level might be partially caused by temperature changes during the casting stop. The upper part of panel 2 (Figure 94) has been cast with stiffer concrete. The height difference within the panel increased to more than 2 m. During the last meters, the concrete level was difficult to trace for the sensors connected to the rebar grid and outside the rebar grid, probably due to the damping effect of stiff old bentonite that remained covering the sensors. Such gradually increasing temperature profiles indicate a high chance of inclusions/anomalies.

To reduce the effect of the ending of the sensor and the top of the panel (sensor not in the trench), 3 m of extra sensor cable could be added to both the end of the sensor and the top of the panel to minimize the boundary effects. These extra meters could be rolled around a steel rod (sensor end) or PVC tube with a diameter larger than the minimum bending radius of the

glass fiber. The extra meters should be fully immersed in the bentonite slurry (or later concrete).

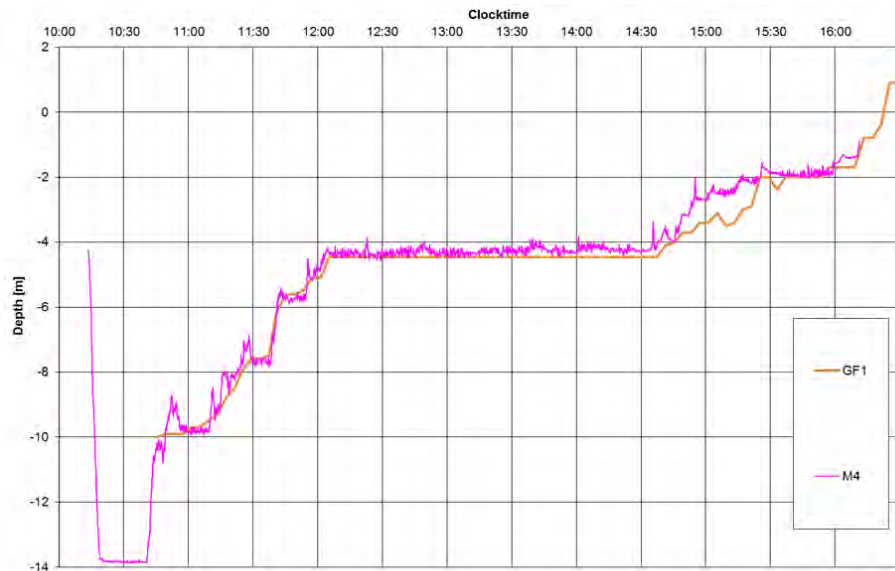


Figure 95: Comparison concrete level from automated mechanical logger (M4) and DTS based concrete level (GF1)

The accuracy of the concrete level recordings with DTS was in the same league as the accuracy obtained with the automated mechanical loggers (Figure 95). If deviations were encountered, this could have been caused by different positions of the DTS sensor and mechanical logger or stiff bentonite-concrete mixture that can be interpreted as concrete by the mechanical logger or lower concrete temperature that was interpreted as bentonite by the DTS levelling system.

The vulnerability of the DTS system proved to be much lower than the vulnerability of the automated mechanical loggers. The space needed for the DTS sensors is almost negligible compared to the automated mechanical loggers.



Figure 96: Automated mechanical loggers at work



Figure 97: Side view of the south face of panel 2 (worst parameters), the western panel 1 is just visible on the left and shows much better concrete

The lessons learned from this project are:

- The thinner DTS sensors with faster readout did not improve spatial accuracy. The acquisition time of 15 seconds could be slightly too short for the Sensornet Oryx DTS, an acquisition time of 1 minute is recommended
- CSL interpretation should primarily be based upon the assumption of bentonite in the inclusion. The calculated volumes could overestimate the actual thickness, but always on the safe side. With anomaly sizes of more than 50 mm, a gradual transition to interpreted volumes based on sandy inclusions could become more realistic.
- Automated mechanical concrete loggers can provide the most detailed level recording, but are vulnerable and require a lot of space. DTS concrete level recording seems very close in accuracy and has proven to be more robust and hardly requiring space. For projects that require detailed concrete level recording, DTS seems the best option.

6.2 Discussion of the tests and results

Three types of measurements have been found useful for detecting anomalies in diaphragm walls: CSL, DTS and ER. These have been tested in field and in laboratory conditions, as described in separate chapters (Chapter 3 Chapter 4 and Chapter 5).

Several aspects of the methods have not been covered in the papers as published, or have been acquired after their submission. Such aspects are addressed in this chapter.

6.2.1 CSL

Prior to the first field and lab tests, Crosshole Sonic Logging seemed the most promising method from a physical point of view (ASTM 2007). It was initially believed that the joint could cause a too severe loss of ultrasonic signal as is also suggested by Mendez et al. (2012). In the firsts tests on site at 'Kruisplein Rotterdam' (§2.3), the operator and co-developer of the PileTest CHUM device, Erez Amir (Amir and Amir 2009), was surprised about the high quality of the signal passing through the joint between two panels. The signal and the interpretability were way above expectations.

In the first tests on the blocks with known anomalies (§2.2), the first arrival time (FAT) of the signal seemed to be linearly correlated with the anomaly dimensions. This led to the conclusion that CSL could be used to assess the presence and size of an anomaly in a joint between diaphragm wall panels. Based upon these results, the contractor of the 'Sporzone Delft' project (§2.4) decided to use CSL on all joints where the retaining wall was closer than 5 m to the neighboring buildings. Within the 'Sporzone' project more than 200 joints were verified with CSL. Only one joint with a clear anomaly was found and repaired with jetgrouting before excavation of the building pit took place (§3.8.2). There were no 'false alarms' encountered, meaning: no CSL detected anomalies showed to be non-faulty in reality. Also, no faults were encountered that were not indicated by CSL.

To help interpretation of CSL data obtained from diaphragm wall joints, test blocks were made in the TU Delft laboratory (§2.5). These tests confirmed the linear correlation between increase of FAT and anomaly size. To make interpretation easier the 'Delay in Arrival Time' (DAT) parameter has been introduced, as described in §3.5.

Finally, the results from the 'Diaphragm wall Test Delft' (§6.1.5.1) have shown that the laboratory based correlations between DAT and anomaly size have reliable predictive value for real anomalies (as compared to well defined anomalies in the laboratory), provided that for estimating the anomaly size, up to 50 mm anomaly thickness, the characteristics of bentonite are used. If the anomaly thickness assuming a bentonite inclusion exceeds 50 mm, the anomaly thickness should also be assessed with the assumption of sand as a filler material. The actual thickness will be within these boundaries. Assuming only bentonite as anomaly material, will always give a safe (over-) estimation of the anomaly size. The two rubber water slots in the joint profile were undistinguishable in the CSL results. The presence of these rubber strips does not seem to influence the CSL results. The strips could however introduce a locally thicker bentonite cake in the joint. This thicker bentonite cake could show up in the CSL results.

During data acquisition, a proper reference level should be used for CSL, to avoid future misinterpretation (see also §6.1.3). The auto-gain function should be checked before application. Not all equipment is directly applicable in auto mode for detecting anomalies in diaphragm walls as was shown in §6.1.3.

Objects with other material than concrete such as steel or air, that remain in the diaphragm wall, can strongly influence the CSL measurements, making interpretation more difficult or impossible (see also §6.1.4).

To prevent opposition of (sub-) contractors, the CSL method should clearly be prescribed in the contract (see also §6.1.1).

Correlation with DTS interpretation showed consistent results (see also §4.8).

6.2.1.1 Field applicability

Between concrete casting of the diaphragm wall panels and excavation of the building pit, there is generally enough time to run the CSL tests. As a result, the testing can be executed without obstructing the building process. Also, the influence of the building process on the measurements can be minimized by choosing the right time window to execute the measurements. The measurement tubes have minimal impact on the panel production. The preferred material for the access tubes is PVC. This material provides a

cleaner signal, is cheaper, is easier to assemble on site and has shown a just as good or better survival rate in the field compared to steel access tubes (§2.3).

6.2.1.2 Interpretation

The interpretation of the CSL measurements is generally straight forward. In most projects, the majority of joints will show no defects, allowing to focus only on a few joints with sub-par measurement results. An expected (based upon site experiences §2.4, §6.1.2 and §6.1.3) 1% to 5% of the tested joints will require more interpretation time. The first step will be to assess the coverage of the anomaly relative to the cross-section of the wall by combining the different CSL scans of the same joint. If the anomaly does not extend to the full width, the chances of a calamity are limited. Only if the full width of the wall is affected, assessment of the anomaly size and material is required. Of course the erosion properties of soil at the same depth should in that stage be evaluated.

Using the reference measurements and project experience, the size of the anomaly can be estimated quite reliably, making preemptive repair decisions possible. The anomaly width determination based on DAT, assumes perfect quality concrete on both sides of the joint. If the concrete has low quality, this will affect the DAT, resulting in an expected relatively large anomaly width. In reality, the anomaly width can be considerably smaller, with adjacent low grade concrete, as has been noticed in e.g. §2.3, §2.4 and §6.1.5.2.

If the concrete quality in part of the wall is low throughout the panel, the DAT may in some cases be locally corrected using the CSL scans parallel to the joint. In such cases, a local base FAT can be assigned to which the DAT is determined for the section with low concrete quality. This should only be done with decent signal quality and if a different concrete quality has been determined in the site tests on each truck load of concrete. If the signal is already deteriorated due to the grainy properties of the concrete and/or anomaly or if there seems to be no reason to suspect a truck load of concrete, it is better to leave the interpretation untouched. Resetting the base FAT locally to compensate for a low quality concrete batch is not recommended as this leads to a less objective interpretation of the measurements.

Future tests with different sound sources (especially lower frequency sources) could help differentiate between different materials in the anomaly. The influence of the adjacent concrete quality will remain an issue to be solved.

6.2.1.3 Cost considerations

The material cost of the PVC measurement tubes, the effort to attach them to the rebar cages and the measurement and interpretation costs are minimal. The total costs are estimated at 2-5% of the construction cost per panel, assuming a measurement rate of 10 joints per day including a preliminary interpretation report.

6.2.2 DTS

Temperature measurements are widely being used to monitor the curing process of concrete (Carino & Lew 2001). Instead of using the traditional temperature sensors like PT100 based sensors (Wikipedia 2015), OTDR technology could be used to obtain a detailed maturity profile (Thevenaz et al, 1998) for example along the joint of a diaphragm wall panel.

At first, the objective was to use the concrete maturity method to evaluate the concrete quality in the joint area. During the first field tests (§2.3), the DTS recorder was already logging the temperature profile during concrete casting. It was possible to track the concrete level during concrete casting using DTS much better than expected based upon the 1 m spatial resolution stated in the device specifications. The maturity measurements on the other hand showed no possibilities for reliable interpretation. The local temperature during curing was primarily influenced by the permeability of the surrounding soil and not by the actual concrete quality. Only with comparative tests, the relative concrete quality may be filtered out, assuming the temperature influence of the soil profile to be equal between the tests.

The possibility to track the concrete presence itself during concrete casting seemed to be a potentially more accurate or more informative method. It was therefor decided to determine the accuracy of tracking the interface between two media with different temperatures in the laboratory (§2.5 and §4.5.3). These tests and the field tests at 'Sporzone Delft' (§2.4 and §6.1.5) showed that tracking the concrete level with DTS is possible with an estimated accuracy of about 0.05 to 0.1 m. Also the shape of the transition of the

temperature profile renders information about the expected quality of the concrete or the chance of anomalies being present.

The field tests in Delft (§2.4) also showed that bentonite refreshing can be monitored with DTS. This even provides the possibility to prevent anomalies: if problems with the bentonite refreshing are being detected, there is still the possibility to brush the joint with the previous panel and/or to refresh the bentonite again.

During the 'Diaphragm wall Test Delft' (§6.1.5.1), the DTS derived concrete levels could be compared with automated mechanical loggers. The results of both level recordings were similar. The automated mechanical loggers seemed to be slightly more accurate but much more vulnerable, more cumbersome and taking much more space above and in the trench than the DTS based method.

6.2.2.1 Field applicability

The measurements need to take place during bentonite refreshing and concrete casting (or only during concrete casting). The sensors will therefore inevitably be exposed to the rough environment of the building site. The field tests have shown that the vulnerability of the sensors is not so much an issue (low failure rate), but the optical systems are vulnerable to dust and moisture.

As a result, DTS will (with current devices) be suitable primarily for semi-research settings, for example, during production of a test panel with a dense rebar grid. Especially the small space requirement of the sensors offers the opportunity to measure the concrete level (or presence) at locations that were previously impossible to monitor.

As a standard replacement of the manual concrete level recordings the current DTS devices are not yet suitable. If a DTS device is developed specifically for concrete level recording, manual concrete level sounding could be only needed as a backup system.

6.2.2.2 Interpretation

A reliable interpretation of the DTS data should be based upon the response curve characteristics that belong to the DTS device that was used. With such a response curve and assumed temperatures and interface levels of the different media in the trench, the measured temperature profile can be

simulated. If no mixing of bentonite and concrete occurs (like it should in a good quality panel), it will be very easy to simulate the measured temperature profile. The more mixing between concrete and bentonite or remaining bentonite are at play, the more difficult it will become to obtain a convincing simulation of the measured temperature profile. Such a situation should be interpreted as a high chance of anomalies.

It is recommended to use sensors in- and outside the rebar cage and attached to the rubber water slot in the joint. If the concrete level between the different sensors starts to deviate much, the chances of an inclusion increase.

Special care should be taken for height calibration of the DTS sensors. This can be done best with a length marking on the sensors. To reduce the boundary effects at both ends of the actual measuring section, 3 m of sensor can be wound around a tube or rod with typically 50 mm diameter (to stay above the minimum bending radius of the sensor, a thick liner will require a larger rod diameter). This coil will ensure a stable temperature recording at the end position.

From the response characteristics it follows that small anomalies will be difficult to recognize in the DTS measurements as the very locally differing temperature will have only a limited effect on the temperature profile. With improving spatial resolution and steeper response curves of newer generation DTS devices, the possibilities for discerning small anomalies are likely to improve.

6.2.2.3 Cost considerations

The price per sensor is limited (in the order of 150 euro per sensor), but the cost of DTS recording and the following interpretation are currently relatively high. In total a 100% of the panel cost should be taken into account. This will not be economical for standard application for all panels. For (semi-) scientific determination of flow behavior, for example in a test panel with very dense rebar grid (e.g. not complying to the Eurocode recommendations for rebar spacing), this could be worth the investment.

6.2.3 ER

In theory, the electrical resistivity of good quality concrete should be higher than the resistivity of soil and/or groundwater (Gunn et al. 2014).

This potentially offers the opportunity to locate anomalies in concrete walls, using an electrical technique.

During a field test with a two electrode setup (see §2.3 and §5.4.1), an anomaly, discovered with CSL, was not clearly recognizable. The CSL measurements indicated an anomaly that extended to only a part of the cross-section of the wall. This could mean that anomalies with partial coverage of the cross section could not be detected or that anomalies could not be detected at all.

To further investigate the possibilities, a test has been setup with a wall with known anomalies in a water basin. This test is mentioned in §2.6 and fully described in §5.4.4. These tests showed that, to obtain useful data, the contact resistance between electrodes and soil should be eliminated with a four-electrode-setup and that the distance between the potential electrodes and the object to be tested should be very small. Generally, the potential electrodes should be closer than 0.2 m to the test object (see §5.4.4). If a global resistivity image, obtained with electrodes at a somewhat larger distance e.g. 0.8 or 1 m, is subtracted from a detailed resistivity image obtained with electrodes at close distance, the resolution can be further enhanced.

6.2.3.1 Field applicability

The ER method will only provide useful information if a 4 electrode-setup is used with the potential electrodes at very short distance to the test object (less than 0.2 m). When using push-in electrodes (CPT based types), the electrodes will deviate from the vertical, resulting in inaccuracy of the distance between electrode and test object and/or collision of the electrode with the test object. The current injection electrodes need to be placed at a rather large distance from the test object, requiring a lot of space for an ER measurement. Not all building sites will have the space available for properly executing ER tests. If space is only available for a two-electrode setup, the test is expected to offer low interpretive value.

Provided that the potential electrodes can be positioned at short distance (for example using boreholes with perforated plastic standpipes), the method still needs reference measurements at a proven high quality joint with the

same geological conditions to compensate for the variation of the soil resistivity parameters.

Potential electrodes at surface level can only be used to estimate the properties of the wall around surface level.

To enhance the image resolution, a global resistivity trend (measured at larger distance) could be subtracted from the resistivity image obtained at short distance, but this will require almost double time in the field and more space at the building site to setup the measurement.

Most projects do not allow for measurements covering a large portion of the site for several days.

On the other hand: if CSL tubes or DTS sensors have not been installed and thus such measurements cannot be executed, ER is more or less the only option to verify the quality of the wall before excavation of the building pit. However, it will be difficult to assign a 'good joint' as reference if no CSL or other data are available.

6.2.3.2 Interpretation

From the field and laboratory tests, it seems that only anomalies that are present in the full cross-section of the wall have a chance to be detected with ER. To compensate for the resistivity properties of the soil layers, the measurements from a proven high quality joint should be used as reference.

The detection limit of anomalies size is exponentially increasing with potential electrode distance to the test object. Depending on the potential electrode distance to the test object as tested in the field, the detection limit of the measurement can be estimated. Generally, only relatively large anomalies that affect the full cross-section can be detected. To assess the quality of a joint as a function of the depth, the potential electrodes (at close range) on both sides of the wall should be able to scan simultaneously vertically along the joint.

6.2.3.3 Cost considerations

The amount of time and cost needed to acquire the measurement data and to make an interpretation of the measurements will not fit in the project planning and budget for most projects.

In most cases, executing repair works based upon CSL or DTS data will be more cost effective than executing ER measurements. Only if CSL or DTS measurements are not available and/or repair with jetgrouting could cause severe side effects, ER measurements can be beneficial.

For testing one joint with the required reference joint, at least four bore holes to the required test depth and two full test days with 2 persons should be taken into account. The same amount of time is required to do a proper interpretation of the results.

Of course the measurements can only be implemented if the equipment can access the required positions.

The potential electrodes should preferably be introduced in the soil using perforated standpipes in boreholes. This will require about two to three days with a drilling rig. The total cost for assessing one doubtful joint is expected to be about 200% of the cost of one panel. This is about half the cost of a single jetgrout column (excluding mobilization costs).

In projects where a jetgrout rig is already on site, repairing a joint will generally be preferable because the chances of the outcome of the ER test to be 'repair' or 'unambiguous' are expected to be more than 50%, provided that the joint was already indicated as subpar based upon another method.

6.3 Recommended measurements

The three techniques addressed in chapters Chapter 3 to Chapter 5 are complementary. Not all projects will demand all three techniques. Figure 98 shows how and when the investigated measurement types can be applied in projects.

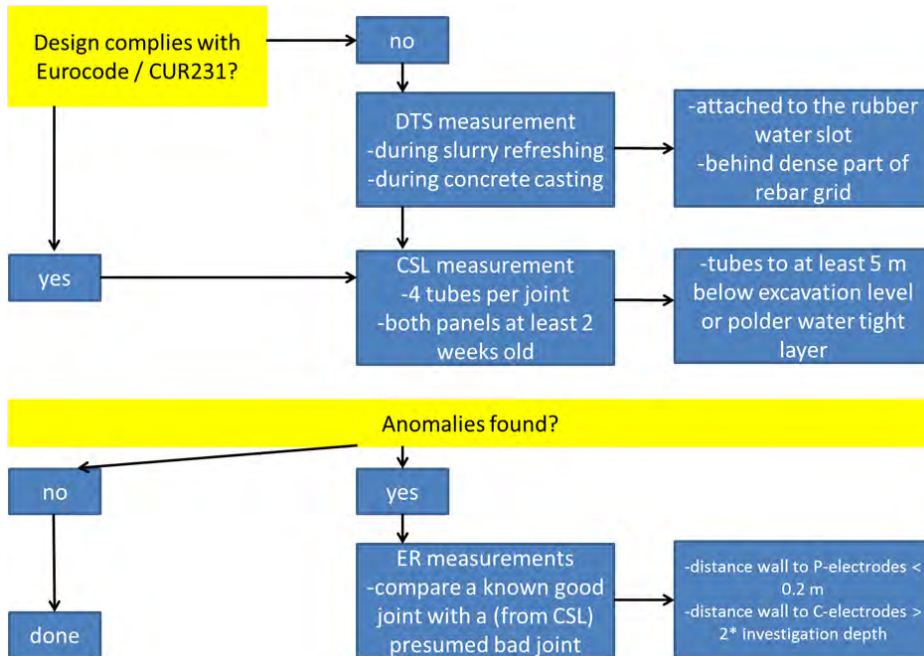


Figure 98: Decision scheme for D-wall testing

Bottom line is that CSL testing should be standard procedure for all D-walls in case of walls retaining sand and foundations close by or other conditions that require a high reliability of water and/or soil tightness.

If the design of the wall cannot comply with the Eurocode or CUR231 recommendations for rebar grid spacing, DTS measurements at critical locations during production of a test panel can provide valuable information about the concrete flow process, as has successfully been used during the research in concrete flow in diaphragm walls by van Dalen (2015).

If in one or more of the before mentioned methods anomalies are recognized, ER measurements could be used to verify the expected permeability across the wall of the anomaly. The cost of this extra measurement and the relatively low reliability should be weighed against the cost and effectiveness of preemptively repairing the presumed defect.

Chapter 7 Conclusions and recommendations⁴

7.1 Conclusions

Diaphragm walls have been widely used as retaining walls for deep excavations due to their risk reducing properties of vibration-less execution and high bending stiffness. A less favorable property of diaphragm walls is the uncertain quality of the joints between panels. Below par joints have caused severe problems during the construction of several underground projects all over the world. After calamities in Amsterdam and Rotterdam (the Netherlands) during metro construction works, it was decided to investigate the possibilities of detecting anomalies in the joints. Starting in 2009 from within the Municipality of Rotterdam and from 2010 onwards continuing at Delft University of Technology with support of the Geolmpuls program, research has been carried out in the laboratory and in several projects.

The research focused on the quality of concrete around the joints between D-wall panels. It is assumed that if the concrete in the joint is of good quality, the joint will be water and soil tight. The quality of the concrete within the panel itself is not considered to be causing calamities. The verticality of the panels has not been studied but must be guaranteed by good craftsmanship and measuring the inclination of the panels.

Within the research project, three techniques for determining the quality of concrete in the area around the joints have been found usable:

- DTS (Distributed Temperature Sensing)
- CSL (Crosshole Sonic Logging)
- ER (Electrical Resistivity)

⁴ This chapter is partly based upon the paper 'Detection of anomalies in diaphragm walls' presented at the Fifth International Symposium on Geotechnical Safety and Risk (ISGSR) 2015 in Rotterdam

An indication of when the measurements can be applied is given in Figure 98.

Generally, CSL must be applied in all projects regardless of the risks in the surroundings. Because of the low measurement costs of CSL, the technique is already cost effective if the only benefit is preventing project delay. Only if the project risk profile is very low as a result of clay layers and/or no neighboring vulnerable objects, CSL measurements could be left out.

DTS measurements will (for the moment) be primarily useful in research settings and for verifying the concrete flow through dense rebar cages. If rebar cages not fulfilling Eurocode and/or CUR231 requirements for rebar spacing are necessary, DTS measurements within the first panels can be used to optimize the concrete characteristics and rebar configuration. Bentonite inclusions in the joint area may be detected if the DTS sensor is included in the rubber water slot.

ER measurements should not be relied upon as primary tool for detecting anomalies in D-walls. As a confirmation tool or to assess the permeability of the wall, it can provide useful information if the potential electrodes are placed close to the wall, in fact closer than 0.2 m.

7.1.1 Crosshole Sonic Logging

Crosshole Sonic Logging (CSL) uses an ultrasonic source and receiver to determine the travel time and signal loss between source and receiver. As the speed of sound in a medium depends on density and stiffness, anomalies containing bentonite or soil can be differentiated from concrete. PVC tubes are attached to the outer corners of the rebar cage to provide access of the source and receiver in the area around the joint. After concrete casting and curing the panels on both sides of a joint, the joint can be scanned by simultaneously lowering source and receiver in all permutable combinations of access tubes. In Chapter 3 a full description of the executed verification tests has been reported.

For several fill materials in an anomaly, the change in First Arrival Time (FAT) and the attenuation of the signal have been determined. The delay in arrival time (DAT) is linearly proportional to the anomaly size (Figure 18). In a similar way, the attenuation also has a correlation with anomaly size (Figure 20).

7.1.1.1 Recommended measurement setup

The preferred material to be used for the tubes is regular PVC. This provides the cleanest signal and has shown to be less vulnerable for damage in the field than steel tubes. The best survival rate for the tubes is obtained when they are attached to the rebar cage on site, just before installation of the rebar cage in the trench. If the rebar cage consists of more than one section and below the top section CSL is still required, PVC offers the possibility to couple several sections quickly and easily using PVC glue and sleeves. The tubes can be attached to the rebar grid by applying tie wraps each meter.

Make sure the position of the measurement tubes relative to the corners of the rebar cage is constant. It is easiest to attach the tubes on the outside of the cage, which also provides for the best signal for imaging the joint. This has not shown to increase the failure rate of the tubes.

After immersion of the rebar cage in the trench, it is recommended (Likins et al. 2004) to fill the measurement tubes with water and to cap them. Make small holes in the caps to prevent pressure build up underneath the caps due to temperature and pressure changes. The water in the tubes will reduce bentonite in-flow in case of a leak in a coupling sleeve. During concrete casting, the water in the tubes will damp the temperature fluctuations, supposedly reducing the chance of debonding. After the concrete casting has finished, check if the caps (used to prevent unwanted objects from entering into the PVC tubes) are still on the measurement tubes. They sometimes pop off due to compression of the PVC tubes and/or heating up due to concrete curing. Experiments with 2 additional tubes in the center of the panel have not shown a better understanding of the geometry of the joint, while increasing the chance of obstructing the concrete flow in the center of the panel, towards the central rubber water slot.

The CSL signal will suffer severe loss in amplitude while crossing the joint. Not all auto-gain algorithms are able to cope with this phenomenon. It is therefore recommended to start with a few tests to evaluate the auto-gain system. If on some scans of the same joint, no useful signal is recorded, manual gain control should be chosen. With manual gain, it is important to use a fixed gain for each type of crossing. Generally, the gain for the scans perpendicular to the joint should be double the gain for the scans parallel to the joint. The scans that run diagonally through the joint generally need a gain three times higher compared to the parallel scans. These values could

be influenced by site specific parameters like the type of concrete and bentonite applied in the production of the wall or the shape of the stop end. It is therefore necessary to test these settings on a few joints before setting them for the large scale production tests. To make comparison between joints possible it is required to keep the gain factors fixed within the project.

Most CSL devices use the top of the measurement tubes as a reference for the measurements. This is not always practical. It is important to be able to refer to a well specified level (for example the national level or WGS84). Often the top of the diaphragm walls will be cut to remove low grade concrete. During these activities, the CSL measurement tubes generally are lost, including the top level of the tubes. As a result, it is important to execute the CSL measurements before demolishing of the upper meters takes place. It is also important to register the actual levels of the top of the measurement tubes (the top level of the tubes is often not equal within a set of four measurement tubes because of the tubes being installed in two different panels and the tubes could have been cut after they were damaged).

7.1.1.2 Interpretation options

For a first evaluation of the CSL results, FAT recordings without deviations can be interpreted as 'there are no anomalies present'.

If severe deviations are noticed, the attenuation at the same depth must be considered in conjunction with FAT. It is also necessary to combine with the other logs of the same joint to assess the volume of the anomaly relative to the cross section of the panel. If the anomaly seems to affect even the scans parallel to the joint, the CSL logs of the joint on the other side of the same panel should be examined in detail as well. If the anomaly was caused by a long term stop of the concrete casting process, there could be a horizontal sandy layer extending to the full cross section of the panel.

To estimate the volume of the anomaly, Figure 18 and Figure 20 can be used. Generally, it is safest to derive the anomaly size upon the DAT assuming bentonite as fill material. By combining all scans of one joint, the affected area and anomaly thickness can be plotted. This information can be used to assess the risk of leakage and/or the need for repair.

7.1.2 Distributed Temperature Sensing

Distributed Temperature Sensing (DTS) uses an optical fiber sensor to measure the local temperature as a function of the position within the sensor. As the different media in the D-wall trench (excavation-bentonite, fresh bentonite and concrete) will have different temperatures, the sequence of media in time (during slurry refreshing or concrete casting) can be registered using DTS. Incomplete or insufficient de-sanding of the bentonite slurry, concrete casting disruption and too dense rebar grid relative to concrete flow parameters (like viscosity) are considered to be the major parameters causing anomalies in D-walls. Theoretically, all of these can be verified using DTS.

To investigate the usability of DTS in this application, it was necessary to determine the response curve of a DTS system (sensor and interrogation device). The typical response curve of the Sensornet Oryx DTS combined with an ACE-TKF CTC 8xMM sensor to an interface between two media with different temperatures is shown in Figure 34. Although the Sensornet Oryx DTS has a stated spatial resolution of 1 m (as per the manufacturers documents), it can be seen in Figure 34 that the influence of a temperature change stretches over a length of 3 m (1.5 m before and after the actual interface between the two media). Each DTS device will have its own characteristic response curve, which is often not supplied by the manufacturer, but the general shape will be comparable.

If the measured temperature profile recorded with a Sensornet Oryx DTS is simulated with the response curve of Figure 34, the position of an interface between two media with different temperatures can be determined with an accuracy of about 0.05 to 0.10 m. This is much more accurate than expected, based upon the 1 m spatial resolution of this specific DTS device. This accuracy has been verified with both laboratory and field tests (Chapter 4).

Most DTS recorders have 4 or more channels. If 4 channels are available it is advised to use fibers to the full depth of the trench at the following locations:

- Attached to a rubber water slot in both joints (2 pcs)
- Inside the rebar cage, near the tremie pipe

- Outside the rebar cage, near the tremie pipe, on the side with the most dense rebar grid (generally the excavation side of the building pit)

7.1.2.1 Interpretation options

Interruption of the concrete flow is generally considered to be causing the most severe defects in diaphragm walls. If two or more profiles overlap, the concrete front has not risen during the interval between the measurements, indicating a casting stop. The number of overlapping profiles times the measurement interval determines the duration of the casting interruption.

If casting restarts after an interruption, the DTS sensors outside the rebar cage and especially those in the joint areas could show a large initial offset compared to the DTS sensor close to the tremie pipe. This is caused by the concrete which has stiffened due to the standstill and which has difficulty regaining the flow through the rebar grid. If the casting interruption was long enough, the fresh concrete could break out of the previous casting front, forming a new front and locking up the sandy bentonite slurry that was collected on top of the previous casting front. This can become visible in the DTS recordings in the joints: the concrete temperature will suddenly appear above the area where the bentonite temperature remains. Before this sudden 'jumping up' of the concrete level, a period of increasing offset between the DTS sensor near the tremie pipe and the DTS sensors in the joints could be visible. The possibilities for detecting this phenomenon are being limited by the spatial resolution of the DTS device. Anomalies smaller than 1 m, will be difficult to discern with current DTS devices. Newer devices with a steeper response curves might be able to improve the detectability of small anomalies.

DTS measurements offer the possibility to monitor the position of the interface between two or more media with different temperatures. With the typical response curve of the DTS device it is possible to simulate the response of the DTS device based upon assumed temperatures of the two media and an assumed position of the interface. By comparing the recorded temperature profile with the simulated profile, the actual interface position can be determined iteratively. If the shape of the measured temperature profile does not fit the response curve shape of the DTS device, this means a system with more than two phases has been present (Figure 40). By superimposing n response curves, a system containing $n+1$ phases can be

simulated. Figure 40 illustrates successful simulation of a three phase system.

A sequence of temperature profiles can be used to simulate the concrete level in time (Figure 47). This shows a far more detailed registration of the casting process than manual measurements.

7.1.3 Electrical Resistivity

The Electrical Resistivity measurement forces an electrical current through an electrode at a distance from one side of the wall to a second current electrode at a distance at the other side of the wall. With two (or more) additional electrodes the local potential very close to the suspected joint is measured. If concrete of a good quality is present in the joint, the electrical resistivity will be high (large potential difference), if the cross section of the joint contains an anomaly (consisting of soil or bentonite), the local resistivity will be lower. The resistivity results of a sound joint are compared to the results of a suspected joint. Local differences indicate an anomaly. A test wall consisting of the reference blocks that were cast for the CSL measurements has been built upon a plastic sheet (Figure 55).

Figure 66 has been constructed using the estimated anomaly cross sections and their detection in the different measurements (0.1, 0.2, 0.4 and 0.8 m distance between potential electrodes and test wall). Even though the number of measurements is limited, it is undeniable that the ability of the ER technique to detect anomalies is strongly influenced by the distance between the potential electrodes and the wall to be tested. Generally speaking, for detecting anomalies that could cause a calamity, the potential electrodes should be closer to the test object than 0.2 m. This results in practical limitations of this technique when push-in electrodes are used. For bored electrode strings such small distances might be realizable between potential electrodes and the object to be tested.

Even though the method is limited, in some cases where repair works with jet grouting are less desirable, ER could be useful for verifying the anomaly estimations made with CSL measurements. In such cases the setup outlined in Figure 68 could be used.

However, in most cases repairing with jet grout will be more cost effective.

7.2 Recommendations

Crosshole Sonic Logging will most probably become the most used type of measurement for assessing the quality of joints between diaphragm walls. It will be valuable to collect measurement data from projects and compare the interpreted anomaly dimensions with the actually discovered dimensions and properties of the anomalies. This will allow for future more accurate determination of anomaly size and properties.

Determining the optimum frequency of the source signal could be typically a field of future academic study. The current ultrasonic signals seem adequate for thin anomalies, but less suitable for thicker or grainy anomalies. By combining high and low frequency measurement results, the image of the joint might be improved for joints that suffer from high signal loss with the current signal sources. Considering that the anomaly sizes that can be detected with current technology will in most cases provide enough information to decide on preemptive repair, the gain to be achieved by even more detailed imaging of the joint must not be overestimated.

Tomographic use of CSL could be a worthy addition to better locate an anomaly horizontally between the measurement tubes.

If a DTS device is going to be produced specifically for monitoring the concrete casting process, specific attention should be given to the automated interpretation of the interface-level between the different media.

Adapting the rubber water slots to include a DTS sensor will simplify implementation of this method. The rubber strips could for example have a prefabricated groove in which the DTS sensor can be mounted on site after the rubber strip has been fixed in the stop end.

The measurements in this research have all been executed with the Sensornet Oryx DTS. Current state-of-the-art DTS devices might be able to provide an even better spatial resolution combined with faster acquisition times. It will be necessary to verify the accuracy of these new DTS devices with response curve tests like the ones described in 4.5.3.

Even though the accuracy and practical value of the ER method in this application has not been convincing, it is worth verifying the detection limits determined in this research in a field situation.

If in a project where CSL has been used, anomalies that extend through the full cross-section of the panel have been found, these positions offer a possibility to verify the ER detection limits and to optimize the proposed field setup (5.4.4.1) of the measurement.

Because pushing in the potential electrodes at close distance to the wall is expected to cause a lot of problems, the potential electrodes can be positioned in perforated stand-pipes (installed in boreholes close to the wall). The current electrodes (at distance) may be pushed in or installed in bore holes as well.

The technique with subtraction of a global image at about 1 m distance from a high resolution image at short distance (less than 0.2 m) seems to offer the best imaging capabilities but this needs field verification.

Crosshole sonic logging has been developed for (large diameter) bored piles. For assessing the quality of these foundation elements, the ASTM D6760 and D4428 codes can be used. As shown in this thesis, CSL can also be used for other in-situ formed elements. For soil mix walls and jetgrouting bodies, the quality might be assessed with CSL, although the variation in material properties may cause difficult interpretation. The installation and survival rate of the measurement tubes could be problematic as well.

Vibro-piles (driven temporary steel casing, which is retracted using a vibrator after being filled with rebar cage and concrete) could be verified with CSL if the rebar cage is equipped with access tubes. Due to the low cost of vibro-piles and the relative small number of problems, adding CSL tubes to all piles does not seem economical. It is worth investigating the typical conditions that seem to cause the majority of problems with vibro-piles. If specific problematic conditions can be identified, in those situations CSL tubes could be added to the rebar cage. CSL can only confirm the quality between the access tubes, e.g. diameter deviations not affecting the core between the tubes cannot be detected.

In all in-situ cast foundation elements DTS can offer useful information about the presence of concrete during the casting process, although in some applications the concrete casting might be too fast to be properly detected with DTS. In some applications (like jetgrouting of soil mixing) installing the fiber-optic-sensors and keeping them in the same position could be difficult. If the concrete casting process is too fast to record, the concrete maturity

Recommendations

principle can be used. If so, the influence of the surrounding soil must be compensated for and could limit the practical resolution of the measurements.

DTS can also be used as an extra source of information during pumping tests of building pits. Permeable locations will probably show up with local changing temperature. It might be necessary to introduce an electrical heating strip combined with the DTS sensor if no temperature contrast with the surrounding groundwater is expected.

References

- Adams, J.C., Hajduk, E.L., Halvarsson, P., Neumann Jr., A., 2009. A case history evaluation of CSL access tube debonding, *Geotechnical Special Publication*, (185), pp. 552-559.
- Akintoye, A.S., MacLeod, M.J., 1996. Risk analysis and management in construction, *International Journal of Project Management*, Vol. 15, No. 1, pp. 31-38
- Amir, J.M., Amir, E.I., 2009. Capabilities and Limitations of Cross Hole Ultrasonic Testing of Piles, *Proc. Conf. Contemporary Topics in Deep Foundation*, ASCE GSP 185, Orlando, pp. 536-543.
- ASTM D6760 – 08. 2008. Standard Test Method for Integrity Testing of Concrete Deep Foundations by Ultrasonic Crosshole Testing
- ASTM D4428 / D4428M – 07. 2007. Standard Test Methods for Crosshole Seismic Testing
- Berkelaar, R. 2011. Risk management during the reconstruction of the underground metrostation Rotterdam Central Station, 3rd International Symposium on Geotechnical Safety and Risk (ISGSR 2011), Vogt, Schuppener, Straub & Bräu (eds) ISBN 978-3-939230-01-4, pp. 643-650.
- Brown, G.A., Tiwari, P. 2010. Using DTS Flow Measurements Below Electrical Submersible Pumps to Optimize Production From Depleted Reservoirs by Changing Injection Support Around the Well, *Proc. SPE Annual Technical Conference and Exhibition*, Florence, Italy, (19–22 September 2010).
- Bruce, D.A., De Paoli, B., Mascardi, C., Mongilardi, E., 1989, Monitoring and quality control of a 100 metre deep diaphragm wall, *International Conference on Piling and Deep Foundations – London 15-18 May 1989*
- Carino, N.J., Lew, H.S. 2001. The maturity method: from theory to application, *proceedings of the 2001 Structures Congress &*

- Exposition, May 21-23, 2001, Washington, D.C., American Society of Civil Engineers, Reston, Virginia, Peter C. Chang, Editor, 2001, 19 p.
- CUR 2010. Handboek diepwanden, Ontwerp en uitvoering, CUR 2010, ISBN-978-90-376-0526-6
- De Doelder, B.R., Slot, A.F.M. 2010. Controle waterdichtheid bouwkuip Metrostation CS, vakblad Geotechniek, oktober 2010.
- DIN 4126, 1986, Cast in-situ diaphragm walls, Deutsche Norm
- DIN 4127, 1986, Diaphragm wall clays for supporting liquids, Deutsche Norm
- Doornenbal, P., Hopman, V., Spruit, R. 2011. High resolution monitoring of temperature in diaphragm wall Concrete, 8th International Symposium on Field Measurements in GeoMechanics (FMGM2011), USB-stick
- Euro Code EN 1538, 2010, Execution of special geotechnical works. Diaphragm walls
- Faro, 2005, http://de.wikipedia.org/wiki/Datei:FARO_Laserscanner_LS.JPG
- Fugro, 2013, Fugro Nieuwsbrief, Jaargang 24, nr 3 november 2013
- Galekamp, H., 2015, Personal communication
- Gunn, D.A., Chambers, J.E., Uhlemann, S., Wilkinson, P.B., Meldrum, P.I., Dijkstra, T.A., Haslam, E., Kirkham, M., Wragg, J., Holyoake, S., Hughes, P.N., Hen-Jones, R., Glendinning, S. 2014. Moisture monitoring in clay embankments using electrical resistivity tomography, Construction and Building Materials
- Hoek, E. 2012. Alternative ground control strategies in underground construction, Keynote address at an International Symposium on "Practices and trends for Financing and Contracting Tunnels and Underground Works", Athens, Greece, on 22-23 March 2012 www.tunnelcontracts2012.com/
- Horb, C. 2005. Plan d'Assurance Qualité, Procedure Travaux, Ausultations Soniques; Port Autonome du Havre, Secretariat d'État Charge des Transports
- Hwang, R.N., Ishihara, K., Lee, W.F. 2007. Forensic Studies for Failure in Construction of An Underground Station of the Kaohsiung MRT System; Forensic Geotechnical Engineering October 2009, International Society for Soilmechanics and Geotechnical Engineering TC 40. p.p. 144-148
- Ihara, I. 2008. Ultrasonic Sensing: Fundamentals and Its Applications to Nondestructive Evaluation; Sensors: Advancements in Modeling, Design Issues, Fabrication and Practical Applications. Springer-Verlag Berlin Heidelberg, ISBN: 978-3-540-69030-6
- Likins, G., Webster, S., Saavedra, M. 2004. Evaluation of Defects and Tomography for CSL, Proceedings of the Seventh International

- Conference on the Application of Stresswave Theory to Piles 2004: Petaling Jaya, Selangor, Malaysia; 381-386.
- Likins, G., Rausche, F., Webster, K., Klesney, A. 2007. Defect analysis for CSL testing. Geotechnical Special Publication, (158). Contemporary Issues in Deep Foundations; Proceedings from Geo-Denver 2007 New Peaks in Geotechnics: Denver, CO. (CD-ROM)
- McDaniel, J.G., Dupont, P. 2000. A Wave Approach to Estimating Frequency-Dependent Damping under Transient Loading. Journal of Sound and Vibration (2000) 231(2), pp. 433-449
- Meinhard, K., Adam, D., Lackner, R. 2014. Temperature measurements to determine the diameter of jetgrouted columns, Recent Developments to Improve Reliability Proceedings-DFI/EFFC 11th International Conference on Piling and Deep Foundations, 2014, Stockholm, Sweden
- Mendez, J. A., Rausche, F., Paulin, J. 2012. Quality Control of Diaphragm Walls by Crosshole Sonic Logging. Full-Scale Testing and Foundation Design: ASCE Geotechnical Special Publication No. 227, pp. 650-663.
- Neville, A.M. 1981 Properties of concrete, 3rd edition, Longman Scientific & Technical, ISBN 0-582-40626-9
- Niederleithinger, E., Hübner, M. and Amir, J.M. 2010. Crosshole Sonic Logging Of Secant Pile Walls - a Feasibility Study. Symposium On The Application Of Geophysics To Environmental And Engineering Problems (SAGEEP), 2, Keystone, Co, pp. 685-693.
- Niederleithinger, E., Garcia, R., 2014, Quality assurance of diaphragm walls by sonar measurements – model study, Proceedings of the Institution of Civil Engineers Geotechnical Engineering 167 April 2014 Issue GE2 Pages 217–226 <http://dx.doi.org/10.1680/geng.13.00038>
- Norme Française NF P94-160-1, 2000, Sols : reconnaissance et essais - Auscultation d'un élément de fondation - Partie 1 : méthode par transparence
- Olson Instruments, 2015, Product description 'NDT System Add-On — Crosshole Sonic Logging' CSL testing device, <http://www.olsoninstruments.com/crosshole-sonic-ndt.php>
- Paikowsky, S.G., Chernauskas, L.R., Hart, L.J., Ealy, C.D., DiMillio, A.F., 2000, Examination of a new cross-hole sonic logging system for integrity testing of drilled shafts, Application of stress-wave theory to piles, Niyama & Beim, 2000 Balkema, Rotterdam, ISBN 90 5809 1503.

- Palm, M. 2012. Single-hole Sonic Logging, A study of possibilities and limitations of detecting flaws in piles, graduation thesis KTH Architecture and the Built Environment
- Pánek, T., Hradecký, J., Šilhán, K. 2008. Application of Electrical Resistivity Tomography (ERT) in the study of various types of slope deformations in anisotropic bedrock: case studies from the Flysch Carpathians, *Studia Geomorphologica Carpatho-Balcanica*, Vol. XLII, 2008: 57-73
- Pellerin, L., 2002, Applications of Electrical and Electromagnetic Methods for Environmental and Geotechnical Investigations , *Surveys in Geophysics*, 23, 101-132
- Pile Dynamics Inc (PDI), 2015, Product description 'CHA' CSL testing device <http://www.pile.com/pdi/products/cha/>
- PileTest, 2015, Product description 'CHUM' CSL testing device, <http://www.piletest.com/Show.asp?page=CHUM>
- Poletto, R.J., Tamaro, G.J. 2011. Repairs of Diaphragm Walls, Lessons Learned, Proceedings of the 36th Annual Conference on Deep Foundations, Boston MA, USA (DFI 2011), USB-stick
- Richtlinië Dichte Schlitzwände, 2002, Österreichische Vereinigung für Beton- und Bautechnik
- Schneider, N., 2014, Qualitätssicherungssystem für Schlitzwandfugen, German Patent: DE 102013205765 A1
- Selker, J. S., Thévenaz, L., Huwald, H., Mallet, A., Luxemburg, W., van de Giesen, N., Stejskal, M., Zeman, J., Westhoff, M. and Parlange, M. B. 2006, Distributed fiber-optic temperature sensing for hydrologic systems, *Water Resour. Res.*, 42, W12202, [doi:10.1029/2006WR005326](https://doi.org/10.1029/2006WR005326)
- Sensornet, 2012. Oryx DTS – Data Sheet, <http://www.sensornet.co.uk/images/PDF/oryx-data-sheet.pdf>
- Sieler, U., Pabst, R., Neweling, G., Moormann, C. 2012. Der Einsturz des Stadtarchivs in Köln. Bauliche Maßnahmen zur Bergung der Archivalien und zur Erkundung der Schadensursache. *BauPortal* (2013) Nr.1, pp. 2-7
- Spruit, R., van der Walle, N.J., Bouman, J.H., van der Hoek, M.J., van de Belt, L.Z. 2003. Measuring underground pipeline infrastructure using fibre optics, conference proceedings, XIIIth ECSMGE, 2003
- Spruit, R. 2011. Diepwanden Kruisplein, Resultaat metingen, Rotterdam Public Works, project report
- Spruit, R., van Tol, A.F., Hopman, V., Broere, W. 2011. Detecting defects in diaphragm walls prior to excavation, 8th International Symposium on Field Measurements in GeoMechanics (FMGM2011), USB-stick

- Spruit, R., van Tol, A.F., Broere, W., Slob, E., Niederleithinger, E. 2014. Detection of anomalies in diaphragm walls with crosshole sonic logging. *Canadian Geotechnical Journal*, 2014, 51:369-380, 10.1139/cgj-2013-0204
- Spruit, R., van Tol, A.F., Broere, W. 2015. Detection of anomalies in diaphragm walls, Fifth International Symposium on Geotechnical Safety and Risk (ISGSR) 2015, Rotterdam, Netherlands
- Stein 2015, product brochure, <http://wequips.com/images/gallery/catalogos/stein/Catalogo%20Ingles/STEIN-Flat%20stop%20end%20element%201000-1500mm.pdf>
- Thevenaz, L., Nikles, M., Fellay, A., Facchini, M., Robert, P.A. 1998. Truly distributed strain and temperature sensing using embedded optical fibers, *Proc. SPIE* 3330, Smart Structures and Materials 1998: Sensory Phenomena and Measurement Instrumentation for Smart Structures and Materials, 301 (July 21, 1998); doi:10.1117/12.316986; <http://dx.doi.org/10.1117/12.316986>
- Tyler, S.W., Selker, J.S., Hausner, M.B., Hatch, C.E., Torgersen, T., Thodal, C.E., Schladow, S.G. 2009. Environmental temperature sensing using Raman spectra DTS fiber-optic methods, *Water Resources Research*, Volume 45, Issue 4, April 2009, DOI: 10.1029/2008WR007052
- Ulrich, B., Günther, T., Rücker, C. 2008. Electrical Resistivity Tomography Methods for Archaeological Prospection, *Layers of Perception. Proceedings of the 35th International Conference on Computer Applications and Quantitative Methods in Archaeology (CAA)*, Berlin, Germany, April 2–6, 2007 (Kolloquien zur Vor- und Frühgeschichte, Vol. 10). Dr. Rudolf Habelt GmbH, Bonn, pp. 25 + CD-ROM.
- Van Dalen, J.H. 2015. Diaphragm walls, optimization of the production process with 3D FEM simulation of flow processes, PhD thesis Delft University of Technology
- Van Tol, A.F., Veenbergen, V., Maertens, J. 2010. Diaphragm walls, a reliable solution for deep excavations in urban areas? DFI and EFFC, London: Deep Foundation Institute, pp. 335-342.
- Van Tol, A.F., Korff, M. 2012. Deep excavations for Amsterdam metro North-South line: An update and lessons learned, *Geotechnical Aspects of Underground Construction in Soft Ground - Proceedings of the 7th International Symposium on Geotechnical Aspects of Underground Construction in Soft Ground*, pp. 37-45.
- Van Tol, A.F., Admiraal, B., Spruit, R., van Dalen, J.H., 2014, Diaphragm Walls, Recent Developments to Improve Reliability Proceedings-DFI/EFFC 11th International Conference on Piling and Deep Foundations, 2014, Stockholm, Sweden

References

- Vanni, D., Geutebrück, E. 2011 Leak detection in complex underground structures using an innovative geophysical method. Proceedings of the seventh International Symposium on Geotechnical Aspects of Underground Construction in Soft Ground, Rome, Italy, 16-18 May 2011– Viggiani (ed), Taylor & Francis Group, London, ISBN 978-0-415-68367-8
- Vié, D. 2004. Rokin Station Amsterdam Franki Cementation Sonic Coring Panel 21, Dienst Metro Amsterdam
- Walz, B., Gerlach, J., Pulsfort, M. 1983 Skript zum Seminar Schlitzwandbauweise, Bergische Universität Gesamthochschule Wuppertal
- Wikipedia. 2015. Resistance thermometer, Wikipedia, the free encyclopedia http://en.wikipedia.org/wiki/Resistance_thermometer
- Wilkinson, P.B., Loke, M.H., Meldrum, P.I., Chambers, J.E., Kuras, O., Gunn, D.A., Ogilvy, R.D. 2012. Practical aspects of applied optimized survey design for electrical resistivity tomography. Geophysical Journal International, Vol. 189, 428-440.

Acknowledgements

I cannot find a satisfactory order in which to thank all that have contributed to this wonderful episode in my life. I feel privileged to have been given this opportunity and to be welcome at so many project sites to do my testing.

The opportunity to execute tests in the field within several projects in the Netherlands has been quite unique. It was a joy to conduct tests on site. The project managers, project directors, contractors etc. that made this possible have made an invaluable contribution to this research. By doing so, they just as well contributed to my motivation for conducting the research.

In particular the Kruisplein Rotterdam and Spoorzone Delft projects, have been exceptionally helpful and have made invaluable contributions to this research.

This research would not have been possible without the support of the Geolmpuls programme, the Municipality of Rotterdam and Delft University of Technology. It is fantastic that these three organizations were able to co-fund this and to make proper arrangements.

I do not want to take the risk of leaving out people. I will therefore at this spot only mention my promotor Frits van Tol and co-promotor Wout Broere. Without their wisdom and experience I would not have completed this quest. For all other people: If you received an invitation for my defense, by mail, email or otherwise, be assured that you are valuable to me and that you have contributed directly or indirectly to this interesting period in my life.

About the author

Rodriaan Spruit was born on the 28th of November 1972 in Schiedam (NL). In 1991 he graduated from the Sint Lyduina Lyceum (Atheneum-B). From 1991 to 1997 he studied Mining and Petroleum Engineering at the Delft University of Technology (NL). His specialization in Engineering Geology was completed with a research into the possibilities to use electromagnetic surveys to map liquefaction sensitive sand layers in earth-quake hazard zones. He conducted EM fieldwork in the area of Herkenbosch (NL) where liquefaction had occurred during the 1992 earth-quake on April the 13th. After graduation he started to work as a geotechnical engineer at the Engineering Department of the Municipality of Rotterdam (at that time part of 'Rotterdam Public Works', now part of 'Rotterdam City Development'). He was involved in very diverse projects, from sewer renewal to bored tunnels, vibration monitoring and trial loading on piles and anchors. He has published several (national and international) papers on case studies and research topics tested and implemented in projects. He is often invited for guest lectures and presentations. He was thesis advisor for several students from Rotterdam Technical School and Delft University of Technology.

He is a 'Laureate of the Hubert Raedschelders award 2011', based upon presentation of his PhD work at the 16th ie.net Geotechnical Innovation Forum, Antwerp, Belgium.

The paper 'Detection of anomalies in diaphragm walls with Crosshole Sonic Logging' (published in Canadian Geotechnical Journal in December 2013) received the 'editors' choice' designation of that journal.